

Y  
RECEIVED BY OST **MAY 28 1986**

**UCRL 15806**

**S/C 5838105**

**UCRL--15806-Rev.1**

**DE86 010789**

**SEISMIC ANALYSIS OF THE  
MIRROR FUSION TEST FACILITY:  
SOIL STRUCTURE INTERACTION ANALYSES  
OF THE AXICELL VACUUM VESSEL**

By

**OLEG R. MASLENIKOV**

**MICHAEL J. HRAZ**

**JAMES J. JOHNSON**

**PREPARED FOR  
LAWRENCE LIVERMORE NATIONAL LABORATORY  
LIVERMORE, CA**

**MARCH 1986**

**DISTRIBUTION OF THIS DOCUMENT IS UNLIMITED**

**PS**

#### **DISCLAIMER**

Work performed under the auspices of the U.S. Department of Energy by Lawrence Livermore National Laboratory under contract number W-7405-ENG-48.

*This document was prepared as an account of work sponsored by an agency of the United States Government. Neither the United States Government nor the University of California nor any of their employees, makes any warranty, express or implied, or assumes any legal liability or responsibility for the accuracy, completeness, or usefulness of any information, apparatus, product, or process disclosed, or represents that its use would not infringe privately owned rights. Reference herein to any specific commercial products, process, or service by trade name, trademark, manufacturer, or otherwise, does not necessarily constitute or imply its endorsement, recommendation, or favoring by the United States Government or the University of California. The views and opinions of authors expressed herein do not necessarily state or reflect those of the United States Government or the University of California, and shall not be used for advertising or product endorsement purposes.*

#### **DISCLAIMER**

*This report was prepared as an account of work sponsored by an agency of the United States Government. Neither the United States Government nor any agency thereof, nor any of their employees, makes any warranty, express or implied, or assumes any legal liability or responsibility for the accuracy, completeness, or usefulness of any information, apparatus, product, or process disclosed, or represents that its use would not infringe privately owned rights. Reference herein to any specific commercial product, process, or service by trade name, trademark, manufacturer, or otherwise does not necessarily constitute or imply its endorsement, recommendation, or favoring by the United States Government or any agency thereof. The views and opinions of authors expressed herein do not necessarily state or reflect those of the United States Government or any agency thereof.*

## TABLE OF CONTENTS

	<u>Page</u>
LIST OF FIGURES . . . . .	v
LIST OF TABLES . . . . .	vi
EXECUTIVE SUMMARY . . . . .	viii
1. INTRODUCTION. . . . .	1-1
1.1 Background . . . . .	1-1
1.2 Description of the MFTF-B Facility . . . . .	1-1
1.3 Objective and Scope. . . . .	1-4
2. METHODS OF ANALYSES . . . . .	2-1
2.1 SSI Analysis of Structures with Rigid Foundations. . . . .	2-1
2.2 Correction for Truncated Modes . . . . .	2-4
3. ELEMENTS OF THE ANALYSES. . . . .	3-1
3.1 Free-field Motion. . . . .	3-1
3.2 Foundation Impedances. . . . .	3-3
3.2.1 Soil Properties . . . . .	3-3
3.2.2 Coupled Impedances for Combined Vessel and Vault Foundations. . . . .	3-5
3.3 Structural Models. . . . .	3-7
3.3.1 Vessel Models . . . . .	3-7
3.3.2 Vault Model . . . . .	3-12
3.3.3 Composite Modal Damping . . . . .	3-12
4. DISCUSSION OF ANALYSES AND RESULTS. . . . .	4-1
4.1 Benchmarking SMA and LLNL Models and Analytical Methods . . . . .	4-3
4.1.1 Effects of Model Differences. . . . .	4-3
4.1.2 Total Effect of Modeling & Analytical Method. . . . .	4-11

TABLE OF CONTENTS (Continued)

	<u>Page</u>
4.2 Results from the Coupled Vessel/Vault SSI Analyses . . . . .	4-18
4.2.1 Effects of SSI and Vessel/Vault Interaction . . . . .	4-19
4.2.2 Comparison of Coupled Vessel/Vault SSI	
Analyses with LLNL Analysis . . . . .	4-26
4.2.3 Effects of Increased Damping in the Vessel. . . . .	4-33
5. CONCLUSIONS AND RECOMMENDATIONS . . . . .	5-1
6. REFERENCES . . . . .	6-1

APPENDIX A - IN-STRUCTURE MAXIMUM ACCELERATIONS,  
DISPLACEMENTS AND RESPONSE SPECTRA  
FROM COUPLED SSI ANALYSES

## LIST OF FIGURES

<u>Figure</u>	<u>Page</u>
1.1 Isometric View of the MFTF-B Facility. . . . .	1-3
2.1 Schematic Representation of the Elements of the Substructure Approach to SSI Analysis . . . . .	2-6
3.1 Response Spectra of Free-field Time Histories at 5% Damping. . . . .	3-2
3.2 Variation of Best Estimate Shear Wave Velocity and Material Damping with Depth. . . . .	3-4
3.3 Vessel and Vault Foundations Showing Discretization Used for Calculating Impedances for Coupled Vessel/Vault SSI Analyses. . . . .	3-6
3.4 Isometric View of the Structural Half-Model of the Axicell Vessel Configuration . . . . .	3-10
3.5 Isometric View of the Structural Model of the Vault. . . . .	3-13

## LIST OF TABLES

<u>Table</u>	<u>Page</u>
3.1 Summary of Significant Modes for the LLNL Axicell Vessel Model. . . . .	3-11
3.2 Summary of Significant Modes for the Axicell Vessel Model with Modified Base Springs by SMA . . . . .	3-11
3.3 Summary of Significant Modes for the Vault Model. . . . .	3-14
4.1 Comparison between SMA and LLNL RESPAN Analysis Results	
A. Summary of Foundation Forces . . . . .	4-5
B. Summary of Vessel End Cell Support Leg Forces. . . . .	4-7
C. Summary of Magnet Hanger and Strut Forces. . . . .	4-9
4.2 Comparison between CLASSI Fixed-Base Analysis and LLNL RESPAN Analysis	
A. Summary of Foundation Forces . . . . .	4-12
B. Summary of Vessel End Cell Support Leg Forces. . . . .	4-14
C. Summary of Magnet Hanger and Strut Forces. . . . .	4-16
4.3 Comparison between CLASSI Coupled SSI and Fixed-Base Analyses	
A. Summary of Foundation Forces . . . . .	4-20
B. Summary of Vessel End Cell Support Leg Forces. . . . .	4-22
C. Summary of Magnet Hanger and Strut Forces. . . . .	4-24
4.4 Comparison between CLASSI Coupled SSI Results and LLNL RESPAN Results	
A. Summary of Foundation Forces . . . . .	4-27
B. Summary of Vessel End Cell Support Leg Forces. . . . .	4-29
C. Summary of Magnet Hanger and Strut Forces. . . . .	4-31
4.5 Comparison between CLASSI Coupled SSI Analyses for 10% Damping and Composite Modal Damping	
A. Summary of Foundation Forces . . . . .	4-34
B. Summary of Vessel End Cell Support Leg Forces. . . . .	4-36
C. Summary of Magnet Hanger and Strut Forces . . . . .	4-38

LIST OF TABLES (Continued)

<u>Table</u>	<u>Page</u>
A.1 CLASSI Coupled SSI Analysis Results	
Summary of Maximum Accelerations. . . . .	
A.2 CLASSI Coupled SSI Analysis Results	
Summary of Maximum Relative Displacements . . . . .	
A. Relative Displacements in the Vessel. . . . .	
B. Relative Displacements in the Vault . . . . .	
C. Relative Displacements between the Vessel and the Vault . . . . .	

## EXECUTIVE SUMMARY

Lawrence Livermore National Laboratory (LLNL) is designing and constructing the Mirror Fusion Test Facility (MFTF-B) for the purpose of conducting magnetic fusion energy experiments. The facility consists of three basic structures: the vacuum vessel, the shielding vault, and Building 431 which surrounds the vault and contains equipment essential to the experiments. Seismic analysis of the Axicell vacuum vessel is the subject of this report. The A-cell, a configuration of the vacuum vessel which has been superseded by the Axicell, was the subject of a preliminary study. The overall characteristics of the two configurations from a seismic response standpoint are similar and the general trends previously observed are similar to those for the Axicell. The specific results reported herein, such as member forces, are applicable to the Axicell configuration only.

The Axicell vessel is a cylindrical stainless steel structure about 180 ft. long, 25 to 35 ft. in diameter, and extending to a height of about 50 ft. above its foundation. It is supported on four foundation mats in an east-to-west pattern, the assembly being essentially symmetrical about the north-south and east-west centerlines of the vessel. The vessel weighs about 8000 kips; its foundation weighs about 6000 kips. The shielding vault is essentially a rectangular box-shaped structure, with a central stiffening buttress, which surrounds the vessel. It is about 238 ft. long by 84 ft. wide and it is about 80 ft. in height. The vault walls are 7 ft. thick and the central buttress is 8 ft. thick. The walls are supported on footings 17-1/2 to 18 ft. wide and 6-1/2 ft. thick. The total weight of the vault including footings is about 70,000 kips. Building 431 is a light steel frame structure surrounding the vault and housing the support equipment and controls for the MFTF experiment.

The objective of this study was to obtain a best estimate of the response of the Axicell vessel to a seismic excitation of 0.25g peak ground acceleration in the free-field. In the course of our study we performed a series of seismic analyses on a model of the Axicell vessel that was identical to the model developed by LLNL except for certain differences in assumed flexibility beneath the vessel's foundation piers and support columns. The

different analyses we performed were: a response spectrum analysis using the same method as LLNL; a fixed-base analysis using the CLASSI methodology; and SSI analyses which included foundation to foundation interaction between the vessel and vault.

- Response spectrum analysis. The response spectrum analyses was performed using computer program RESPAN. Its purpose was to provide a benchmark between the two structural models. Response was calculated for the MFTF design response spectra, at 5% damping, reduced by a factor of 25%. The results were compared with the LLNL results to determine the effects of the differences in modeling assumptions at the foundation pier and column bases.
- Fixed-base analysis. We performed a fixed-base analysis using computer program CLASSI to benchmark the combined effects of differences in modeling assumptions and analytical methods, and to provide a basis for comparison of the subsequent SSI analyses of the vessel. The fixed-base analysis was made with 5% damping in the vessel and used as input motion free-field time histories whose spectra loosely matched the MFTF design spectra.
- SSI analysis of the vessel including through-soil coupling with the vault. Because the vault is significantly more massive than the vessel and is founded in close proximity to the vessel, through-soil coupling between the two is expected to be significant. The motion of the vault is likely to induce similar motions in the vessel. SSI analysis of the vessel including this through-soil coupling was performed. The dynamic model of the vault was based on the model developed by Foster Engineering, Inc. and was used for our seismic analysis of the vault. This forms our best estimate analysis. Building 431 was not included since its motion is not likely to induce significant motion in the vessel or vault due to its mass and foundation conditions. We performed analyses for three sets of soil properties bracketing the estimated range of uncertainty in soil modulus. For these analyses we used composite modal damping for the vessel

to reflect different damping levels in different structural members. We also performed an SSI analysis using a damping ratio of 10% in all modes to study this effect on response.

All of the CLASSI analyses performed here were for a 0.25g design earthquake. Design response spectra were specified, for which artificial acceleration time histories were generated. Three components of motion were treated simultaneously -- two horizontal and the vertical. Results were obtained in the form of time histories; peak values are presented here for comparison purposes. The CLASSI methodology was used to perform the SSI analyses. This is an implementation of the substructure approach. All of the analysis results include a correction for excluded modes or "missing mass."

In-structure response of the vessel reported here takes the form of maximum accelerations and response spectra at 56 locations, maximum foundation forces for 8 elements where the vessel supports connect with the foundation mats, maximum forces at 8 locations where vessel support legs are connected to the end cell piers, maximum forces in 66 magnet hangers, and maximum relative displacements between 6 locations on the vessel and 15 locations on the vault.

Our results are presented in this report as tables of comparisons of specific member forces from our analyses and the analyses performed by LLNL. Also presented are tables of maximum accelerations and relative displacements and plots of response spectra at various selected locations. Based on these results we made the following observations. In general, we observed a reduction of about 20% in calculated vessel forces due to the combined effect of SSI and interaction with the vault. This was based on comparisons between our CLASSI fixed-base and SSI analyses. However, a comparison of our RESPAN results with LLNL results showed that the differences in the way that the foundation flexibility beneath the foundation piers and support columns was modeled led to significant increases in forces and moments at the bases of the piers. After an extensive study of these modeling differences, we concluded that our representation of the foundation flexibility was more appropriate for the seismic analysis of the vessel. The differences due to modeling assumptions are reflected in all our analyses. Our best estimate of vessel response is summarized in Tables 4.4A to 4.4C. We recommend that

## 1. INTRODUCTION

### 1.1 BACKGROUND

The Mirror Fusion Test Facility (MFTF-B), located at the Lawrence Livermore National Laboratory, Livermore, CA, is the site of one of the latest in a series of experiments, sponsored by the U.S. DOE, studying the potential of magnetic fusion energy. As part of the design of the facility, seismic analyses were performed on each of the major structures - the vacuum vessel, the shielding vault and the enclosure building. The basic objectives of the analyses are to provide seismic design information in the form of member forces in the structures, foundation forces, and in-structure response spectra for the definition of the design environment for equipment.

Seismic analysis of the Axicell vacuum vessel is the subject of this report. The Axicell is a configuration of the vacuum vessel which supersedes the A-cell, which was the subject of a previous study by SMA, reported in Reference 1. Soil structure interaction (SSI) was an important phenomenon to be considered in the analyses. The CLASSI family of computer programs was used. The analyses performed ranged in complexity from fixed-base to SSI analyses including through-soil coupling between the vessel and the vault. The main features of the structures are summarized below.

### 1.2 DESCRIPTION OF THE MFTF-B FACILITY

The MFTF-B facility consists of three basic structures (Fig. 1.1): the vacuum vessel within which fusion experiments are conducted, a massive reinforced concrete shielding vault which surrounds the vessel, and a steel frame building enclosing both vault and vessel and housing equipment essential to the experiments.

The vacuum vessel is a cylindrical stainless steel structure about 180 ft. long, 25 to 35 ft. in diameter, and extending to a height of about 50 ft. above its foundation. It is supported on four foundation mats oriented in an east-to-west array, the assembly being essentially symmetrical about the north-south and east-west centerlines of the vessel. The vessel itself

consists of three sections or cells. The east and west end cells house the large Yin-Yang magnets. Each end cell is supported by four large (16 ft. x 13 ft.) piers. The end foundation slabs under the piers are about 4 ft. thick and about 50 ft. square with a 22 ft. square hole in the center. The center cell connecting the two end cells houses a series of solenoids and is supported by the two inside foundation slabs, each 4 ft. thick and about 25 ft. x 50 ft., and by the center buttress of the vault. The support system for the center cell consists of two box beams, oriented longitudinally beneath the vessel, on which the vessel legs rest. The box beams in turn, are supported by steel braced column systems on the two inside foundation slabs. They also receive vertical support only from the vault center buttress. For all analyses performed on the vessel, the array of four foundations was assumed to behave as a rigid body for calculating soil impedances (i.e. the stiffness of the foundations themselves in conjunction with the stiffening effect of the vessel and supporting structure induces rigid behavior). However, additional flexibility was superposed as part of the structural model to account for differential rocking of the separate slabs in the longitudinal direction as well as slab flexibility between the piers of the end cells. The vessel weighs about 8000 kips; its foundation weighs about 6000 kips.

The vault is a rectangular box-shaped structure with a central stiffening buttress. In plan view, its exterior dimensions are 238 ft. x 84 ft. In elevation the structure extends 80-1/2 ft. from the base of the foundation to the top of the cap beam. It is embedded 27-1/2 ft. Removable precast prestressed interlocking T-beams form the roof. The vault walls are 7 ft. thick and are supported on footings about 18 ft. wide and 6-1/2 ft. thick. The eastern half of the vault was constructed for prior experiments and uses concrete block walls above grade; the western half was added for the MFTF-B experiments and is a post-tensioned monolithic concrete structure. The total weight of the vault including footings is about 70,000 kips. The vault is the subject of a separate study by SMA, reported in Reference 2.

Building 431 is a light steel frame structure about 300 ft. long, 160 ft. wide and 100 ft. high, with concrete floor and low bay roof diaphragms. The eastern portion was built for prior experiments; the extension to the west was added for the MFTF-B experiments. A trussed roof system spans

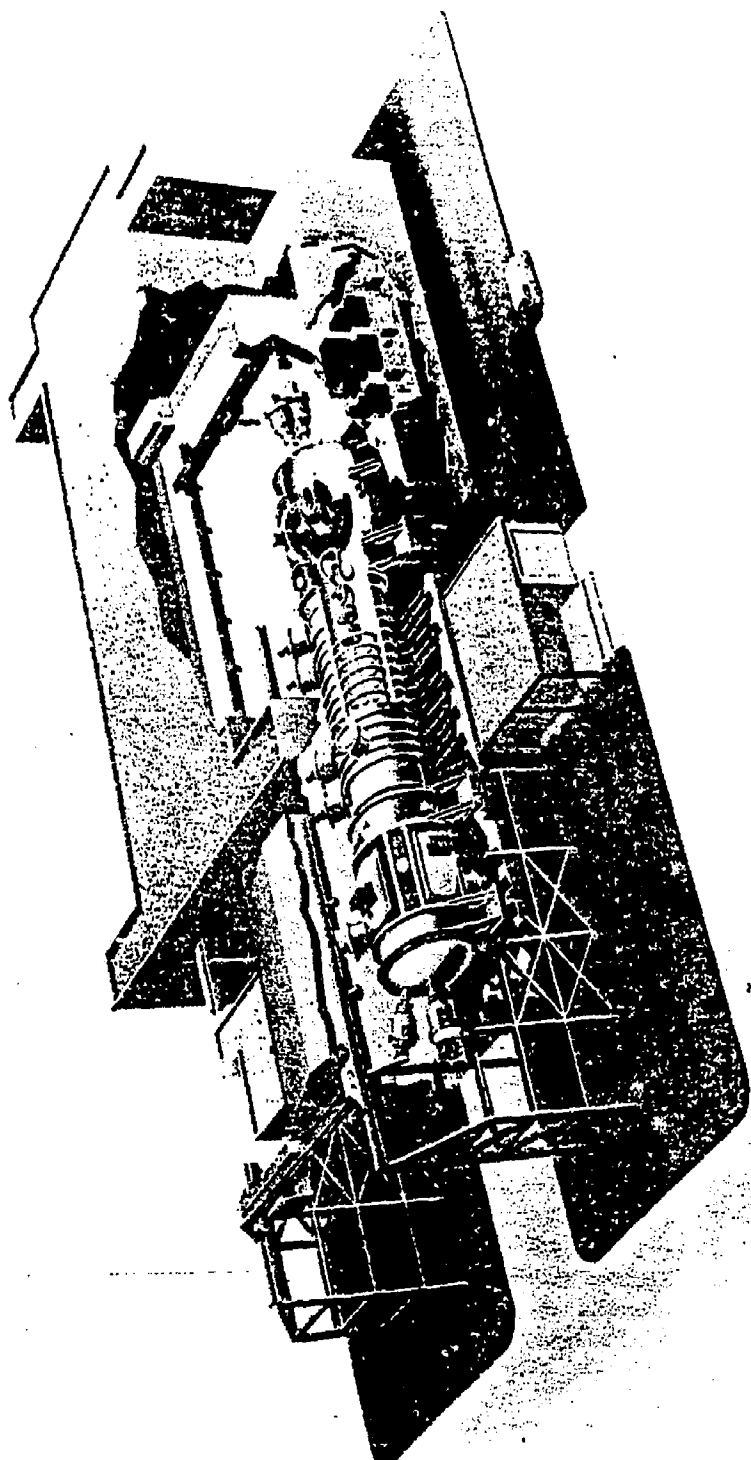


Fig. 1.1 Isometric View of NEPR-B Facility.

the high bay area supporting a tar and gravel roof over corrugated metal decking. The lateral force resisting system is a combination of diagonal cross-bracing and moment resistant frames. Column bases in the pre-existing portion of the building are supported by piers. Columns in the extension are supported by a combined pier and shear beam arrangement. The total weight of the building and equipment is about 6000 kips. Because of the size and location of the vault, the effects of building 431 on the vessel are considered to be relatively insignificant and it was not included in the study reported herein. However, a detailed study of building 431 was conducted by SMA and is the subject of a separate report (Ref. 3).

### 1.3 OBJECTIVES AND SCOPE

The objectives of this study were to perform seismic analyses of the MFTF-B Axicell vacuum vessel configuration to provide LLNL with our best estimate of its response to a 0.25g earthquake excitation. Analyses were performed for two foundation support conditions: fixed-base and soil-structure interaction (SSI) including through-soil coupling with the vault. The latter case is our best estimate of the behavior of the vessel. The relative mass and close proximity of the vault to the vessel was expected to affect significantly the dynamic response of the vessel. Motions of the vault are likely to drive the vessel. The fixed-base analysis serves two purposes. First, it serves to benchmark the fixed-base LLNL response spectrum analysis. Second, it serves as a basis of comparison for the subsequent SSI analyses performed herein. The coupled SSI analysis was performed for three soil property estimates to account for uncertainties in their values.

This report is organized as follows:

Section 2 describes the methods of SSI analysis used in this study. The computer programs denoted CLASSI were used extensively. CLASSI is an implementation of the substructure approach to SSI. In all analyses, corrections for truncated modes or "missing mass" were made. These corrections are applied in the time domain and are described in Sec. 2.

Section 3 presents the elements of the analyses -- free-field

member forces in these tables be reviewed and used for comparison with design capacities. If significant yielding should be observed to occur in any major structural elements, a reanalysis using degraded structural properties would obtain better estimates of response.

motion, foundation impedances for the coupled vessel-vault system, and the structure models of the vessel and vault.

Section 4 presents numerical results and comparisons between the various analysis scenarios.

Section 5 contains conclusions and recommendations.

## 2. METHODS OF ANALYSIS

### 2.1 SSI ANALYSIS OF STRUCTURES WITH RIGID FOUNDATIONS

The substructure approach to SSI analysis of structures with assumed rigid foundations is depicted schematically in Fig. 2.1. The key elements of the approach are: specifying the free-field ground motion; calculating the foundation input motion; calculating the foundation impedances; determining the dynamic characteristics of the structure, and performing the SSI analysis, i.e. combining the previous steps to calculate the response of the coupled soil-structure system. Each aspect is described below. The computer programs denoted CLASSI (Ref. 4) were used for the analysis.

Free-field ground motion. Specification of the free-field ground motion entails specifying the control point, the frequency characteristics of the control motion (typically, time histories or response spectra), and the spatial variation of the motion. For the MFTF vessel analysis, the control point was specified on the surface of the soil, the control motion consisted of acceleration time histories generated to match the design ground response spectra, and, in all cases, no spatial variation of motion has been assumed, i.e. the foundation input motion has been assumed identical to the free-field ground motion.

Foundation input motion. In general, the foundation input motion differs from the free-field ground motion in all cases, except for surface foundations subjected to vertically incident waves. First, the free-field motion varies with soil depth. Second, the soil-foundation interface scatters waves because points on the foundation are constrained to move according to its geometry and stiffness. The foundation input motion  $\{U^*(\omega)\}$  is related to the free-field ground motion by means of a transformation defined by a scattering matrix  $[S(\omega)]$ , which is complex valued and frequency dependent:

$$\{U^*(\omega)\} = [S(\omega)] \{f(\omega)\} \quad (2.1)$$

The vector  $\{f(\omega)\}$  is the complex Fourier transform of the free-field ground motion, which contains its complete description. For the MFTF vessel SSI

analysis, scattering effects were not included. This retains some conservatism albeit unquantified.

Foundation impedances. Foundation impedances [ $K_s(\omega)$ ] describe the force-displacement characteristics of the soil. They depend on the soil configuration and material behavior, the frequency of the excitation, and the geometry of the foundation. In general, for a linear elastic or viscoelastic material and a uniform or horizontally stratified soil deposit, each element of the impedance matrix is complex-valued and frequency dependent. For a rigid foundation, the impedance matrix is a 6 x 6 which relates a resultant set of forces and moments to the six rigid-body degrees-of-freedom. Foundation impedances are calculated using the CLASSI programs CLAY and CLAN. When foundation-to-foundation interaction is included as in our analysis of the coupled vessel-vault system, the impedance matrix increases in size to include through-soil coupling of the foundations. For a two foundation system, e.g. vessel and vault with each foundation assumed to behave rigidly, the impedance matrix is a 12 x 12.

Structure model. The dynamic characteristics of the structures to be analyzed are described by their fixed-base eigensystem and modal damping factors. The structures dynamic characteristics are then projected to a point on the foundation at which the total motion of the foundation, including SSI effects, is determined. Typically, structural data for CLASSI is calculated using the finite element program SAP4 or GEMINI, in conjunction with the post processor INSSIN.

SSI analysis. The final step in the substructure approach is the actual SSI analysis. The results of the previous steps -- foundation input motion, foundation impedances, and structure model -- are combined to solve the equations of motion for the coupled soil-structure system. For a single rigid foundation, the SSI response computation requires solution of, at most, six simultaneous equations -- the response of the foundation. The formulation is in the frequency domain. Hence, one can write the equation of motion for the unknown harmonic foundation response  $[U] \exp(i\omega t)$  for any frequency  $\omega$ , about a reference point normally selected on the foundation.

$$(-\omega^2([M_0] + [M_b(\omega)]) + [K_s(\omega)])\{U\} = [K_s(\omega)]\{U^*\} \quad (2.2)$$

Equation 2.2 separates the effects due to scattering from those caused by interaction between soil, structure, and foundation. The effects of scattering are included in the foundation input motion  $\{U^*\}$ . The interaction effects of the structure, foundation, and soil are represented in the term

$$-\omega^2([M_0] + [M_b(\omega)]) + [K_s(\omega)]$$

where  $[M_0]$  is the mass matrix of the foundation,  $[M_b(\omega)]$  is the frequency-dependent equivalent mass matrix of the structure, and  $[K_s(\omega)]$  is the impedance matrix of the foundation. The total motion  $\{U\}$  of the foundation results from a combination of both types of effects.

The equivalent mass matrix of the structure, when multiplied by  $\omega^2$ , represents the force-displacement relationship of the structure subjected to base excitations. All of the physical and dynamic characteristics of the structure pertinent to the solution are contained in it:

$$[M_b(\omega)] = [M_{bo}] + [\Gamma]^T[D(\omega)][\Gamma] \quad (2.3a)$$

The matrix  $[M_{bo}]$  is the  $6 \times 6$  mass matrix of the structure for rigid translations and rotations about the reference point:

$$[M_{bo}] = [\alpha]^T[M][\alpha] \quad (2.3b)$$

where  $[M]$  is the mass matrix of the structure and  $[\alpha]$  defines the node point locations relative to the reference point.  $[M_{bo}]$  is independent of frequency.

The second term on the right-hand side of Eq. 2.3a represents the dynamic behavior of the structure using its fixed-base modes. The matrix  $[\Gamma]$  comprises the modal participation factors for base translations and rotations:

$$\{\Gamma\} = \{\phi\}^T [M] \{\alpha\} \quad (2.3c)$$

where the columns of  $\{\phi\}$  are the mass normalized fixed-base mode shapes. Finally, the diagonal matrix  $[D(\omega)]$  contains the dynamic amplification factors  $D_j(\omega)$  for each fixed-base mode of the structure:

$$D_j(\omega) = \frac{(\omega/\omega_j)^2}{(1-\omega^2/\omega_j^2) + 2i\beta_j(\omega/\omega_j)} \quad (j = 1, nf) \quad (2.3d)$$

where

$\omega_j$  = the frequency of the  $j$ th fixed-base mode,

$\beta_j$  = the modal damping ratio of the  $j$ th fixed-base mode,

$nf$  = the number of fixed-base modes included in the solution.

Note that the term  $[M_{bo}(\omega)]$  is complex-valued for damped structures. Once the equations of motion (eq. 2.2) are solved for the response  $\{U\}$  of the foundation (three translations and three rotations), in-structure response may be obtained simply as

$$\{U_{STR}(\omega)\} = \{\alpha\} \{U(\omega)\} + \{\phi\}^T [D(\omega)] \{\Gamma\} \{U(\omega)\} \quad (2.4)$$

## 2.2 CORRECTION FOR TRUNCATED MODES

As part of this effort, we developed and implemented a method to correct the dynamic responses calculated by CLASSI to account for the effects of higher modes of the vessel not included in the dynamic analysis. This is referred to as modal truncation effects, excluded modes effects, or "missing mass" effects. Depending on the location in the structure where forces are being calculated, these effects can be significant, even predominant.

The procedure involves performing a static analysis of the structure, applying load vectors consisting of the portion of the nodal point masses not included in the dynamic analysis. Six load vectors are applied; one each for the six foundation degrees-of-freedom. The resulting element

stresses become influence coefficients relating element stress to foundation acceleration. Again six values are obtained — each value relates element stress to a foundation degree-of-freedom acceleration. These influence coefficients are applied to the six acceleration time histories of the foundation and then added by direct superposition to the dynamic response. Because this method of combination uses algebraic summation, the total force can be greater or less than the dynamic portion — it is a function of the phase relationship between the foundation motions and the dynamic response. All results presented here include corrections for modal truncation.

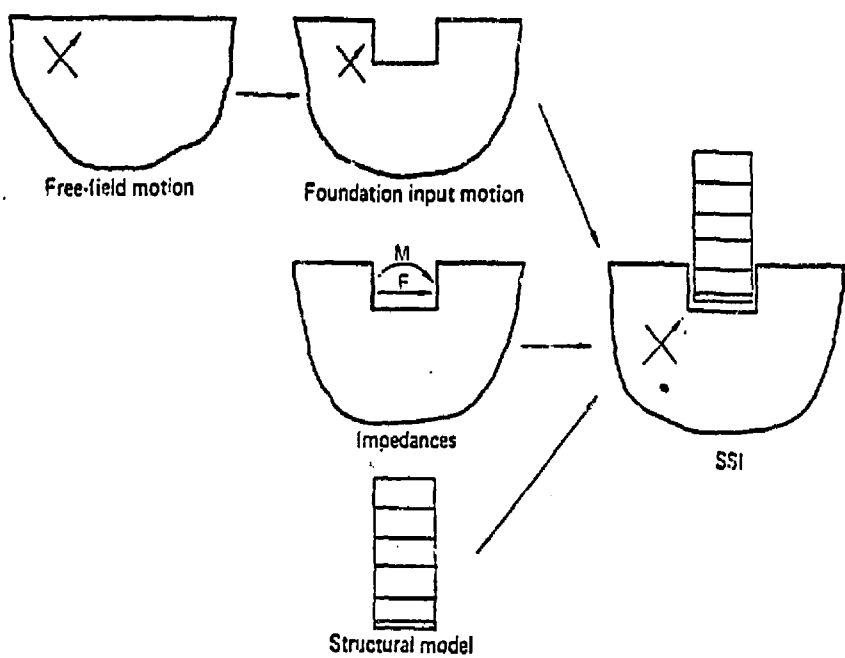


Fig. 2.1 Schematic Representation of the Elements of the Substructure Approach to SSI Analysis.

### 3. ELEMENTS OF THE ANALYSES

Soil-structure interaction (SSI) analysis by the substructure approach using the CLASSI family of computer programs uses three basic elements of data. These are the definition of the earthquake in the free-field; the foundation impedances, which depend on the foundation geometry and the dynamic soil properties; and the dynamic characteristics of the structure. These elements are discussed separately below.

#### 3.1. FREE-FIELD MOTION

The free-field ground motions used in the present analyses were three acceleration time histories, two horizontal components and the vertical component, generated to match the MFTF design ground response spectra. These time histories were generated with the program SIMQKE. The time histories were digitized at a time interval of 0.01 seconds, and have a duration of 18.0 seconds followed by a 2.5 second quiet zone. In accordance with the MFTF design criteria, the horizontal components were scaled to a zero period acceleration (ZPA) of 0.25g; the vertical component has a ZPA of 0.17g. Figure 3.1 shows response spectra at 5% damping for each component compared with the MFTF design spectrum.

Before proceeding, selected observations concerning the definition of the free-field ground motion are in order. Definition of the design earthquake as a single set of time histories whose response spectra approximate the design ground response spectra does not constitute a unique definition. No single set of time histories uniquely define corresponding response spectra. This is especially true for broad-band design ground response spectra intended to represent a range of possible earthquakes rather than a single event. The standard practice for the seismic analysis of commercial nuclear power plants is to generate artificial acceleration time histories whose response spectra envelope the design ground response spectra. This practice can add significant conservatism. For the present analyses, we sought a best estimate fit as evidenced in Fig. 3.1 rather than introducing artificial conservatism. An additional point is that seismic responses calculated by a response spectrum analysis procedure will not match

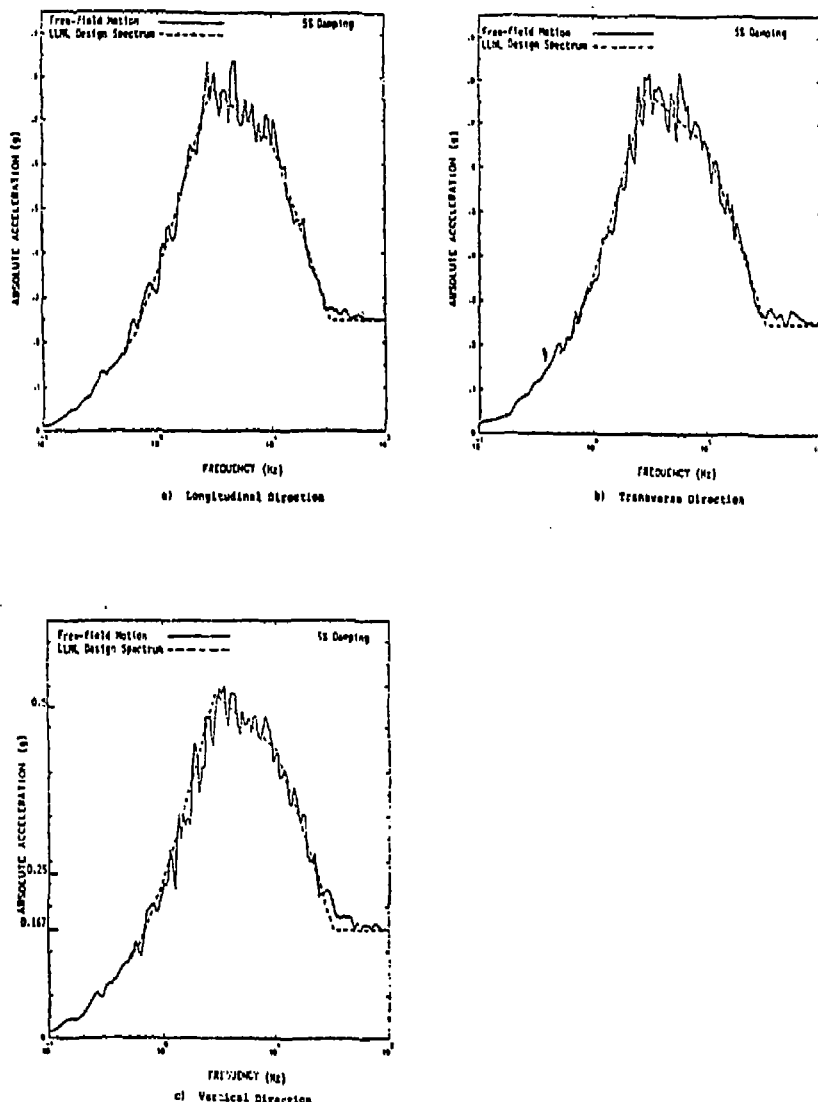


Fig. 3.1 Response Spectra of Free-field Time Histories at 5% Damping.

exactly those calculated by a time history procedure -- minor differences are to be expected.

For all seismic analyses performed on the vessel (i.e. fixed-base, and SSI analyses assuming it to be coupled with the vault through-the-soil), the foundation input motion was assumed to be identical to the free-field motions defined on the ground surface. This is equivalent to ignoring wave scattering effects for the vessel and the vault. Ignoring this phenomenon adds a degree of conservatism albeit difficult to quantify.

### 3.2 FOUNDATION IMPEDANCES

The force-displacement characteristics of the soil are represented by complex-valued frequency-dependent functions denoted foundation impedances. The impedances represent the effects of soil stiffness and damping (including both material and radiation damping) on the foundation. The soil deposit at the site is modeled as a horizontally layered half-space with different properties in each layer (shear modulus, material damping, mass density and Poisson's ratio). The impedance functions are calculated based on this definition of the soil deposit together with a description of the geometry of the soil-foundation interface.

#### 3.2.1 Soil Properties

The soil properties used for the calculation of foundation impedances were best estimate values for a 0.25g ground surface excitation obtained from the study by the NTED Geotechnical Group of LLNL (Ref. 5). Figure 3.2 shows profiles of the best estimate shear wave velocities and damping ratios vs. soil depth. These values are mean value properties obtained from multiple SHAKE analyses using least squares fit strength data obtained from the site of building 431. Other properties defining the site that did not vary with depth were unit weight (130pcf) and Poisson's ratio (0.42). Our SSI analysis including vessel-vault interaction was performed for these best estimate properties and for a stiffer and a softer soil as described in Sec. 4.3.

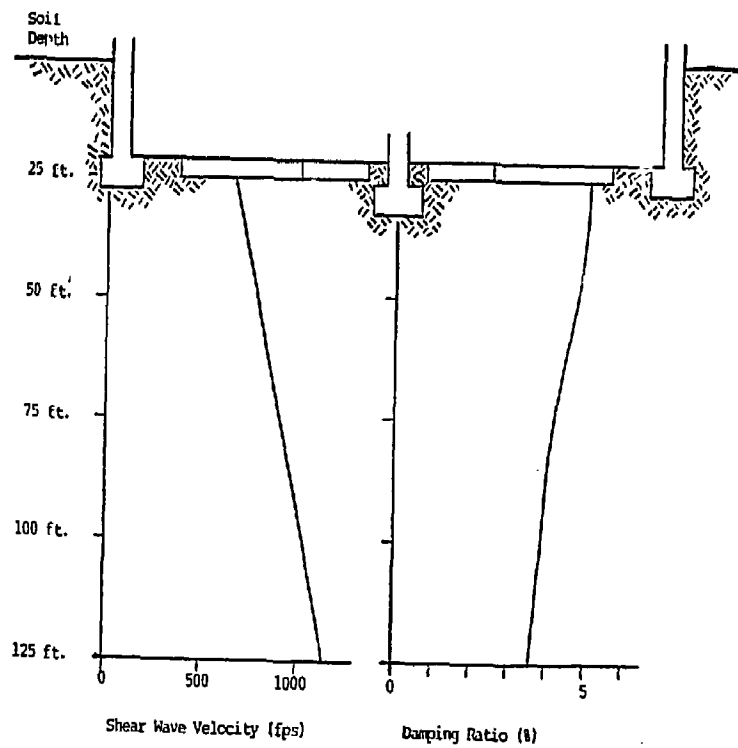


Fig. 3.2 Variation of Best Estimate Shear Wave Velocity and Material Damping with Depth.

### 3.2.2 Coupled Impedances for Combined Vessel and Vault Foundation System

For our SSI analyses of the vessel, which included the interaction effect between the vessel and vault foundations, we computed impedance functions that included coupling between the foundations through the soil. For the calculation of impedances, each foundation was assumed to behave as a single rigid body.

For the vessel foundation, we assumed all slabs were rigidly connected so that the assembly moved as a single rigid body. Effects of differential rocking between slabs in the longitudinal direction and of slab flexibility between the piers of the end cells were included using rotational springs attached to the fixed-base structural model.

The behavior of the vault, including flexibility in its foundation, was investigated in Ref. 2. The effect of flexibility of the vault foundation was found to be significant on stresses in the vault. However, it is not expected to have a significant effect on foundation-to-foundation interaction with the vessel.

The procedure used to compute the impedances involved first using the CLASSI program GLAY to calculate Green's functions, which are steady state dynamic force/displacement relationships between a point source and observation points at various specified distances on the surface of the layered half-space. This was done for a number of specified frequencies. The Green's functions were then used, along with a discretized model of the soil-foundation interface, to generate the foundation impedance functions at the specified frequencies. This was accomplished using CLASSI program CLAN. Figure 3.3 shows the model of the coupled vessel/vault foundation geometry including its discretization into a number of rectangular subregions. The force/displacement relationships between each pair of subregions were calculated by integration of the Green's functions over the subregion areas. The impedance functions were calculated by applying the constraints of rigid body motion between all subregions of each foundation to obtain a  $12 \times 12$  complex-valued impedance matrix at each specified frequency. The impedance matrices give the total steady state dynamic force/displacement relationship,

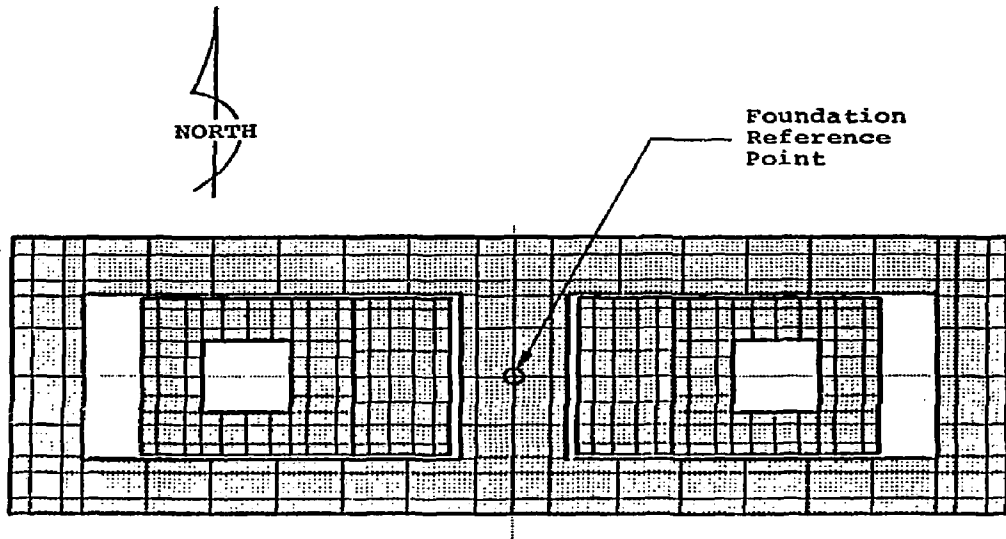


Fig. 3.3 Vessel and Vault Foundations Showing Discretization Used for Calculating Impedances for Coupled Vessel/Vault SSI Analyses.

including phase information, of the rigid massless foundations on the soil deposit. Figure 3.3 shows that the vault foundation and the vessel foundation slabs are very close to each other along the north and south vault walls. Therefore we could expect to see strong coupling between the foundation, and in fact the coupling terms of the 12 x 12 impedance matrix (not shown) are large. It should be noted however, that this coupling is only through the soil; no direct contact between foundations is assumed.

### 3.3 STRUCTURAL MODELS

#### 3.3.1 Vessel Models

The structural model of the vessel used in our analysis was taken from the dynamic model of the Axicell vessel configuration developed by LLNL. This model is shown in Fig. 3.4. The model assumes the vessel is symmetric about the north-south plane at its center and was constructed as two half-models, one having symmetric and the other antisymmetric boundary conditions at the plane of symmetry. The assumption of symmetry of the vessel results in a decoupling of modal response into either purely symmetric or purely antisymmetric motion and thus allows the use of the two half-models.

The support configuration used in the LLNL Axicell model differs from that used in the previous A-cell model in that it includes rotational springs at the bases of the beam elements modeling the end cell piers and center cell columns and knees which rest on the foundation mats. In the A-cell model, these elements were fixed rigidly to the base. The purpose of the rotational springs was to represent the flexibility of the foundation mats and the soil beneath them. Spring constants were calculated based on simple beam-on-elastic-foundation methods.

The LLNL eigenvalue extraction analyses calculated 75 modes (up to 33.0 Hz.) for the symmetric model and 75 modes (up to 33.2 Hz.) for the antisymmetric model. Of these, the 38 modes having the greatest participation in each direction were used for the response spectrum analysis in that direction — that is, a different set of 38 modes was used in each direction. These modes accounted for 86.6% of the total mass of the vessel in

the transverse direction, 88.1% in the longitudinal direction and 55.9% in the vertical direction. Table 3.1 summarizes the most significant modes occurring in both half-models. The table includes all modes from either model having at least one percent participation.

The model used for our analyses was adapted from the LLNL model. The difference between the two models was in the way in which the foundation springs were applied. For our CLASSI analyses, the gross effects of soil flexibility were modeled using impedance functions which assumed that the array of foundation mats moved as a single rigid body. We modeled local foundation and soil flexibility effects (rocking) in a way similar to that used by LLNL. For the end cell piers, we added to the LLNL model elements connecting the pier bases, which represented the foundation slab. We used fully cracked concrete section properties to model the stiffness of these elements. We also included rocking springs, similar to LLNL, which modeled the local rocking flexibility of the soil directly beneath each pier. The spring stiffnesses we used were obtained using commonly accepted soil spring formulas for square footings (Ref. 6). As a result of the above modeling technique, our stiffness at the bases of the piers was about forty percent higher than that used by LLNL. Additionally the coupling between pier bases due to our basemat elements increased the effective stiffness significantly. At the bases of the columns and knees beneath the center cell, we modeled the rocking flexibility by adding to the model plate elements representing the four foot thick basemat.

After the above modifications were made and verified, our work on the structural model of the vessel consisted of performing eigenvalue extraction analyses, manipulating the resulting data to put it into a form that can be read by the CLASSI response calculation program, SSIN, and collating the data from the two half-models into a single data set representing the full dynamic characteristics of the total structure. The fully automated procedure consisted of the following steps:

- Perform the modal extraction analyses and obtain modal frequencies, mode shapes and the mass matrix for each half-model. Reorganize these dynamic characteristics into a file

structure that can be read by subsequent programs.

- Use these dynamic characteristics to calculate for each half-model, modal participation factors, the rigid-body mass matrix, and modal coordinates and rigid-body transformation vectors of specified responses. This data is calculated relative to a specified reference point at which the foundation impedances are calculated. Apply appropriate scaling factors to account for the mass of a full model.
- Merge the results of the separate half-model calculations to obtain data describing the dynamic properties of the total structure.

Table 3.2 gives a summary of the results of this process. Included in the table are the frequency and mass participation for each mode having at least one percent participation. Also, listed for each mode is an equivalent height in inches above the foundation base at which the participating mass acts.

It should be noted that the coordinate systems used for the CLASSI analyses and for the LLNL analyses are different. The LLNL calculations were made with an origin located at the plane of symmetry, on the centerline of the vessel (elev. +11 ft.). The origin for the CLASSI analyses (also called the foundation reference point) was located at the same point horizontally, but at an elevation of -25 ft., at the bottom of the foundation slabs. Additionally, because CLASSI requires that the Z-axis be vertical, the coordinate system used by LLNL had to be transformed by rotation of the axes. The correspondence between the LLNL system and the CLASSI system are tabulated below:

<u>Direction</u>	<u>LLNL</u>	<u>CLASSI</u>
Longitudinal (E-W)	Z	X
Transverse (N-S)	X	Y
Vertical	Y	Z

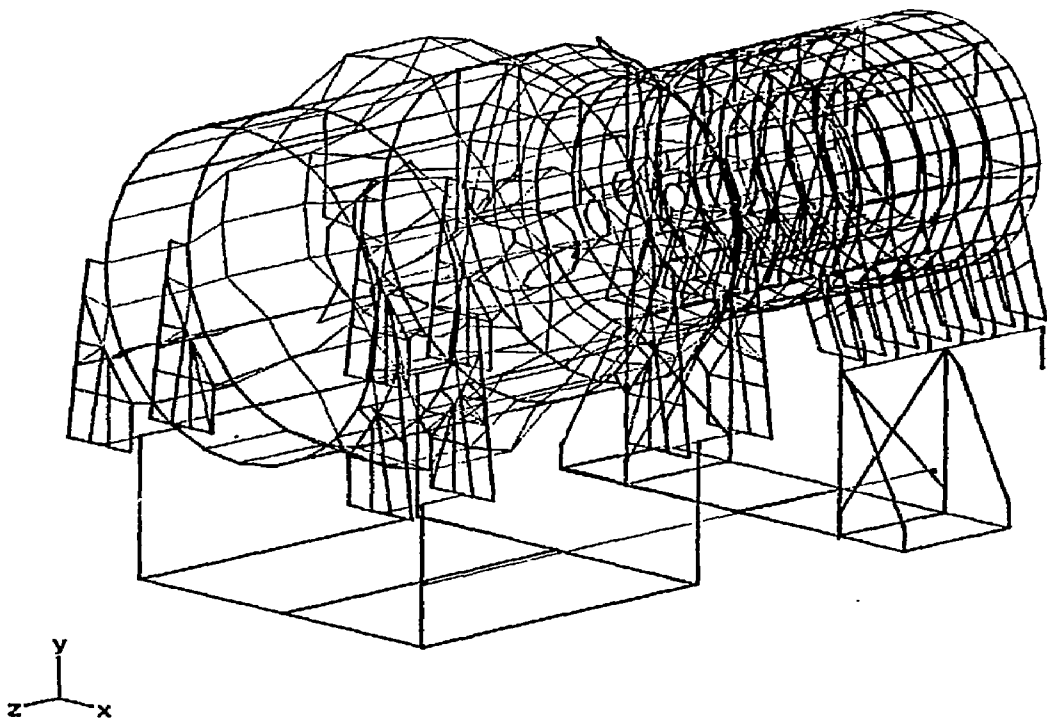


Fig. 3.4 Isometric View of the Structural Half-Model of the Axicell Vessel Configuration.

TABLE 3.1: SIGNIFICANT MODES FOR LNL AXICELL VESSEL MODEL

MODE	FREQUENCY (HZ)	LONGITUDINAL MPF(%)	TRANSVERSE MPF(%)	VERTICAL MPF(%)
2	3.04	.00	68.23	.09
3	4.37	75.99	.00	.00
4	5.15	.00	7.20	.34
6	6.10	.00	.95	1.00
7	6.35	.00	.00	17.91
17	8.29	.00	.03	3.50
20	9.57	.00	.06	3.73
24	10.63	.00	.48	1.40
28	11.30	.00	.04	1.40
42	13.74	.00	3.06	.48
53	15.62	.00	.33	2.33
61	17.03	.00	.08	2.46
73	18.45	.00	.00	1.08
87	19.85	.00	.01	1.74
97	21.20	5.44	.00	.00
106	23.46	.00	.01	1.22
109	24.61	.00	.00	1.13
117	27.55	.00	.01	2.32

TABLE 3.2: SIGNIFICANT MODES FOR SMA AXICELL VESSEL MODEL

MODE	FREQUENCY (HZ)	DAMPING	LONGITUDINAL		TRANSVERSE		VERTICAL		TORSIONAL	
			MPF	HT	MPF	HT	MPF	HT	MPF	HT
1	3.33	.054	.00	.0	63.30	340.3	.16	.00	.00	.00
2	3.36	.056	.35	52.1	.00	.0	.00	.00	59.18	.00
3	3.93	.045	75.35	381.2	.00	.0	.00	.00	.22	.00
4	5.28	.071	.00	.0	8.76	125.6	.37	.00	.00	.00
5	5.98	.045	.08	140.2	.00	.0	.00	.00	9.96	.00
6	6.35	.036	.00	.0	.30	20.7	10.97	.00	.00	.00
8	6.45	.043	.00	.0	1.45	53.1	8.42	.00	.00	.00
12	7.35	.038	.00	.0	1.12	67.4	.01	.03	.00	.00
17	8.29	.036	.00	.0	.08	19.3	3.19	.00	.00	.00
20	9.63	.025	.00	.0	.06	15.2	3.80	.00	.00	.00
24	10.63	.033	.00	.0	.50	37.3	1.43	.00	.00	.00
28	11.32	.036	.00	.0	.05	11.9	1.28	.00	.00	.00
37	12.92	.034	.09	.0	.06	6.8	1.08	.00	.00	.00
46	14.23	.041	.00	.0	3.67	7.0	.57	.00	.00	.00
47	14.47	.040	.02	72.1	.00	.0	.00	.00	4.28	.00
48	14.79	.039	.00	.0	.65	13.0	1.54	.00	.00	.00
53	15.43	.039	.00	.0	.45	15.3	1.66	.00	.00	.00
69	17.66	.037	.00	.0	.06	11.3	1.53	.00	.00	.00
73	18.46	.037	.00	.0	1.09	9.1	.82	.00	.00	.00
74	18.60	.039	.07	18.6	.00	.0	.00	.00	1.72	.00
90	20.64	.049	.00	.0	.00	3.6	2.00	.00	.00	.00
95	21.80	.045	1.87	69.2	.00	.0	.00	.00	.02	.00
103	23.71	.037	.00	.0	.06	10.0	2.21	.00	.00	.00
111	27.70	.033	.00	.0	.01	.0	2.78	.00	.00	.00

### 3.3.2 Vault Model

The structural model of the vault used for the coupled vault/vessel SSI analyses was the fixed-base finite element model used for our previous vault seismic analyses (Ref. 2). Figure 3.5 shows an isometric view of the finite element mesh. The model was based on the EASE2 model developed by Foster Engineering, Inc. (FEI) for their vault seismic design calculations.

Reference 2 examined in detail the SSI response of the vault for a number of structure and foundation behavioral assumptions. SSI analysis of the final configuration of the vault assumed no hinge at the blockwall-retaining wall interface and a flexible foundation. This configuration is the one that was used for the coupled SSI analyses reported herein.

The dynamic data for the vault model contains 115 modes of vibration and included frequencies in excess of 50 Hz. These modes accounted for 74.5% of the total mass in the longitudinal direction, 78.5% in the transverse direction and 69.3% in the vertical direction. The frequencies and percent mass participation of the significant modes are summarized in Table 3.3. For all modes we used 5% damping in the SSI analyses.

The system of physical units to define the vault model was kip-ft-sec. Because this was not compatible with the system in which the vessel model was defined (lb-in-sec), the vault model data was converted to the vessel system by applying appropriate scale factors to the mass matrix, mode shapes, node point coordinates and modal coordinates used to compute acceleration response in the structure.

### 3.3.3 Composite Modal Damping

Preliminary estimates of stress levels, as well as the variety of materials and construction methods used in the vessel indicated that different portions of the vessel could be expected to exhibit different damping behavior. Specifically for the CLASSI SSI analyses of the vessel we made the following assumptions for damping:

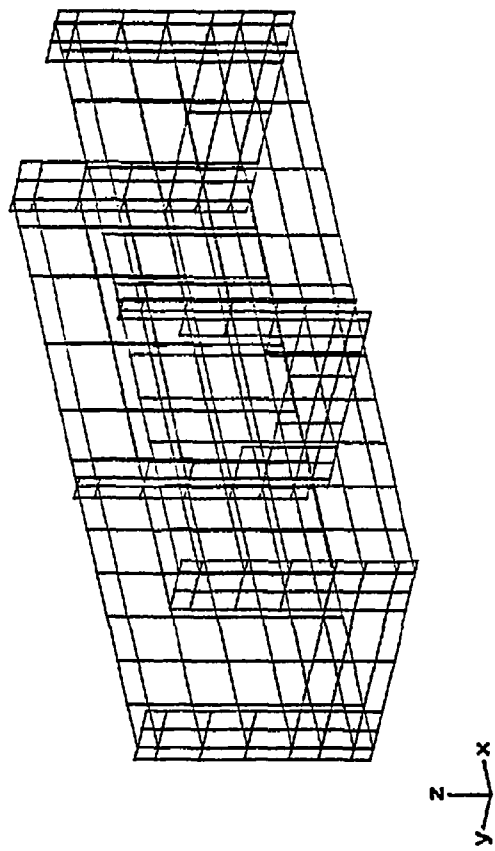


Fig. 3.5 Isometric View of the Structural Model of the Vault.

TABLE 3.3: SIGNIFICANT MODES FOR VAULT MODEL

MODE	FREQUENCY MODAL DAMPING (HZ)	LONGITUDINAL		TRANSVERSE		VERTICAL		TORSIONAL	
		MPF (%)	HT (IN)	MPF (%)	HT (IN)	MPF (%)	HT (%)	MPF (%)	HT (%)
2	2.02	.050	.00	.0	22.11	255.5	.00	8.50	
4	3.23	.050	.00	.0	17.20	219.1	.00	13.10	
5	4.21	.050	.00	.0	4.47	110.9	.00	.24	
7	5.15	.050	.00	.0	.27	34.0	.00	6.21	
9	5.42	.050	.00	.0	3.50	18.5	.00	.56	
13	5.57	.050	.00	.0	1.93	23.7	.00	3.07	
15	5.88	.050	.00	.0	.87	43.8	.00	1.85	
17	6.19	.050	.00	.0	.36	34.2	.00	5.43	
18	6.19	.050	1.48	66.5	.00	.0	.00	.00	
19	6.93	.050	2.90	87.5	.00	.0	.00	.00	
20	6.97	.050	.00	.0	3.01	100.5	.00	.32	
21	7.57	.050	15.26	206.4	.00	.0	.00	.00	
22	7.62	.050	.00	.0	.94	59.5	.00	1.04	
23	9.24	.050	3.47	110.1	.00	.0	.00	.00	
24	9.26	.050	.00	.0	.01	8.6	.00	4.95	
25	10.10	.050	18.01	237.7	.00	.0	.00	.00	
26	10.17	.050	.00	.0	.01	1.3	.00	5.44	
29	13.70	.050	1.61	72.3	.00	.0	.00	.00	
30	13.71	.050	.00	.0	1.36	19.9	.00	.07	
32	14.19	.050	.00	.0	.51	6.7	.00	1.55	
33	15.15	.050	.00	.0	7.03	5.0	.00	1.93	
37	15.91	.050	2.99	73.0	.00	.0	.00	.00	
43	17.03	.050	8.51	108.0	.00	.0	.00	.00	
44	17.03	.050	.00	.0	.00	2.6	.00	1.55	
45	17.62	.050	6.53	83.6	.00	.0	.01	.00	
47	19.25	.050	.00	.0	.64	9.7	.00	1.56	
57	27.05	.050	.00	.0	4.70	6.5	.00	.39	
59	27.53	.050	.00	.0	.14	34.7	.00	5.52	
61	29.80	.050	1.33	90.5	.00	.0	.02	.00	
65	30.08	.050	.00	.0	1.76	22.5	.00	.92	
69	31.03	.050	.03	301.4	.00	.0	23.98	.00	
70	31.67	.050	.02	323.1	.00	.0	3.79	.00	
74	32.46	.050	.11	194.3	.00	.0	31.56	.00	
75	33.42	.050	.00	.0	.12	27.4	.00	2.45	
78	34.37	.050	.00	351.6	.00	.0	3.97	.00	
79	35.49	.050	3.27	15.7	.00	.0	.26	.00	
90	39.57	.050	.42	168.5	.00	.0	1.24	.00	
92	39.62	.050	.00	.0	1.42	1.2	.00	1.23	
112	52.68	.050	.00	6.4	1.13	9.5	.00	.33	
115	53.95	.050	1.30	39.0	.06	5.1	.00	.05	

#### 4. DISCUSSION OF ANALYSES AND RESULTS

We performed three dynamic response analyses of the Axicell vessel. The first was a response spectrum analysis using the computer program RESPAN and the MFTF design spectra, at 5% damping, which were used by LLNL for their analyses. The purpose of this was to benchmark the differences between the LLNL and SMA versions of the vessel model. This is discussed in Section 4.1.1.

The second analysis was a fixed-base analysis, using the CLASSI program SSIN, in which the free-field ground surface motions were applied directly to the base of the structure and rotations at the base (rocking and torsion) were restrained. All modes contained 5% damping. The results from the fixed-base analysis were compared with those from the LLNL response spectrum analysis to benchmark the cumulative differences between models and analysis methods. This is discussed in Section 4.1.2.

The third analysis performed was an SSI analysis of the vessel and vault, coupled together through the soil and excited by the same free-field motions. Composite modal damping was used for the vessel. This represents our best estimate of the actual behavior of the vessel during a 0.25g earthquake. The results of the coupled SSI analysis were compared first with those from the vessel fixed-base CLASSI analysis to study the effect of SSI and the vault on the response of the vessel; second, they were compared with those from the LLNL fixed-base response spectrum analyses as an aid in checking them against design capacities of various structural elements in the vessel and on its foundation.

We reanalyzed the coupled SSI case to study what effect an increase in damping used for the vessel had on our results. For this case, we assumed that a constant 10% damping ratio occurs for all vessel modes. We compared these results with those from our coupled SSI analysis with composite modal damping. A discussion of the coupled SSI analyses we performed and the comparisons we made is found in Section 4.2.

In all CLASSI analyses, we corrected the dynamic force response

results for the effects of truncated modes or "missing mass." These corrections were made in the form of time histories which were added to the dynamic response time histories resulting from the CLASSI analyses. The correction procedure is discussed in detail in Sec. 2.2.

For both the fixed-base analysis and the SSI analyses, we obtained in-structure response on the vessel at a number of locations specified by LLNL. For our analyses, each LLNL response consists of a pair of responses, one in the modeled (east) half of the vessel and the other in the reflected (west) half. The responses we obtained include the following:

- Maximum foundation forces at eight locations where the vessel supports are connected to the reinforced concrete foundation mats and resultant forces under each of the mats.
- Maximum forces at eight locations where vessel support legs are connected to the end cell piers.
- Maximum hanger forces in 66 hangers connecting the magnets to the vessel and to each other.
- Maximum accelerations and response spectra at 40 locations on the vessel and 16 locations on the vault for the coupled SSI analyses. (Appendix A)
- Maximum relative displacements between 6 locations on the vessel, 15 locations on the vault and between the reference locations on the vessel and vault from which the other relative displacements were calculated. Relative displacements were obtained from the coupled SSI analysis only. (Appendix A)

For the SSI analyses we additionally computed maximum accelerations and response spectra of the vessel foundation at the foundation reference point. Results were obtained for all six degrees-of-freedom of the rigid foundation assembly.

The following subsections discuss the results of our analyses and the comparisons made. Section 4.1 discusses the SMA response spectrum and fixed-base CLASSI results and compares them with the response spectrum analysis results obtained by LLNL. Section 4.2 discusses our coupled vessel/vault SSI analyses. These provided us with our best estimates of vessel response. Section 4.2.1 provides a study of the combined effects of SSI and of interaction with the vault by comparing the fixed-base and coupled

vessel/vault CLASSI analyses. Section 4.2.2 discusses our final analyses of the coupled vessel/vault system over a range of soil properties and compares their envelope with the response spectrum analysis results obtained by LLNL for use in design. Section 4.2.3 discusses the effects of increasing damping in the vessel to 10% for all modes.

Before continuing with the discussion of results, a note should be made regarding the terminology used in the subsequent subsections. Because of the differences in the coordinate systems used by LLNL and CLASSI, directions will be referred to as longitudinal (east-west), transverse (north-south) and vertical. For direct forces the use of these terms is clear. For bending moments the following terminology will be adopted. "Longitudinal Bending Moment" means bending in the vertical plane oriented in the longitudinal direction (i.e. bending about the transverse axis). "Transverse Bending Moment" means bending in the vertical plane oriented in the transverse direction (i.e. bending about the longitudinal axis).

The discussions in the remainder of this section are limited to various comparisons of maximum forces. For a summary of maximum accelerations, response spectra and relative displacements the reader is referred to Appendix A.

#### 4.1 BENCHMARKING SMA AND LLNL MODELS AND ANALYTICAL METHODS

##### 4.1.1 Effects of Model Differences

In order to obtain a benchmark between our CLASSI results and the LLNL response spectrum results, we performed two dynamic analyses. The first was a set of response spectrum analyses, using program RESPAN. We performed separate response spectrum analyses for longitudinal, transverse and vertical earthquake components using the MFTF design response spectra for 5% damping. For each direction we used the 38 highest participating modes from the appropriate half-model. To be consistent with the LLNL analysis, we factored the design spectra by a factor of 0.75 reflecting a predicted general reduction due to SSI. Modal responses were combined by the SRSS method, as were the responses to the individual earthquake components. We compared our

results with the LLNL RESPAN results to isolate differences in response caused by the differences in modeling techniques between the two models, in particular the modeling of local rocking foundation flexibility beneath piers and support columns and knees. Tables 4.1A to 4.1C summarize our comparisons for vessel foundation forces, forces in the end cell support legs and magnet hanger and strut forces.

Differences in modeling techniques had a significant effect on moments in the piers supporting the end cells (Table 4.1A). Bending moments in the longitudinal direction (i.e. about the transverse axis) from our analysis were about twice the LLNL moments. Our transverse bending moments (about the longitudinal axis) were 15% to 20% higher. Longitudinal shear forces were about 20% higher, but transverse shear forces did not differ. Vertical (axial) forces in the piers were reduced by about 20%. Forces at the bases of the support columns in the center cell were generally reduced by about 20% for all significant components except axial forces which were reduced to about 40% of the LLNL values.

Forces in the vessel support legs connected to the end cell piers (Table 4.1B) generally increased. Longitudinal shear forces and bending moments increased by about 35%. Transverse shear forces increased by about 5% while transverse bending moments increased by about 20%. As was the case with the piers, axial (vertical) forces decreased by about 20%.

Hanger and strut forces (Table 4.1C) from our analyses varied overall less than 5% from the LLNL values with a maximum difference of 18%.

The significant increases (factors of 2) in the longitudinal bending moments in the end cell piers are a direct result of the increased rotational stiffness beneath them. This increase is not nearly as apparent in the transverse moments (15% increases) possibly because of differences in the relative stiffnesses between the end cell and center cell support systems in the two directions. It also should be noted that the most significant moments in the piers are in the transverse direction, the largest transverse moment being nearly three times the largest longitudinal moment in our analysis. Consequently, resultant bending moments were increased by only about 20%.

TABLE 4.1A: COMPARISON BETWEEN SMA AND LLNL RESPAW ANALYSIS RESULTS  
SUMMARY OF FOUNDATION FORCES

PAGE 2

ELEM	COMPONENT	GLOBAL-X				GLOBAL-Y				GLOBAL-Z				VECTOR SUM		
		SMA	LLNL	SMA	LLNL	SMA	LLNL	SMA	LLNL	SMA	LLNL	SMA	LLNL	SMA	LLNL	SMA
388	AXIAL FORCE (1)	207	283	.731	.25	19	1.332	203	553	.367	.291	622	.468			
	LONG SHR (2)	15	21	.737	3	2	1.210	224	274	.810	.225	275	.817			
	TRANS SHR (3)	11	11	.981	3	2	1.220	4	4	1.043	12	12	.998			
	TORSN MNT (4)	306	412	.743	29	27	1.070	95	74	1.201	322	420	.767			
	TRANS MNT (5)	4020	5140	.782	350	261	1.341	427	369	1.157	4058	5160	.786			
	LONG MNT (6)	50	80	.620	16	13	1.183	1510	1750	.863	1511	1752	.862			
	TRANS MNT (11)	3730	4840	.771	327	269	1.216	329	463	.711	3759	4970	.772			
	LONG MNT (12)	393	517	.760	65	72	1.194	8010	9690	.027	8020	9704	.026			
389	AXIAL FORCE (1)	184	248	.739	22	18	1.229	184	550	.335	261	604	.432			
	LONG SHR (2)	15	19	.786	3	2	1.526	219	273	.802	220	274	.802			
	TRANS SHR (3)	1	1	1.057	2	1	1.333	3	5	.518	3	5	.631			
	TORSN MNT (4)	343	455	.754	37	28	1.305	112	83	1.354	363	463	.783			
	TRANS MNT (5)	3960	5070	.781	359	282	1.309	62	454	1.414	4029	5098	.790			
	LONG MNT (6)	34	73	.469	20	18	1.913	1480	1750	.846	1481	1752	.845			
	TRANS MNT (11)	3940	5070	.777	301	274	1.391	575	589	.976	4000	5111	.783			
	LONG MNT (12)	411	489	.840	94	57	1.655	780	9670	.811	7851	9663	.811			
390	AXIAL FORCE (1)	.177	232	.763	30	24	1.269	75	421	.177	194	481	.404			
	LONG SHR (2)	19	23	.810	3	2	1.448	214	248	.863	215	249	.863			
	TRANS SHR (3)	5	4	1.155	4	3	1.134	10	6	1.074	12	8	1.561			
	TORSN MNT (4)	294	344	.855	30	23	1.280	22	72	.310	296	352	.812			
	TRANS MNT (5)	4060	4870	.834	413	310	1.332	268	424	.632	4090	4898	.835			
	LONG MNT (6)	26	10	2.462	6	6	.894	2170	1660	1.307	2170	1660	1.307			
	TRANS MNT (11)	4030	4860	.829	426	350	1.217	563	503	.966	4091	4907	.834			
	LONG MNT (12)	571	664	.860	61	51	1.566	6380	8040	.948	8400	8865	.948			
391	AXIAL FORCE (1)	169	220	.768	28	20	1.431	73	421	.174	186	475	.392			
	LONG SHR (2)	17	21	.805	2	2	1.320	211	247	.854	212	248	.854			
	TRANS SHR (3)	11	12	.934	4	3	1.367	11	6	1.779	16	14	1.155			
	TORSN MNT (4)	339	379	.892	38	23	1.661	37	80	.466	342	388	.802			
	TRANS MNT (5)	4330	5070	.854	488	334	1.461	372	462	.805	4373	5102	.857			
	LONG MNT (6)	20	15	1.305	9	5	1.688	2140	1560	1.289	2140	1660	1.209			
	TRANS MNT (11)	4650	5420	.858	568	376	1.505	674	633	1.065	4733	5170	.865			
	LONG MNT (12)	495	583	.849	64	48	1.335	6250	8830	.934	6265	8849	.934			
400	AXIAL FORCE (1)	21	20	1.030	50	41	1.231	371	394	.942	375	397	.945			
	LONG SHR (2)	3	2	1.660	2	1	1.901	875	1050	.033	875	1050	.033			
	TRANS SHR (3)	423	555	.762	39	31	1.248	14	13	1.336	425	556	.764			
	TORSN MNT (4)	3500	3210	1.080	758	683	1.110	3450	2610	1.322	4973	4193	1.186			
	TRANS MNT (5)	149000	156000	.955	11800	9530	1.303	3160	2140	1.477	149500	156248	.957			
	LONG MNT (6)	128	824	.755	127	561	.226	73800	177000	.417	73800	177003	.417			
	TRANS MNT (11)	150000	157000	.955	11900	8680	1.307	3190	2150	1.484	150505	157249	.957			
	LONG MNT (12)	122	821	.149	123	560	.220	75500	179000	.422	75500	179003	.422			

TABLE 4.1A: CONT.

245	AXIAL FORCE (1)	43	39	1.113	81	96	.839	109	139	.704	142	173	.821
	LONG SHR (2)	17	25	.689	15	15	1.041	210	160	1.312	211	163	1.299
	TRANS SHR (3)	230	228	1.009	51	25	2.055	27	17	1.630	237	230	1.031
	TORSN MNT (4)	4310	2840	1.518	1540	1558	.994	8820	7840	1.125	9937	8161	1.172
	TRANS MNT (5)	81700	71600	1.141	13100	4190	3.126	0310	3060	2.153	81160	71826	1.158
	LONG MNT (6)	3300	2910	1.134	2240	842	2.660	28000	12000	2.460	29075	12377	2.349
	TRANS MNT (11)	86300	76100	1.134	10000	4090	3.423	8910	4160	2.125	87874	76323	1.151
	LONG MNT (12)	3640	3410	1.057	2490	1050	2.371	33000	15200	2.171	32293	15613	2.132
246	AXIAL FORCE (1)	39	36	1.078	85	89	.956	213	293	.842	233	271	.860
	LONG SHR (2)	11	13	.823	20	11	1.754	287	179	1.275	228	179	1.276
	TRANS SHR (3)	334	347	.963	46	16	3.025	52	33	1.573	342	349	.979
	TORSN MNT (4)	4950	2760	1.793	1450	2200	.659	6890	7860	1.131	10278	8616	1.193
	TRANS MNT (5)	69700	61300	1.137	13200	6300	2.095	7800	3120	2.281	71366	61718	1.156
	LONG MNT (6)	4390	3370	1.303	2490	1010	2.416	27700	11300	2.451	20152	11835	2.379
	TRANS MNT (11)	76400	68300	1.119	14000	6350	2.205	8770	3820	2.296	78160	68701	1.130
	LONG MNT (12)	4450	3550	1.254	2600	1150	2.435	32200	14900	2.161	32626	15350	2.124
247	AXIAL FORCE (1)	420	537	.782	72	76	.955	110	33	3.323	440	543	.810
	LONG SHR (2)	17	24	.728	14	9	1.544	210	159	1.321	211	161	1.312
	TRANS SHR (3)	260	254	1.024	18	11	1.575	17	12	1.410	261	255	1.026
	TORSN MNT (4)	7210	6890	1.830	1610	1220	1.344	6180	6120	.963	9637	10873	.806
	TRANS MNT (5)	69800	57000	1.194	3000	1050	2.103	4870	2270	2.145	69281	57874	1.197
	LONG MNT (6)	2980	2770	1.076	2200	842	2.708	27200	11300	2.497	27459	11655	2.354
	TRANS MNT (11)	74100	62600	1.100	4100	1850	2.259	5110	2480	2.060	74394	62076	1.163
	LONG MNT (12)	3300	3220	1.025	2500	849	2.634	31400	14500	2.166	31672	14884	2.128
248	AXIAL FORCE (1)	329	425	.774	96	91	1.053	93	61	1.522	355	439	.809
	LONG SHR (2)	12	13	.865	17	12	1.487	212	165	1.285	213	166	1.294
	TRANS SHR (3)	284	286	.993	20	12	1.681	31	16	1.563	286	287	.999
	TORSN MNT (4)	1360	2950	.461	1770	1990	.089	6540	6100	1.022	6910	7323	.944
	TRANS MNT (5)	57100	47800	1.195	4260	2190	1.945	3800	2130	1.784	57385	47898	1.198
	LONG MNT (6)	5470	4180	1.309	2420	782	3.095	26300	11000	2.397	26972	11793	2.287
	TRANS MNT (11)	62700	53600	1.170	4580	2230	2.054	4340	2110	1.801	63017	53701	1.173
	LONG MNT (12)	5590	4390	1.273	2720	916	2.969	30500	14200	2.148	31127	14891	2.090
305	AXIAL FORCE (1)	115	90	1.281	262	335	.782	519	314	1.653	593	468	1.267
	LONG SHR (2)	28	32	.861	26	21	1.203	859	661	1.300	660	682	1.299
	TRANS SHR (3)	1100	1110	.991	112	40	2.635	116	68	1.706	1112	1113	.999
	TORSN MNT (4)	44000	44500	.989	35300	16500	2.139	8840	10400	.850	57099	48587	1.175
	TRANS MNT (5)	463000	208000	2.226	38600	9550	4.042	44200	18500	2.309	466704	209039	2.233
	LONG MNT (6)	25100	34300	.732	19200	16400	1.171	156000	101000	1.545	159168	107919	1.475
	TRANS MNT (11)	459000	210000	2.186	36100	9560	3.985	43700	18700	2.337	462647	211048	2.192
	LONG MNT (12)	25000	3430	.727	19100	16400	1.165	153000	103000	1.485	158201	109024	1.482

UNITS: FORCES - KIPS  
MOMENTS - KIP-IN

TABLE 4.1B: COMPARISON BETWEEN SMA AND LLNL RCFSPAN ANALYSIS RESULTS  
SUMMARY OF VESSEL END CELL SUPPORT LEG FORCES

ELEM	COMPONENT	GLOBAL-X				GLOBAL-Y				GLOBAL-Z				VECTOR SUM		
		SMA	LLNL	SMA	LLNL	SMA	LLNL	SMA	LLNL	SMA	LLNL	SMA	LLNL	SMA	LLNL	SMA
253	AXIAL FORCE (1)	19	8	2.257	34	40	.853	85	109	.702	94	117	.805			
	LONG SHR (2)	1	1	.702	0	1	.051	9	6	1.371	9	6	1.363			
	TRANS SHR (3)	74	87	.853	27	10	2.685	37	39	.959	87	95	.911			
	TORSN MNT (4)	14	14	.986	4	6	.614	153	115	1.330	154	116	1.325			
	TRANS MNT (5)	10700	9430	1.135	4080	2680	1.522	4560	5260	.867	12356	11125	1.108			
	LONG MNT (6)	29	41	.701	20	24	1.162	510	395	1.387	550	398	1.381			
	TRANS MNT (11)	10000	9470	1.140	4090	2680	1.526	4500	5280	.867	12424	11169	1.112			
	LONG MNT (12)	29	41	.703	28	24	1.160	552	398	1.387	554	401	1.381			
259	AXIAL FORCE (1)	32	13	2.524	32	37	.870	60	86	.794	82	94	.867			
	LONG SHR (2)	0	0	.856	1	0	1.747	7	5	1.336	7	5	1.335			
	TRANS SHR (3)	117	137	.854	24	12	2.000	56	47	1.150	131	145	.902			
	TORSN MNT (4)	10	13	.773	3	3	1.147	70	56	1.236	70	58	1.210			
	TRANS MNT (5)	7550	6230	1.212	3650	3250	1.123	3900	3690	1.092	9283	7932	1.170			
	LONG MNT (6)	21	26	.815	31	15	2.060	457	339	1.349	459	340	1.347			
	TRANS MNT (11)	7610	6300	1.208	3660	3260	1.123	4010	3700	1.084	9348	8001	1.168			
	LONG MNT (12)	21	26	.820	31	15	2.059	460	341	1.349	462	342	1.348			
265	AXIAL FORCE (1)	26	38	.653	46	58	.800	108	247	.761	195	257	.761			
	LONG SHR (2)	15	22	.603	9	5	1.665	169	138	1.370	190	140	1.357			
	TRANS SHR (3)	134	112	1.196	19	23	.836	50	45	1.130	144	123	1.177			
	TORSN MNT (4)	81	151	.535	149	153	.974	3310	2530	1.308	3314	2539	1.305			
	TRANS MNT (5)	35300	26900	1.312	3710	4090	.907	6350	5500	1.155	36058	27760	1.299			
	LONG MNT (6)	913	1350	.676	624	369	1.691	12300	8910	1.380	12350	9019	1.369			
	TRANS MNT (11)	35300	27000	1.307	3710	4080	.908	6370	5520	1.154	36062	27859	1.294			
	LONG MNT (12)	920	1360	.676	628	371	1.693	12400	8980	1.381	12450	9090	1.370			
272	AXIAL FORCE (1)	45	34	1.320	53	54	.991	275	338	.814	284	344	.825			
	LONG SHR (2)	9	9	1.010	13	5	2.440	200	157	1.325	209	157	1.326			
	TRANS SHR (3)	199	181	1.098	19	23	.831	20	21	.971	201	104	1.094			
	TORSN MNT (4)	436	624	.699	214	252	.849	4730	3690	1.205	4755	3741	1.271			
	TRANS MNT (5)	10500	4150	2.554	3800	3670	1.035	6270	7810	.803	12889	9575	1.346			
	LONG MNT (6)	577	704	.820	858	352	2.438	13000	9680	1.343	13041	9712	1.343			
	TRANS MNT (11)	10700	4170	2.566	3800	3660	1.038	6280	7820	.803	12976	9568	1.353			
	LONG MNT (12)	581	708	.821	865	355	2.437	13100	9760	1.342	13141	9792	1.342			
280	AXIAL FORCE (1)	210	283	.742	42	45	.918	104	201	.517	238	350	.600			
	LONG SHR (2)	15	20	.730	6	4	2.111	191	139	1.374	192	141	1.365			
	TRANS SHR (3)	171	178	.961	14	8	1.897	15	20	.747	178	179	.961			
	TORSN MNT (4)	179	165	1.085	136	106	1.283	5980	4370	1.364	5964	4374	1.363			
	TRANS MNT (5)	26800	22300	1.202	2790	3280	.851	2280	3370	.677	27041	22791	1.187			
	LONG MNT (6)	1250	1700	.735	674	330	2.042	13900	9948	1.398	13972	10090	1.385			
	TRANS MNT (11)	26800	22400	1.196	2800	3290	.851	2280	3380	.675	27042	22891	1.181			
	LONG MNT (12)	1260	1710	.737	678	332	2.042	14000	10000	1.400	14073	10151	1.386			

1 TABLE 4.1B: CONT.

286	AXIAL FORCE (1)	129	184	.665	57	.998	123	229	.537	187	306	.613	
	LONG SHR (2)	8	9	.901	11	1.863	191	195	1.357	195	143	1.316	
	TRANS SHR (3)	138	150	.920	15	1.094	20	22	.907	140	152	.921	
	TRANS MNT (4)	163	183	1.110	212	2.363	6070	4530	1.300	6077	4535	1.300	
	TRANS MNT (5)	9260	5100	1.802	3720	4270	.071	1650	2800	.577	10115	7289	.392
	LONG MNT (6)	615	741	.870	807	542	1.667	10000	10200	1.313	10443	10241	1.371
	TRANS MNT (11)	9330	5210	1.791	3720	4270	.871	1660	2870	.576	10181	7322	1.390
	LONG MNT (12)	619	745	.871	892	535	1.657	14100	10300	1.369	14143	10341	1.368
292	AXIAL FORCE (1)	210	254	.927	32	1.095	215	177	1.215	302	311	.971	
	LONG SHR (2)	1	1	.893	0	1.731	?	5	1.395	7	5	1.399	
	TRANS SHR (3)	76	60	1.271	17	1.272	3	15	.222	78	63	1.237	
	TRANS MNT (4)	9	11	.797	3	1.3	636	50	1.257	51	41	1.220	
	TRANS MNT (5)	3710	4530	.819	1670	1130	1.478	3590	3510	1.014	5426	5859	.966
	LONG MNT (6)	32	39	.814	16	1.9	1.769	357	222	1.417	359	255	1.406
	TRANS MNT (11)	3700	4520	.827	1600	1130	1.487	3590	3510	1.014	5450	5851	.931
	LONG MNT (12)	32	40	.816	16	1.9	1.764	361	235	1.415	363	258	1.405
299	AXIAL FORCE (1)	201	231	.870	39	1.066	219	172	1.273	300	290	1.033	
	LONG SHR (2)	0	0	1.384	0	1.262	7	5	1.367	7	5	1.367	
	TRANS SHR (3)	129	114	1.132	21	20	1.010	11	10	1.069	131	116	1.129
	TRANS MNT (4)	4	7	.564	3	4	.896	53	1.245	54	43	1.232	
	TRANS MNT (5)	3530	2220	1.590	1780	1860	.977	3910	3800	1.009	5560	4912	1.148
	LONG MNT (6)	19	13	1.466	22	15	1.073	361	1.303	362	1.362	1.361	
	TRANS MNT (11)	3600	2170	1.659	1790	1810	.957	3900	3880	1.005	5601	4923	1.161
	LONG MNT (12)	19	13	1.459	22	15	1.067	365	263	1.389	366	264	1.388

UNITS: FORCES - KIPS  
MOMENTS - KIP-IN

TABLE 4.1C: COMPARISON BETWEEN SMA AND LLNL RESPON ANALYSIS RESULTS  
SUMMARY OF MAGNETIC HARRIER AND STRUT FORCES

ELEM	COMPONENT	GLOBAL-X				GLOBAL-Y				GLOBAL-Z				VECTOR SUM			
		SMA	LLNL	SMA	LLNL	SMA	LLNL	SMA	LLNL	SMA	LLNL	SMA	LLNL	SMA	LLNL	SMA	LLNL
313	AXIAL FORCE (1)	245	236	1.038	54	57	.919	25	19	1.298	252	244	1.035				
314	AXIAL FORCE (1)	232	223	1.010	59	36	1.659	32	53	1.058	212	228	1.061				
315	AXIAL FORCE (1)	270	266	1.015	162	195	.831	56	53	1.058	320	334	.957				
316	AXIAL FORCE (1)	530	530	.991	50	39	1.256	66	51	1.290	536	539	.995				
317	AXIAL FORCE (1)	449	445	1.009	59	47	1.263	263	278	.946	524	527	.994				
318	AXIAL FORCE (1)	441	430	1.026	119	78	1.534	347	345	1.005	574	577	1.030				
319	AXIAL FORCE (1)	33	26	1.165	60	61	.927	0	7	1.00	69	68	1.014				
320	AXIAL FORCE (1)	15	14	1.103	24	22	1.086	5	4	1.117	29	26	1.091				
321	AXIAL FORCE (1)	66	70	.913	21	22	.929	8	8	.830	70	74	.940				
322	AXIAL FORCE (1)	7	9	.760	18	17	1.061	6	9	.672	21	22	.955				
323	AXIAL FORCE (1)	4	5	.730	7	5	1.328	3	6	.611	9	10	.934				
324	AXIAL FORCE (1)	33	35	.916	14	14	1.007	4	5	.654	36	38	.953				
325	AXIAL FORCE (1)	331	32	.992	23	26	.895	33	36	.920	137	139	.985				
326	AXIAL FORCE (1)	32	32	1.009	23	25	.811	62	61	.978	76	79	.959				
327	AXIAL FORCE (1)	58	57	1.010	20	18	1.109	54	54	.985	82	81	1.008				
328	AXIAL FORCE (1)	103	102	1.010	20	12	1.661	67	66	1.008	122	122	1.017				
329	AXIAL FORCE (1)	8	6	1.186	18	20	.919	16	17	.953	26	27	.949				
330	AXIAL FORCE (1)	20	22	.940	10	9	1.031	22	22	1.009	32	32	.980				
331	AXIAL FORCE (1)	48	49	.981	23	22	1.036	15	18	.929	55	56	.977				
332	AXIAL FORCE (1)	31	29	1.031	36	31	1.055	27	26	1.050	55	51	1.069				
333	AXIAL FORCE (1)	6	6	1.031	9	9	1.032	3	3	.932	11	12	.923				
334	AXIAL FORCE (1)	6	6	1.019	15	15	1.027	4	5	.677	17	17	.937				
335	AXIAL FORCE (1)	30	33	.987	15	14	1.065	4	6	.733	34	34	.944				
336	AXIAL FORCE (1)	6	6	1.082	7	9	.781	2	4	.571	10	12	.853				
337	AXIAL FORCE (1)	6	5	1.158	11	12	.927	4	5	.761	13	14	.936				
338	AXIAL FORCE (1)	32	32	.987	13	14	.970	4	4	.919	34	35	.984				
339	AXIAL FORCE (1)	7	7	1.039	12	13	.968	4	5	.710	15	15	.967				
340	AXIAL FORCE (1)	58	61	1.150	12	13	.961	4	5	.703	15	15	.969				
341	AXIAL FORCE (1)	55	55	1.060	32	22	1.195	7	5	1.369	67	59	1.130				
342	AXIAL FORCE (1)	13	14	.868	16	15	1.039	45	45	1.000	50	50	.993				
343	AXIAL FORCE (1)	18	22	.847	10	12	1.039	4	4	1.028	49	50	.989				
344	AXIAL FORCE (1)	13	13	.992	16	16	1.006	40	39	1.008	45	44	1.006				
345	AXIAL FORCE (1)	27	27	1.147	26	19	1.325	47	41	1.143	63	53	1.176				
346	AXIAL FORCE (1)	6	5	1.078	6	6	.905	1	3	.537	8	9	.948				
347	AXIAL FORCE (1)	5	4	1.280	6	6	.967	2	3	.538	8	8	1.081				
348	AXIAL FORCE (1)	16	16	1.000	8	7	1.243	1	1	.928	18	17	1.010				
349	AXIAL FORCE (1)	9	10	.882	13	13	.985	2	3	.676	16	16	.938				
350	AXIAL FORCE (1)	6	6	.991	13	13	1.000	3	4	.750	14	15	.983				
351	AXIAL FORCE (1)	33	32	1.038	19	17	1.123	5	6	.833	38	37	1.045				
352	AXIAL FORCE (1)	7	7	1.030	12	12	.975	1	1	.907	14	14	.967				
353	AXIAL FORCE (1)	4	4	.986	12	12	1.043	1	1	.929	13	14	.915				
354	AXIAL FORCE (1)	40	39	1.039	25	23	1.095	6	6	.697	16	16	1.044				
355	AXIAL FORCE (1)	6	7	.787	7	7	.986	25	24	1.038	26	26	1.010				
356	AXIAL FORCE (1)	6	7	.949	6	6	.576	25	24	1.042	26	25	1.032				
357	AXIAL FORCE (1)	6	7	.926	8	7	1.083	24	23	1.066	26	25	1.050				
358	AXIAL FORCE (1)	11	9	1.178	11	10	1.040	25	23	1.061	27	27	1.073				
359	AXIAL FORCE (1)	2	3	.855	2	2	.955	0	0	.939	9	9	1.015				
360	AXIAL FORCE (1)	2	2	1.074	3	3	.922	9	9	1.017	10	10	1.012				
361	AXIAL FORCE (1)	5	4	1.100	4	3	1.325	9	8	1.114	11	11	1.143				
362	AXIAL FORCE (1)	2	2	1.005	3	3	.934	10	10	1.010	11	11	1.005				
363	AXIAL FORCE (1)	14	17	.855	8	10	.899	35	34	1.026	39	39	.990				

TABLE 4.1C: CONT.

364	AXIAL FORCE (1)	11	10	1.048	13	13	1.016	31	31	1.006	35	35	1.011
365	AXIAL FORCE (1)	27	24	1.143	22	16	1.392	37	32	1.145	51	43	1.181
366	AXIAL FORCE (1)	10	11	.920	13	13	1.039	36	36	.997	39	40	.996
367	AXIAL FORCE (1)	2	3	.655	4	4	.959	10	10	1.036	11	11	.019
368	AXIAL FORCE (1)	8	8	1.020	5	4	1.134	9	10	.969	13	13	1.004
369	AXIAL FORCE (1)	2	2	.936	4	4	.912	9	8	1.051	10	9	1.028
370	AXIAL FORCE (1)	6	6	1.077	4	3	1.274	11	10	1.101	14	12	1.110
371	AXIAL FORCE (1)	1	1	.942	1	2	.919	4	4	1.035	5	5	1.015
372	AXIAL FORCE (1)	1	1	.945	1	2	.895	4	4	1.047	5	5	1.027
373	AXIAL FORCE (1)	1	1	1.032	2	2	1.000	4	4	1.065	5	5	1.054
374	AXIAL FORCE (1)	1	1	1.100	2	2	.933	4	4	1.060	5	5	1.042
375	AXIAL FORCE (1)	4	6	.739	6	6	.966	13	13	1.023	15	15	.979
376	AXIAL FORCE (1)	5	5	.912	5	5	.917	13	13	1.039	15	15	1.009
377	AXIAL FORCE (1)	5	6	.829	6	6	1.042	13	12	1.067	15	15	1.029
378	AXIAL FORCE (1)	8	7	1.173	8	8	1.022	13	12	1.073	10	16	1.077

UNITS: FORCE - KIPS

#### 4.1.2 Total Effect of Modeling and Analytical Method

The second dynamic analysis we performed was a CLASSI fixed-base analysis. For this analysis, we used the free-field time histories, described in Section 3.1, applied directly to the base of the model. Global foundation rotations were restrained; only the local rocking which was included in the structural model was included. We assumed a uniform 5% damping throughout the vessel, to be consistent with the LLNL analysis. We compared the CLASSI fixed-base results with the LLNL results to benchmark the differences in response caused by the cumulative effects of differences in the models, in the analytical methods and in the definitions of the input motions. Again, to be consistent with the LLNL results, we applied a factor of 0.75 to our fixed-base results.

Tables 4.2A through 4.2C show our comparison between the CLASSI fixed-base analysis and the LLNL analysis. The CLASSI values shown in these tables have been scaled by a factor of 0.75 to be consistent with the LLNL results which were calculated based on a reduced design response spectrum that was used for input. Also note that two CLASSI values are given for each force component listed. These values are for corresponding locations on either side of the plane of symmetry. They are different because of earthquake component phase information that is retained in the CLASSI analysis but not in a response spectrum analysis. For our comparison we took the averages of the CLASSI pairs of results and divided them by the LLNL results.

Our comparison resulted in ratios that were generally slightly higher than the ratios obtained from the RESPAN comparisons previously discussed. In the end cell piers (Table 4.2A), forces and moments increased by about 10%. Moments in the center cell columns increased by about 20% to values about equal to LLNL values. Forces in the vessel end cell support legs (Table 4.2B) increased by about 5%. Magnet hanger and strut forces (Table 4.2C) generally decreased slightly.

In general the differences between the fixed-base analysis and the SMA response spectrum analysis were fairly uniform and within the range of differences one would expect from comparisons between the CLASSI Fourier

TABLE 4.2A: COMPARISON BETWEEN CLASSI FIXED BASE AND LLNL RESPAN ANALYSIS  
SUMMARY OF FOUNDATION FORCES

ELMT	COMPONENT	(1) LLNL RESPAN ANALYSIS	(2) .75 X FIXED BASE ANALYSIS	RATIO (2) (1)
COLUMN BASES SUPPORTING CENTER CELL BOX BEAMS				
388	AXIAL FORCE (1)	621.5	295.5	.480
	LONGITUDINAL SHEAR (2)	274.8	230.1	.856
	TRANSVERSE SHEAR (3)	11.6	12.4	1.013
	TORSIONAL MOMENT (4)	419.5	396.7	.919
	TRANSVERSE MOMENT (5)	5159.8	5047.4	.956
	LONGITUDINAL MOMENT (6)	1751.9	1596.5	.906
	TRANSVERSE MOMENT (11)	4869.5	4703.9	.946
	LONGITUDINAL MOMENT (12)	9704.0	8266.6	.866
389	AXIAL FORCE (1)	604.0	299.0	.479
	LONGITUDINAL SHEAR (2)	273.7	238.3	.856
	TRANSVERSE SHEAR (3)	5.1	3.7	.711
	TORSIONAL MOMENT (4)	463.3	435.4	.947
	TRANSVERSE MOMENT (5)	5099.1	4694.7	.925
	LONGITUDINAL MOMENT (6)	1751.6	1558.9	.903
	TRANSVERSE MOMENT (11)	5111.4	4949.4	.959
	LONGITUDINAL MOMENT (12)	9682.5	8480.3	.865
390	AXIAL FORCE (1)	481.3	227.2	.462
	LONGITUDINAL SHEAR (2)	249.1	231.5	.904
	TRANSVERSE SHEAR (3)	7.0	12.5	1.581
	TORSIONAL MOMENT (4)	352.1	379.9	1.053
	TRANSVERSE MOMENT (5)	4869.2	5169.5	1.043
	LONGITUDINAL MOMENT (6)	1660.0	2892.4	1.777
	TRANSVERSE MOMENT (11)	4907.3	5171.2	1.038
	LONGITUDINAL MOMENT (12)	8665.1	9004.5	.994
391	AXIAL FORCE (1)	475.4	209.2	.455
	LONGITUDINAL SHEAR (2)	247.9	220.2	.907
	TRANSVERSE SHEAR (3)	13.8	17.1	1.291
	TORSIONAL MOMENT (4)	388.1	438.2	1.182
	TRANSVERSE MOMENT (5)	5102.0	5535.1	1.083
	LONGITUDINAL MOMENT (6)	1660.1	2274.3	1.373
	TRANSVERSE MOMENT (11)	5469.8	6022.1	1.104
	LONGITUDINAL MOMENT (12)	8849.4	8659.4	.994
400	AXIAL FORCE (1)	396.6	368.7	1.001
	LONGITUDINAL SHEAR (2)	1050.0	928.1	.883
	TRANSVERSE SHEAR (3)	556.0	537.7	.958
	TORSIONAL MOMENT (4)	4193.2	5179.3	1.398
	TRANSVERSE MOMENT (5)	156247.7	183278.9	1.166
	LONGITUDINAL MOMENT (6)	177002.8	78012.2	.441
	TRANSVERSE MOMENT (11)	157249.0	184352.6	1.165
	LONGITUDINAL MOMENT (12)	179002.8	79901.3	.447

TABLE 4.2A: CONT.

PIER BASES IN END CELL					
245	AXIAL FORCE (1)	173.3	202.5	182.7	1.111
	LONGITUDINAL SHEAR (2)	162.6	231.4	227.5	1.411
	TRANSVERSE SHEAR (3)	229.9	282.7	282.0	1.184
	TORSIONAL MOMENT (4)	8481.4	9494.3	10809.1	1.197
	TRANSVERSE MOMENT (5)	71626.3	86108.7	78859.1	1.148
	LONGITUDINAL MOMENT (6)	12376.5	30304.3	29992.3	2.436
	TRANSVERSE MOMENT (11)	76323.3	91717.8	84061.8	1.152
	LONGITUDINAL MOMENT (12)	15613.2	34778.5	34491.4	2.218
246	AXIAL FORCE (1)	270.6	240.2	271.8	.946
	LONGITUDINAL SHEAR (2)	178.8	244.9	252.4	1.390
	TRANSVERSE SHEAR (3)	348.9	382.5	353.0	1.054
	TORSIONAL MOMENT (4)	8816.1	10333.4	11159.1	1.282
	TRANSVERSE MOMENT (5)	61717.7	74599.0	68393.4	1.159
	LONGITUDINAL MOMENT (6)	11835.0	30290.1	29029.4	2.505
	TRANSVERSE MOMENT (11)	68700.8	82179.3	75461.1	1.147
	LONGITUDINAL MOMENT (12)	15360.2	75111.4	34016.7	2.250
247	AXIAL FORCE (1)	543.3	495.9	460.3	.880
	LONGITUDINAL SHEAR (2)	161.0	232.9	221.4	1.411
	TRANSVERSE SHEAR (3)	254.5	349.1	329.2	1.333
	TORSIONAL MOMENT (4)	10872.9	10592.1	9937.5	.944
	TRANSVERSE MOMENT (5)	57874.1	60798.9	76337.5	1.358
	LONGITUDINAL MOMENT (6)	11666.0	29195.5	29815.4	2.444
	TRANSVERSE MOMENT (11)	62876.2	87745.3	82983.4	1.359
	LONGITUDINAL MOMENT (12)	14883.5	32559.9	33199.6	2.214
248	AXIAL FORCE (1)	439.0	365.3	400.1	.872
	LONGITUDINAL SHEAR (2)	165.9	234.0	230.1	1.398
	TRANSVERSE SHEAR (3)	286.7	374.7	357.8	1.277
	TORSIONAL MOMENT (4)	7322.7	6666.2	6622.4	.907
	TRANSVERSE MOMENT (5)	47897.5	66545.4	65228.1	1.397
	LONGITUDINAL MOMENT (6)	11793.4	29736.6	27449.3	2.382
	TRANSVERSE MOMENT (11)	53700.5	75977.4	72409.8	1.382
	LONGITUDINAL MOMENT (12)	14891.3	33311.5	32005.4	2.193
305	AXIAL FORCE (1)	467.9	792.4	874.5	1.781
	LONGITUDINAL SHEAR (2)	662.1	943.1	931.2	1.415
	TRANSVERSE SHEAR (3)	1112.8	1388.8	1300.0	1.209
	TORSIONAL MOMENT (4)	48585.6	43148.6	41663.9	.873
	TRANSVERSE MOMENT (5)	209039.4	521665.8	493133.1	2.427
	LONGITUDINAL MOMENT (6)	107918.7	165896.1	163953.4	1.528
	TRANSVERSE MOMENT (11)	211047.6	516072.2	487953.2	2.379
	LONGITUDINAL MOMENT (12)	109824.0	162129.1	160274.8	1.468

UNITS: FORCES - KIPS  
MOMENTS - KIP-IN

TABLE 4.2B: COMPARISON BETWEEN CLASSI FIXED BASE AND LLNL RESPAN ANALYSIS  
SUMMARY OF VESSEL END CELL SUPPORT LEG FORCES

ELMT NO.	COMPONENT	(1) LLNL RESPAN ANALYSIS		(2) .75 X FIXED BASE ANALYSIS		RATIO (2) (1)
		116.5	104.9	100.0	100.0	
253	AXIAL FORCE (1)	116.5	104.9	100.0	100.0	.880
	LONGITUDINAL SHEAR (2)	6.3	9.1	9.0	9.0	1.429
	TRANSVERSE SHEAR (3)	95.4	100.0	85.5	85.5	.972
	TORSIONAL MOMENT (4)	116.0	159.4	162.0	162.0	1.386
	TRANSVERSE MOMENT (5)	11125.4	13111.9	11883.0	11883.0	1.123
	LONGITUDINAL MOMENT (6)	397.8	580.4	570.6	570.6	1.447
	TRANSVERSE MOMENT (11)	11169.8	13161.6	11924.0	11924.0	1.123
259	LONGITUDINAL MOMENT (12)	400.9	584.7	574.8	574.8	1.446
	AXIAL FORCE (1)	94.2	98.5	90.0	90.0	1.000
	LONGITUDINAL SHEAR (2)	5.0	7.0	7.1	7.1	1.410
	TRANSVERSE SHEAR (3)	145.3	125.3	129.9	129.9	.879
	TORSIONAL MOMENT (4)	57.8	71.0	75.4	75.4	1.256
	TRANSVERSE MOMENT (5)	7932.1	8588.4	10059.9	10059.9	1.175
	LONGITUDINAL MOMENT (6)	340.3	481.3	487.5	487.5	1.423
265	TRANSVERSE MOMENT (11)	8000.5	8624.1	10155.5	10155.5	1.174
	LONGITUDINAL MOMENT (12)	342.3	484.5	499.9	499.9	1.425
	AXIAL FORCE (1)	255.5	202.3	208.6	208.6	.801
	LONGITUDINAL SHEAR (2)	139.8	199.1	197.9	197.9	1.420
	TRANSVERSE SHEAR (3)	122.6	145.9	142.8	142.8	1.178
	TORSIONAL MOMENT (4)	2539.1	3470.4	3519.5	3519.5	1.376
	TRANSVERSE MOMENT (5)	27759.5	35307.5	32883.1	32883.1	1.229
272	LONGITUDINAL MOMENT (6)	9018.2	13016.1	12889.3	12889.3	1.436
	TRANSVERSE MOMENT (11)	27659.9	35385.5	32940.1	32940.1	1.225
	LONGITUDINAL MOMENT (12)	9090.0	13114.6	12997.2	12997.2	1.435
	AXIAL FORCE (1)	343.9	262.0	321.5	321.5	.848
	LONGITUDINAL SHEAR (2)	157.3	219.1	223.3	223.3	1.403
	TRANSVERSE SHEAR (3)	183.6	218.8	198.6	198.6	1.137
	TORSIONAL MOMENT (4)	3741.0	4885.7	5059.2	5059.2	1.330
280	TRANSVERSE MOMENT (5)	9575.4	15442.3	16267.3	16267.3	1.466
	LONGITUDINAL MOMENT (6)	9711.9	13644.1	13902.7	13902.7	1.418
	TRANSVERSE MOMENT (11)	9568.4	15534.8	16262.6	16262.6	1.472
	LONGITUDINAL MOMENT (12)	9792.1	13751.5	14012.6	14012.6	1.418
	AXIAL FORCE (11)	350.0	259.0	251.2	251.2	.729
	LONGITUDINAL SHEAR (2)	140.5	202.3	198.9	198.9	1.428
	TRANSVERSE SHEAR (3)	179.3	186.3	169.9	169.9	.994
286	TORSIONAL MOMENT (4)	4374.4	6334.5	6227.7	6227.7	1.436
	TRANSVERSE MOMENT (5)	22790.5	27009.9	24384.4	24384.4	1.127
	LONGITUDINAL MOMENT (6)	10089.7	14702.9	14498.9	14498.9	1.447
	TRANSVERSE MOMENT (11)	22891.2	27105.5	24453.1	24453.1	1.126
	LONGITUDINAL MOMENT (12)	10150.6	14802.2	14596.2	14596.2	1.448
	AXIAL FORCE (11)	305.5	229.1	184.9	184.9	.678
	LONGITUDINAL SHEAR (2)	143.4	204.5	206.8	206.8	1.434
	TRANSVERSE SHEAR (3)	152.1	155.0	145.6	145.6	.998
	TORSIONAL MOMENT (4)	4533.3	6401.1	6474.4	6474.4	1.420
	TRANSVERSE MOMENT (5)	7268.6	10300.7	9708.4	9708.4	1.376
	LONGITUDINAL MOMENT (6)	10240.7	14651.0	14591.1	14591.1	1.457
	TRANSVERSE MOMENT (11)	7322.2	10366.1	9770.2	9770.2	1.375
	LONGITUDINAL MOMENT (12)	10340.8	14955.4	15095.8	15095.8	1.453

TABLE 4.28 CONT.

292	AXIAL FORCE (1)	311.2	355.3	330.8	1.102
	LONGITUDINAL SHEAR (2)	5.0	7.3	7.1	1.451
	TRANSVERSE SHEAR (3)	63.0	94.6	93.9	1.495
	TORSIONAL MOMENT (4)	41.3	55.4	50.6	1.293
	TRANSVERSE MOMENT (5)	5859.1	5170.5	5229.2	.887
	LONGITUDINAL MOMENT (6)	255.2	378.1	371.8	1.469
	TRANSVERSE MOMENT (11)	5951.4	5190.3	5254.4	.892
	LONGITUDINAL MOMENT (12)	259.2	381.8	375.4	1.466
299	AXIAL FORCE (1)	290.3	298.3	330.2	1.083
	LONGITUDINAL SHEAR (2)	5.1	7.3	7.5	1.446
	TRANSVERSE SHEAR (3)	116.2	153.7	151.1	1.312
	TORSIONAL MOMENT (4)	43.4	54.7	57.7	1.293
	TRANSVERSE MOMENT (5)	4841.7	5669.4	6388.2	1.245
	LONGITUDINAL MOMENT (6)	261.0	379.0	389.9	1.467
	TRANSVERSE MOMENT (11)	4822.9	5712.1	6429.6	1.259
	LONGITUDINAL MOMENT (12)	263.8	382.7	392.6	1.470

UNITS: FORCES - KIPS  
 MOMENTS - KIP-IN

TABLE 4.20: COMPARISON BETWEEN CLASSIC FIXED BASE AND LLNL RESPAN ANALYSIS  
SUMMARY OF MAGNET HANGER AND STRUT FORCES

ELMT NO.	(1) LLNL RESPAN ANALYSIS	(2) .75 X FIXED BASE ANALYSIS	RATIO (2) (1)
313	243.6	265.6	1.042
314	227.7	248.2	1.048
315	334.1	293.9	.886
316	539.9	505.0	.953
317	526.9	570.4	1.022
318	556.7	582.5	1.040
319	67.9	56.6	.818
320	26.3	27.2	1.024
321	74.4	73.5	.950
322	21.5	16.9	.763
323	9.6	5.5	.669
324	39.1	43.1	1.113
325	139.2	146.1	.992
326	79.2	75.1	.957
327	81.0	95.6	1.040
328	122.2	125.7	1.047
329	25.9	26.7	.941
330	32.1	33.6	.999
331	56.3	53.7	.941
332	51.4	51.1	.929
333	13.4	11.5	.899
334	16.9	13.5	.846
335	36.1	40.3	1.088
336	11.7	9.2	.799
337	14.2	9.3	.712
338	34.9	39.0	1.065
339	15.1	11.4	.765
340	15.0	13.4	.839
341	59.4	66.1	1.072
342	90.0	46.3	1.009
343	49.9	52.7	1.003
344	44.2	49.1	1.066
345	53.2	52.1	1.089
346	8.8	4.4	.505
347	8.2	4.6	.541
348	16.9	20.7	1.208
349	16.8	11.5	.691
350	14.5	10.3	.724
351	36.6	41.2	1.121
352	14.2	10.4	.740
353	14.1	9.4	.662
354	46.0	50.0	1.077
355	25.6	25.7	1.048
356	25.3	26.6	1.064
357	24.7	28.1	1.061
358	26.9	27.3	1.026
359	8.5	9.4	1.071
360	9.9	11.1	1.101
361	9.1	9.2	1.081
362	10.5	10.7	1.066

TABLE 4.2C CONT.

363	39.1	41.3	37.5	1.008
364	34.9	39.0	34.9	1.057
365	43.1	42.6	52.7	1.104
366	39.5	36.7	42.7	1.004
367	10.9	10.7	12.4	1.068
368	13.0	14.1	11.8	.999
369	9.4	11.2	8.9	1.072
370	12.2	12.5	13.7	1.073
371	4.7	4.5	5.4	1.049
372	4.6	4.8	5.0	1.051
373	4.5	5.0	4.8	1.081
374	4.7	5.1	4.8	1.051
375	15.2	14.1	16.6	1.007
376	14.9	14.7	15.1	1.001
377	14.5	15.6	13.9	1.019
378	16.3	15.8	16.2	1.001

UNITS: FORCES - KIPS

methodology and the response spectrum method. Thus, the major source of differences is the method of modeling the local foundation rocking springs.

#### 4.2 RESULTS FROM THE COUPLED VESSEL/VAULT SSI ANALYSES

Our best estimate of vessel response to a 0.25g earthquake excitation is obtained from our CLASSI SSI analysis of the vessel and vault together, coupled through the soil. These analyses include the two major effects which influence vessel response and cause it to differ from results calculated from the fixed-base analysis: SSI and interaction with the vault. The effect of SSI is to modify the motions on the foundation from three translational free-field motions to a set of six motions (three translational, two rocking and a torsional component). The effects of the assumed rigid foundation mats are included with a 6 x 6 matrix of translational, rocking, torsional and coupling terms. Energy radiated away from the structure ("radiation damping") is included in the foundation impedances.

Interaction with the vault (often termed "structure-to-structure interaction") describes the dynamic effects of the vessel and vault on each other and is dependent on the relative masses of the two structures as well as their stiffness and damping characteristics, proximity of their foundations, and the flexibility and damping of the soil deposit.

The two effects discussed above were studied individually in our previous analyses of the A-cell vessel (Ref. 1). Generally, the same trends observed for the A-cell vessel occur here although some differences occur due to the differences in dynamic properties of the A-cell and Axicell models. Only the cumulative effects of SSI and interaction with the vault are discussed in this report.

We analyzed the coupled vessel/vault/soil system for three sets of soil properties to account for uncertainties in their values. The three sets of soil properties were: the best estimate properties discussed in Section 3.2.1 which are denoted "nominal" properties; "stiff" properties for which the soil shear moduli were 1.5 times the nominal values; and "soft" properties for

which the soil shear moduli were 1/1.5 or 2/3 times the nominal values. The same soil material damping was used for all sets of properties. For all coupled SSI analyses we used composite modal damping in the vessel to reflect differences in damping in different parts of the vessel.

#### 4.2.1 Effects of SSI and Vessel/Vault Interaction

We compared the results of our CLASSI coupled SSI analysis for nominal soil properties with our CLASSI fixed-base analysis to study the effect that SSI and interaction with the vault had on vessel response. For these comparisons we used the unfactored fixed-base results (i.e. no 25% reduction). For each response we calculated the ratio of the greater of the two (east half vs. west half) coupled SSI results to the greater of the two fixed-base results. Our results are shown in Tables 4.3A through 4.3C.

Our comparison showed that the combined effect of SSI and interaction with the vault resulted in an overall reduction of about 20% in vessel forces. Foundation forces (Table 4.3A) generally were reduced about 20% in the transverse direction and 25% in the longitudinal direction. Reductions in the end cell piers were generally less than those in the center cell, averaging about 15% for transverse force components and 20% for longitudinal components. In the center cell the reduction was about 22% for transverse forces and about 29% for longitudinal forces. For the vessel support legs in the end cells (Table 4.3B), the force reduction was about 15% in the transverse direction and about 30% in the longitudinal direction. Forces in the magnet hangers and struts (Table 4.3C) were generally reduced by about 15%. Horizontal strut forces were generally reduced from 20% to 30%, averaging about a 25% reduction, while vertical hangers experienced an overall increase of about 8%.

The overall reduction of forces experienced by the vessel was not as great as the 25% we had previously anticipated. This is probably due to the decrease in the natural frequencies of the vessel caused by the increased flexibility beneath the foundation piers and columns. This increased flexibility resulted in vessel frequencies that were much closer to the vault frequencies and probably caused increased amplification because of this. It

TABLE 4.3A: COMPARISON BETWEEN CLASSI COUPLED SSI AND FIXED BASED ANALYSIS  
SUMMARY OF FOUNDATION FORCES

ELMT NO.	COMPONENT	(1) FIXED BASE ANALYSIS		(2) COUPLED SSI ANALYSIS		RATIO (2) (1)
		(1)	(2)	(1)	(2)	
COLUMN BASES SUPPORTING CENTER CELL BOX BEAM						
388	AXIAL FORCE (1)	394.0	401.2	358.1	363.6	.906
	LONGITUDINAL SHEAR (2)	306.8	320.3	228.4	210.2	.713
	TRANSVERSE SHEAR (3)	16.6	14.7	11.8	13.5	.814
	TORSIONAL MOMENT (4)	529.9	499.6	438.9	388.9	.830
	TRANSVERSE MOMENT (5)	6729.8	6426.9	5234.9	4653.3	.778
	LONGITUDINAL MOMENT (6)	2126.6	2103.6	1422.5	1494.2	.702
	TRANSVERSE MOMENT (11)	6271.8	6012.1	4891.7	4400.7	.780
	LONGITUDINAL MOMENT (12)	11022.1	11388.3	8039.2	7496.6	.706
389	AXIAL FORCE (1)	398.7	373.3	341.8	334.4	.857
	LONGITUDINAL SHEAR (2)	317.8	306.7	212.5	225.0	.708
	TRANSVERSE SHEAR (3)	4.9	4.8	4.3	4.0	.872
	TORSIONAL MOMENT (4)	580.6	589.2	417.1	456.4	.792
	TRANSVERSE MOMENT (5)	6526.2	6433.6	4651.2	4968.7	.761
	LONGITUDINAL MOMENT (6)	2091.7	2129.2	1535.7	1405.6	.722
	TRANSVERSE MOMENT (11)	6599.2	6472.8	4743.0	4978.2	.754
	LONGITUDINAL MOMENT (12)	11307.1	11022.2	7700.0	7930.0	.701
390	AXIAL FORCE (1)	302.9	299.6	244.3	216.9	.806
	LONGITUDINAL SHEAR (2)	308.6	291.8	201.4	222.4	.721
	TRANSVERSE SHEAR (3)	16.6	16.1	14.0	12.8	.842
	TORSIONAL MOMENT (4)	506.6	491.5	387.4	357.3	.765
	TRANSVERSE MOMENT (5)	6891.3	6729.9	5094.3	4744.1	.739
	LONGITUDINAL MOMENT (6)	3056.6	3037.4	2077.4	2122.1	.694
	TRANSVERSE MOMENT (11)	6894.9	6655.5	5253.2	4602.5	.763
	LONGITUDINAL MOMENT (12)	12006.0	11499.5	7820.9	6572.7	.714
391	AXIAL FORCE (1)	279.0	298.6	211.7	217.7	.729
	LONGITUDINAL SHEAR (2)	293.5	305.8	224.7	203.3	.735
	TRANSVERSE SHEAR (3)	22.8	24.8	19.2	20.0	.809
	TORSIONAL MOMENT (4)	584.2	576.9	408.3	425.4	.729
	TRANSVERSE MOMENT (5)	7380.1	7349.7	5071.0	5291.7	.716
	LONGITUDINAL MOMENT (6)	3032.4	3045.3	2165.9	2060.0	.711
	TRANSVERSE MOMENT (11)	6029.5	6068.4	5525.4	5883.0	.727
	LONGITUDINAL MOMENT (12)	11544.6	11914.2	8682.5	7900.1	.729
400	AXIAL FORCE (1)	491.6	566.9	417.1	417.3	.736
	LONGITUDINAL SHEAR (2)	1237.5	1235.2	864.7	852.8	.693
	TRANSVERSE SHEAR (3)	717.0	703.6	521.1	509.9	.727
	TORSIONAL MOMENT (4)	6905.8	8723.5	12060.1	9128.6	1.382
	TRANSVERSE MOMENT (5)	244371.9	241260.4	176265.0	173293.2	.721
	LONGITUDINAL MOMENT (6)	104016.3	104102.2	72535.9	71402.9	.697
	TRANSVERSE MOMENT (11)	245816.9	242578.7	177304.2	174310.9	.721
	LONGITUDINAL MOMENT (12)	106535.1	106616.3	74295.5	73138.5	.697

TABLE 4.3A CONT.

PIER BASES IN END CELL						
245	AXIAL FORCE (1)	270.0	243.7	203.4	233.5	.865
	LONGITUDINAL SHEAR (2)	308.6	303.3	267.9	246.5	.868
	TRANSVERSE SHEAR (3)	376.9	349.3	339.0	311.1	.899
	TORSIONAL MOMENT (4)	12659.1	14412.1	11473.5	9627.5	.796
	TRANSVERSE MOMENT (5)	114811.6	103145.5	104359.6	92599.5	.909
	LONGITUDINAL MOMENT (6)	40405.7	39988.8	30913.4	27901.5	.765
	TRANSVERSE MOMENT (11)	122290.4	112092.4	111059.5	98739.8	.908
	LONGITUDINAL MOMENT (12)	46371.3	45998.5	36115.0	32359.4	.779
246	AXIAL FORCE (1)	320.3	362.4	305.7	339.2	.936
	LONGITUDINAL SHEAR (2)	326.6	336.5	278.3	269.0	.827
	TRANSVERSE SHEAR (3)	510.0	470.6	441.2	416.0	.865
	TORSIONAL MOMENT (4)	14577.9	14877.5	10908.1	13295.8	.894
	TRANSVERSE MOMENT (5)	95462.0	91191.3	69372.8	62159.0	.899
	LONGITUDINAL MOMENT (6)	40366.7	38705.8	27252.0	30624.3	.763
	TRANSVERSE MOMENT (11)	109572.4	100614.9	98154.7	90486.5	.896
	LONGITUDINAL MOMENT (12)	46815.2	45355.5	32082.4	36078.6	.771
247	AXIAL FORCE (1)	661.2	613.7	541.3	601.2	.909
	LONGITUDINAL SHEAR (2)	310.5	295.3	265.6	250.1	.855
	TRANSVERSE SHEAR (3)	465.5	438.9	371.2	338.8	.797
	TORSIONAL MOMENT (4)	14122.7	13250.0	11918.2	12565.6	.890
	TRANSVERSE MOMENT (5)	107731.9	101863.3	86126.2	79980.8	.799
	LONGITUDINAL MOMENT (6)	37554.0	36420.5	29358.4	27049.6	.764
	TRANSVERSE MOMENT (11)	116933.7	110645.4	93457.0	86733.2	.759
	LONGITUDINAL MOMENT (12)	43599.8	44266.1	34413.3	31595.7	.777
248	AXIAL FORCE (1)	487.0	533.5	469.8	541.4	1.015
	LONGITUDINAL SHEAR (2)	312.0	306.8	257.3	263.9	.848
	TRANSVERSE SHEAR (3)	499.6	477.0	383.7	376.3	.768
	TORSIONAL MOMENT (4)	8889.3	8829.9	6379.1	6882.9	.774
	TRANSVERSE MOMENT (5)	91393.9	86594.1	73063.4	68839.6	.799
	LONGITUDINAL MOMENT (6)	38315.5	36999.0	27402.4	31179.8	.814
	TRANSVERSE MOMENT (11)	101303.2	96546.4	80562.0	76240.2	.795
	LONGITUDINAL MOMENT (12)	44415.4	42673.9	31937.8	36457.1	.821
305	AXIAL FORCE (1)	1056.5	1166.0	967.5	1034.9	.888
	LONGITUDINAL SHEAR (2)	1257.4	1241.6	1063.8	1029.3	.846
	TRANSVERSE SHEAR (3)	1851.7	1733.3	1535.0	1440.8	.829
	TORSIONAL MOMENT (4)	57531.4	55551.8	65246.7	50724.0	1.134
	TRANSVERSE MOMENT (5)	695594.4	657690.9	597941.2	573379.7	.860
	LONGITUDINAL MOMENT (6)	221194.7	216604.6	165953.9	154904.4	.750
	TRANSVERSE MOMENT (11)	688086.3	650604.2	591648.5	567646.2	.860
	LONGITUDINAL MOMENT (12)	216172.1	213699.8	161684.9	151216.2	.749

UNITS: FORCES - KIPS  
MOMENTS - KIP-IN

TABLE 4.3B: COMPARISON BETWEEN CLASSI COUPLED SSI AND FIXED BASED ANALYSIS  
SUMMARY OF VESSEL END CELL SUPPORT LEG FORCES

ELMT NO.	COMPONENT	(1) FIXED BASE ANALYSIS		(2) COUPLED SSI ANALYSIS		RATIO (2) (1)
		139.9	133.4	108.2	103.6	
253	AXIAL FORCE (1)	139.9	133.4	108.2	103.6	.773
	LONGITUDINAL SHEAR (2)	12.1	12.0	8.5	8.2	.704
	TRANSVERSE SHEAR (3)	133.3	114.0	118.2	112.0	.886
	TORSIONAL MOMENT (4)	212.5	216.0	154.7	140.4	.716
	TRANSVERSE MOMENT (5)	17482.5	15844.0	16179.6	15925.0	.925
	LONGITUDINAL MOMENT (6)	773.9	760.8	532.1	516.0	.688
	TRANSVERSE MOMENT (11)	17548.8	15988.6	16238.4	15980.0	.925
	LONGITUDINAL MOMENT (12)	779.6	756.4	535.1	519.9	.688
259	AXIAL FORCE (1)	131.3	120.0	106.5	91.6	.811
	LONGITUDINAL SHEAR (2)	9.4	9.5	6.7	6.5	.701
	TRANSVERSE SHEAR (3)	167.1	173.3	155.6	148.8	.898
	TORSIONAL MOMENT (4)	94.6	100.5	74.8	65.0	.744
	TRANSVERSE MOMENT (5)	11424.5	13454.6	10963.2	10685.1	.815
	LONGITUDINAL MOMENT (6)	641.7	650.0	446.0	435.8	.686
	TRANSVERSE MOMENT (11)	11498.8	13540.7	11048.6	10762.1	.816
	LONGITUDINAL MOMENT (12)	646.1	654.5	449.1	438.8	.686
265	AXIAL FORCE (1)	259.7	278.1	209.3	231.8	.834
	LONGITUDINAL SHEAR (2)	255.5	263.9	186.5	173.7	.703
	TRANSVERSE SHEAR (3)	194.6	190.4	171.2	183.1	.941
	TORSIONAL MOMENT (4)	4627.2	4692.6	3206.6	3175.4	.683
	TRANSVERSE MOMENT (5)	47076.7	43844.1	37956.7	38361.5	.815
	LONGITUDINAL MOMENT (6)	17354.8	17185.8	12102.6	11354.1	.697
	TRANSVERSE MOMENT (11)	47154.1	43920.2	36029.7	38452.4	.815
	LONGITUDINAL MOMENT (12)	17466.2	17316.3	12194.9	11440.0	.697
272	AXIAL FORCE (1)	348.4	428.8	329.5	314.7	.768
	LONGITUDINAL SHEAR (2)	290.8	297.7	206.6	194.2	.694
	TRANSVERSE SHEAR (3)	291.8	264.8	263.2	225.8	.802
	TORSIONAL MOMENT (4)	6527.6	6744.3	4761.3	4390.2	.706
	TRANSVERSE MOMENT (5)	20599.7	16835.4	17897.3	15784.4	.869
	LONGITUDINAL MOMENT (6)	18192.1	18537.0	12750.6	12212.2	.668
	TRANSVERSE MOMENT (11)	20713.1	18923.5	18019.4	15875.0	.870
	LONGITUDINAL MOMENT (12)	18335.3	18683.5	12852.2	12307.8	.688
280	AXIAL FORCE (1)	345.3	335.0	329.3	275.6	.954
	LONGITUDINAL SHEAR (2)	269.7	265.2	187.8	175.1	.696
	TRANSVERSE SHEAR (3)	248.4	225.6	223.5	189.3	.800
	TORSIONAL MOMENT (4)	6446.0	6303.7	5699.3	5663.2	.675
	TRANSVERSE MOMENT (5)	38013.2	32465.9	31911.2	29471.9	.886
	LONGITUDINAL MOMENT (6)	19603.9	19331.8	13740.4	12761.7	.701
	TRANSVERSE MOMENT (11)	36142.0	32604.1	32025.8	29557.3	.666
	LONGITUDINAL MOMENT (12)	19736.3	19461.5	13832.3	12847.2	.701

TABLE 4.3B CONT.

286	AXIAL FORCE (1)	305.5	246.5	304.1	237.2	.995
	LONGITUDINAL SHEAR (2)	272.8	275.7	189.4	183.6	.687
	TRANSVERSE SHEAR (3)	206.7	194.1	174.2	170.3	.843
	TORSIONAL MOMENT (4)	854.8	8632.6	5668.6	5770.7	.682
	TRANSVERSE MOMENT (5)	13734.3	12944.6	12267.4	12559.7	.915
	LONGITUDINAL MOMENT (6)	19902.4	19988.2	13660.5	13262.1	.683
	TRANSVERSE MOMENT (11)	13821.4	13026.9	12348.7	12654.3	.916
	LONGITUDINAL MOMENT (12)	19940.5	20127.7	13756.4	13355.1	.683
292	AXIAL FORCE (1)	473.7	441.1	375.1	434.5	.917
	LONGITUDINAL SHEAR (2)	9.7	9.5	6.9	6.5	.706
	TRANSVERSE SHEAR (3)	125.1	125.0	96.1	95.1	.763
	TORSIONAL MOMENT (4)	73.9	67.4	48.6	56.1	.759
	TRANSVERSE MOMENT (5)	6894.0	6972.3	5939.8	4686.9	.852
	LONGITUDINAL MOMENT (6)	504.2	495.7	352.0	323.4	.699
	TRANSVERSE MOMENT (11)	6920.4	7005.8	5562.7	4727.3	.851
	LONGITUDINAL MOMENT (12)	509.1	500.5	355.5	331.7	.698
299	AXIAL FORCE (1)	397.7	440.3	408.5	390.1	.929
	LONGITUDINAL SHEAR (2)	9.7	10.0	7.2	6.6	.716
	TRANSVERSE SHEAR (3)	204.9	201.5	148.5	147.6	.725
	TORSIONAL MOMENT (4)	72.9	76.9	53.3	50.1	.694
	TRANSVERSE MOMENT (5)	7559.2	6517.6	5391.6	7259.0	.853
	LONGITUDINAL MOMENT (6)	505.4	518.5	361.6	335.9	.699
	TRANSVERSE MOMENT (11)	7616.1	8572.9	5465.3	7321.3	.854
	LONGITUDINAL MOMENT (12)	510.2	523.5	365.2	339.2	.698

UNITS: FORCES - KIPS  
MOMENTS - KIP-IN

TABLE 4.3C: COMPARISON BETWEEN CLASS1 COUPLED SSI AND FIXED BASE ANALYSIS  
SUMMARY OF MAGNET HANGER AND STRUT FORCES

ELMNT NO.	(1) FIXED BASE ANALYSIS	(2) COUPLED SSI ANALYSIS	RATIO (2) (1)
313	354.1	322.8	.892
314	330.9	305.4	.741
315	390.6	398.7	.869
316	674.7	694.2	.810
317	760.6	675.7	.803
318	776.7	767.5	.760
319	75.5	72.6	.945
320	36.3	35.6	.97
321	98.1	90.4	.856
322	22.5	21.2	.952
323	7.4	9.7	.759
324	57.5	55.6	.982
325	197.4	167.1	.845
326	100.1	104.1	.951
327	114.0	110.6	.915
328	168.9	172.3	.970
329	35.5	31.9	.895
330	44.7	40.9	.905
331	71.6	69.7	.945
332	68.2	73.5	.905
333	15.3	16.9	.885
334	18.0	20.2	.895
335	53.7	51.1	.945
336	12.2	12.6	.959
337	12.4	14.5	.830
338	52.0	49.8	.945
339	15.2	16.4	.923
340	17.9	15.6	.935
341	88.1	82.7	.925
342	61.7	72.6	.845
343	70.2	63.1	.895
344	65.5	60.3	.925
345	69.4	65.1	.945
346	5.9	5.9	1.000
347	6.1	5.8	.959
348	27.6	26.7	.959
349	15.3	15.8	.985
350	13.8	14.3	.923
351	54.9	54.4	.985
352	13.9	14.1	.985
353	12.5	12.5	1.000
354	66.6	65.4	.985
355	34.3	37.3	.915
356	35.5	36.3	.970
357	37.5	32.4	.867
358	36.3	37.2	.970
359	12.5	11.7	.959
360	14.8	14.2	.959
361	12.2	14.1	.859
362	14.3	15.7	.915
363	55.1	49.9	.895
364	52.0	46.5	.895

TABLE 4.3C CONT.

365	56.8	70.2	42.0	47.9	.683
366	56.9	56.9	42.0	39.9	.738
367	14.2	16.5	12.0	11.4	.726
368	18.8	15.8	12.8	12.4	.685
369	15.0	11.9	10.2	10.8	.718
370	16.6	18.3	14.6	12.5	.799
371	6.0	7.2	5.8	4.9	.809
372	6.3	6.7	4.6	5.1	.756
373	6.7	6.4	5.1	4.9	.755
374	6.9	6.4	4.8	5.1	.737
375	18.8	22.2	18.4	15.5	.828
376	19.6	20.1	14.6	16.9	.840
377	20.9	18.5	16.9	16.2	.809
378	21.1	22.4	15.9	17.0	.760

UNITS: FORCES - KIPS

should be noted that for our previous analyses of the A-cell vessel configuration (Ref. 1), where the vessel frequencies were further separated from the vault frequencies, forces in the vessel experienced a much greater reduction (over 30%) due to SSI and interaction with the vault.

#### 4.2.2 Comparison of Coupled Vessel/Vault SSI Analyses with LLNL Analysis

We compared the results of our coupled SSI analysis for the three different soil property assumptions (best estimate shear moduli, 2/3 and 1.5 of best estimate moduli) with the results of the LLNL response spectrum analysis. For each force response we calculated a ratio consisting of the maximum of six values from our CLASSI analyses (east side and west side for each soil property case) divided by the LLNL value. The results for vessel forces are summarized in Tables 4.4A through 4.4C. Overall, the coupled SSI forces averaged about 40% higher than the LLNL results. On the foundations (Table 4.4A), ratios were about equal to the overall average. For the end cell piers it was higher (almost 80%). Transverse forces and moments were about 50% higher than the LLNL values; longitudinal shear forces were higher by about 70% and longitudinal moments were higher by factors ranging from about 2.5 to 2.8 (average 2.7) times the LLNL values. Axial forces were about 30% higher. As was briefly mentioned in Section 4.1.1, the transverse bending moments were considerably higher than the longitudinal ones; the resultant moments were about 55% higher. For the center cell support columns, ratios were much lower. Moments averaged about 10% higher than LLNL values. Longitudinal shear forces were reduced by about 5% (transverse shears were insignificant). Axial forces were reduced by about 45%.

For the vessel support legs in the end cells (Table 4.4B) our coupled SSI values averaged about 45% higher than LLNL values. Ratios between moments varied between 1.03 and 1.9. Transverse moments averaged about 50% higher; longitudinal moments were about 55% higher. Shears varied from about 10% to 60% higher. Vertical forces varied from a reduction of about 6% to an increase of about 40%.

Ratios between magnet hanger and strut forces (Table 4.4C) varied between a maximum reduction of about 15% to a maximum increase of almost 55%

TABLE 4.4A: COMPARISON BETWEEN CLASSI COUPLED SSI AND LLNL RESPAN ANALYSIS  
SUMMARY OF FOUNDATION FORCES

PAGE 2

ELMT NO.	COMPONENT	LLNL RESPAN ANALYSIS		COUPLED SSI ANALYSIS				MAX CPLD	MAX CPL LLNL
		SOFT SOIL	NOMINAL SOIL	STIFF SOIL	MAX CPLD				
<b>COLUMN BASES SUPPORTING CENTER CELL BOX BEAM</b>									
388	AXIAL FORCE (1)	621.5	357.9	329.3	350.1	363.6	340.6	366.1	366.1 STIFF .509
	LONGITUDINAL SHEAR (2)	274.8	224.1	191.7	220.4	210.2	245.5	260.1	260.1 STIFF .947
	TRANSVERSE SHEAR (3)	11.6	11.0	12.4	11.8	13.5	13.4	13.3	13.5 NOM 1.166
	TORSIONAL MOMENT (4)	419.5	383.0	357.4	430.9	308.9	473.2	396.2	473.2 STIFF 1.126
	TRANSVERSE MOMENT (5)	5159.8	4577.8	4100.2	5244.9	4653.3	5730.6	5098.0	5730.6 STIFF 1.111
	LONGITUDINAL MOMENT (6)	1751.9	1392.7	1140.1	1422.5	1194.2	1677.9	1730.7	1730.7 STIFF 1.989
	TRANSVERSE MOMENT (11)	4869.5	4265.8	4169.0	4881.7	4100.7	5350.5	4006.0	5350.5 STIFF 1.009
	LONGITUDINAL MOMENT (12)	5704.0	7889.8	6967.8	6039.2	7406.5	6784.4	9271.2	9271.2 STIFF .955
389	AXIAL FORCE (1)	604.0	310.7	323.7	341.8	334.4	340.2	336.8	341.8 NOM .566
	LONGITUDINAL SHEAR (2)	273.7	199.3	218.3	212.5	225.0	255.3	249.0	255.3 STIFF .933
	TRANSVERSE SHEAR (3)	5.1	4.1	4.2	4.3	4.0	4.4	4.0	4.4 STIFF .867
	TORSIONAL MOMENT (4)	463.3	389.7	410.9	417.1	466.4	442.2	506.4	506.4 STIFF 1.093
	TRANSVERSE MOMENT (5)	5098.1	4424.4	4403.4	4651.2	4968.7	5209.7	5418.0	5418.0 STIFF 1.063
	LONGITUDINAL MOMENT (6)	1751.6	1446.3	1363.5	1536.7	1405.6	1702.2	1701.9	1702.2 STIFF .972
	TRANSVERSE MOMENT (11)	5111.4	4474.2	4160.3	4743.0	4970.2	5295.1	5420.0	5420.0 STIFF 1.062
	LONGITUDINAL MOMENT (12)	5982.5	7225.3	7695.8	7700.0	7930.0	9104.9	8924.1	9104.9 STIFF .910
390	AXIAL FORCE (1)	481.3	207.6	225.5	244.3	216.9	269.7	211.7	269.7 STIFF .560
	LONGITUDINAL SHEAR (2)	249.1	186.0	212.6	201.4	222.4	241.9	242.5	242.5 STIFF .973
	TRANSVERSE SHEAR (3)	7.8	10.5	11.0	14.0	12.0	14.4	14.5	14.5 STIFF 1.867
	TORSIONAL MOMENT (4)	352.1	347.5	336.8	387.4	357.3	427.4	392.0	427.4 STIFF 1.214
	TRANSVERSE MOMENT (5)	4898.2	4554.9	4480.1	5094.3	4744.1	5684.1	5326.7	5684.1 STIFF 1.160
	LONGITUDINAL MOMENT (6)	1660.0	2023.3	2000.0	2077.4	2121.2	2422.2	284.4	2484.4 STIFF 1.497
	TRANSVERSE MOMENT (11)	4967.3	4645.3	4511.3	5263.2	4802.5	5837.7	5285.5	5837.7 STIFF 1.190
	LONGITUDINAL MOMENT (12)	8865.1	7418.1	8174.6	7820.9	8572.7	9438.1	9516.4	9516.4 STIFF 1.073
391	AXIAL FORCE (1)	475.4	195.0	194.5	211.7	217.7	232.6	241.5	241.5 STIFF .508
	LONGITUDINAL SHEAR (2)	247.9	213.3	185.3	224.7	203.3	241.3	242.6	242.6 STIFF .979
	TRANSVERSE SHEAR (3)	13.8	21.3	17.0	19.2	20.0	19.1	21.6	21.6 STIFF 1.560
	TORSIONAL MOMENT (4)	380.1	389.3	390.1	408.3	425.1	459.3	470.0	470.0 STIFF 1.211
	TRANSVERSE MOMENT (5)	5102.0	4801.6	4829.8	5071.0	5201.7	5728.5	5904.9	5904.9 STIFF 1.157
	LONGITUDINAL MOMENT (6)	1660.1	2043.2	1991.1	2165.9	2060.0	2453.4	2445.1	2453.4 STIFF 1.478
	TRANSVERSE MOMENT (11)	5469.8	5209.3	5261.7	5525.4	5863.0	6106.3	6530.7	6530.7 STIFF 1.194
	LONGITUDINAL MOMENT (12)	6849.4	6228.5	7378.1	6592.5	7900.1	9451.7	9479.4	9479.4 STIFF 1.071
400	AXIAL FORCE (1)	396.6	412.3	329.5	417.1	417.3	422.2	461.6	461.6 STIFF 1.164
	LONGITUDINAL SHEAR (2)	1050.0	829.7	816.8	864.7	852.8	993.2	1003.5	1003.5 STIFF .956
	TRANSVERSE SHEAR (3)	555.0	476.7	474.7	521.1	509.9	582.6	567.9	582.6 STIFF 1.048
	TORSIONAL MOMENT (4)	4183.2	12827.3	10397.3	12060.1	9128.6	1137.1	8889.5	12827.3 SOFT 3.059
	TRANSVERSE MOMENT (5)	156247.7	160448.3	60522.8	176265.0	73293.2	198092.1	94108.7	198092.1 STIFF 1.260
	LONGITUDINAL MOMENT (6)	177002.8	69503.3	68104.1	72535.9	71402.9	83304.8	84187.7	84187.7 STIFF 1.476
	TRANSVERSE MOMENT (11)	15729.0	161408.1	6172.4	177304.2	74310.9	199266.3	95254.0	199266.3 STIFF 1.267
	LONGITUDINAL MOMENT (12)	179002.8	71191.9	69046.3	74295.6	73138.5	85326.4	86230.3	86230.3 STIFF .482

TABLE 4.4A CONT.

PIER BASES IN END CELL											
245	AXIAL FORCE (1)	173.3	228.3	201.7	203.4	233.5	210.9	250.3	250.3	STIFF	1.444
	LONGITUDINAL SHEAR (2)	162.6	254.4	243.0	267.9	246.5	277.0	281.3	281.3	STIFF	1.730
	TRANSVERSE SHEAR (3)	229.9	208.8	279.7	339.0	311.1	351.2	318.7	351.2	STIFF	1.527
	TORSIONAL MOMENT (4)	8681.4	11337.8	8722.6	11473.6	9627.5	11063.2	11107.4	11473.6	NOM	1.353
	TRANSVERSE MOMENT (5)	71026.3	91091.6	82203.6	104359.6	92590.5	108730.5	98325.4	108730.5	STIFF	1.514
	LONGITUDINAL MOMENT (6)	12376.5	29148.0	26367.2	30913.4	27901.5	32465.7	31126.9	31126.9	STIFF	2.757
	TRANSVERSE MOMENT (11)	76323.3	96655.5	87469.4	111050.5	90730.0	115723.5	92659.1	115723.5	STIFF	1.516
	LONGITUDINAL MOMENT (12)	15613.2	34188.9	31226.9	36115.0	32359.4	37908.1	30752.4	38752.4	STIFF	2.516
246	AXIAL FORCE (1)	270.6	318.6	286.6	305.7	339.2	321.3	358.8	358.0	STIFF	1.326
	LONGITUDINAL SHEAR (2)	178.8	276.0	256.1	278.3	269.0	293.5	293.6	293.6	STIFF	1.642
	TRANSVERSE SHEAR (3)	348.9	376.7	370.7	441.4	416.0	465.5	429.3	465.5	STIFF	1.334
	TORSIONAL MOMENT (4)	8616.1	9912.1	13041.1	10900.1	13295.0	10756.2	12583.6	13295.0	NOM	1.543
	TRANSVERSE MOMENT (5)	61717.7	78824.5	73934.0	89372.0	82150.0	93469.0	84370.2	93469.0	STIFF	1.514
	LONGITUDINAL MOMENT (6)	11835.0	26907.2	29221.6	27252.0	30824.3	33083.4	32301.3	33683.4	STIFF	2.816
	TRANSVERSE MOMENT (11)	68700.8	86108.9	81246.5	98154.7	90406.5	102641.3	92973.8	102641.3	STIFF	1.494
	LONGITUDINAL MOMENT (12)	15360.2	31431.9	34329.0	32083.0	36707.6	39557.0	37903.4	39557.0	STIFF	2.575
247	AXIAL FORCE (1)	543.3	517.7	520.7	541.3	601.2	577.2	649.0	649.0	STIFF	1.194
	LONGITUDINAL SHEAR (2)	161.0	253.3	245.0	265.6	250.1	276.4	279.0	276.4	STIFF	1.717
	TRANSVERSE SHEAR (3)	254.5	327.4	319.2	371.2	330.8	399.6	363.1	399.6	STIFF	1.570
	TORSIONAL MOMENT (4)	10872.9	10888.3	11065.1	11818.2	12565.6	11554.9	13166.3	13166.3	STIFF	1.211
	TRANSVERSE MOMENT (5)	57874.1	75041.9	73053.4	86126.2	79900.8	93581.6	86637.7	93581.6	STIFF	1.617
	LONGITUDINAL MOMENT (6)	71655.0	28584.9	25350.4	29358.4	27040.6	30523.4	33025.0	33025.0	STIFF	2.031
	TRANSVERSE MOMENT (11)	62876.2	81651.4	79467.5	9357.0	86733.2	101612.0	93940.7	101612.0	STIFF	1.616
	LONGITUDINAL MOMENT (12)	14693.5	33614.0	20247.7	34413.3	31595.7	39825.6	38502.2	38502.2	STIFF	2.507
248	AXIAL FORCE (1)	439.0	443.3	516.8	469.8	541.4	483.0	541.2	541.4	NOM	1.233
	LONGITUDINAL SHEAR (2)	165.9	261.9	251.8	257.3	263.9	280.9	278.7	280.9	STIFF	1.693
	TRANSVERSE SHEAR (3)	286.7	347.9	348.3	303.7	376.3	416.9	403.9	416.9	STIFF	1.454
	TORSIONAL MOMENT (4)	7322.7	6286.5	6005.5	6379.1	6802.8	6764.2	6349.1	6349.1	STIFF	1.140
	TRANSVERSE MOMENT (5)	47897.5	64280.6	61961.1	73063.4	68030.6	70024.6	73779.3	70024.6	STIFF	1.616
	LONGITUDINAL MOMENT (6)	11793.4	21810.4	20624.6	27102.4	31179.8	32493.2	32331.8	32493.2	STIFF	2.792
	TRANSVERSE MOMENT (11)	53700.5	70675.7	68805.2	80562.0	76240.2	87180.3	81073.6	87180.3	STIFF	1.623
	LONGITUDINAL MOMENT (12)	14891.3	30040.3	33465.6	31937.8	36457.1	30065.3	39505.6	38505.6	STIFF	2.506
305	AXIAL FORCE (1)	1467.9	895.3	934.4	967.5	1034.9	1013.6	1014.1	1034.9	NOM	2.212
	LONGITUDINAL SHEAR (2)	662.1	1039.4	978.7	1063.8	1029.3	1106.1	1116.9	1116.9	STIFF	1.607
	TRANSVERSE SHEAR (3)	1112.0	1329.6	1313.9	1535.0	1440.0	1633.1	1511.1	1633.1	STIFF	1.468
	TORSIONAL MOMENT (4)	48566.6	49305.6	49565.9	65246.7	50724.0	60603.1	43470.5	65246.7	NOM	1.343
	TRANSVERSE MOMENT (5)	209039.4	53626.0	21482.6	587941.2	73379.7	627058.0	97220.6	627058.0	STIFF	3.004
	LONGITUDINAL MOMENT (6)	107918.7	163987.5	44670.9	165953.9	54904.4	185713.0	87265.3	187625.3	STIFF	1.730
	TRANSVERSE MOMENT (11)	211047.6	530156.5	16562.1	591848.5	67664.6	621417.3	91200.9	621417.3	STIFF	2.944
	LONGITUDINAL MOMENT (12)	109824.0	159833.2	40003.7	161864.9	51216.2	181310.4	63363.2	183363.2	STIFF	1.670

UNITS: FORCES - KIPS  
MOMENTS - KIP-IN

TABLE 4.4B: COMPARISON BETWEEN CLASSI COUPLED SSI RESULTS AND LLNL RESPAN RESULTS  
SUMMARY OF VESSEL END CELL SUPPORT LEG FORCES

PAGE 2

ELMT NO.	COMPONENT	LLNL RESPAN ANALYSIS			COUPLED SSI ANALYSIS			MAX CPLD LLNL
		SOFT SOIL	NOMINAL SOIL	STIFF SOIL	MAX CPLD			
253	AXIAL FORCE (1)	116.5	99.7	97.8	108.2	103.6	108.9	108.9 STIFF .935
	LONGITUDINAL SHEAR (2)	6.3	8.1	7.9	8.5	8.2	9.4	10.0 NOM 1.578
	TRANSVERSE SHEAR (3)	95.4	107.0	99.9	118.2	112.0	115.5	118.2 NOM 1.239
	TORSIONAL MOMENT (4)	116.0	147.4	132.1	154.7	140.4	166.2	176.4 STIFF 1.520
	TRANSVERSE MOMENT (5)	11125.4	14867.1	14081.5	16179.6	15925.0	15937.3	16463.0 STIFF 1.480
	LONGITUDINAL MOMENT (6)	397.8	505.1	492.6	532.1	516.0	594.6	627.6 STIFF 1.578
253	TRANSVERSE MOMENT (11)	11168.8	14900.8	1429.8	16230.4	15980.0	15993.2	16519.1 STIFF 1.479
	LONGITUDINAL MOMENT (12)	400.9	500.0	496.3	536.1	519.9	593.0	632.3 STIFF 1.577
	AXIAL FORCE (1)	94.2	94.0	75.8	106.5	91.8	111.2	111.2 STIFF 1.180
	LONGITUDINAL SHEAR (2)	5.0	6.4	6.2	6.7	6.5	7.8	7.8 STIFF 1.547
	TRANSVERSE SHEAR (3)	145.3	136.5	135.0	155.6	140.0	157.7	147.6 STIFF 1.086
	TORSIONAL MOMENT (4)	57.0	71.1	59.2	74.0	65.0	76.7	81.7 STIFF 1.115
253	TRANSVERSE MOMENT (5)	7932.1	10504.3	10019.0	10989.2	10606.1	10572.0	10267.9 NOM 1.393
	LONGITUDINAL MOMENT (6)	340.3	426.3	413.5	496.0	435.8	520.1	513.3 STIFF 1.528
	TRANSVERSE MOMENT (11)	8000.5	10563.7	10088.4	11049.6	10762.1	10652.6	10339.9 NOM 1.361
	LONGITUDINAL MOMENT (12)	342.3	429.3	416.4	449.1	430.8	523.6	516.9 STIFF 1.530
	AXIAL FORCE (1)	256.5	202.9	212.7	209.3	231.8	217.4	263.7 STIFF 1.028
	LONGITUDINAL SHEAR (2)	139.0	177.0	165.7	186.5	173.7	204.3	217.1 STIFF 1.553
253	TRANSVERSE SHEAR (3)	122.6	152.0	166.8	171.2	183.1	176.0	185.7 STIFF 1.515
	TORSIONAL MOMENT (4)	2539.1	3076.1	3013.9	3206.6	3175.4	3691.0	3784.0 STIFF 1.490
	TRANSVERSE MOMENT (5)	27759.5	34020.9	35298.0	37956.7	30361.5	41714.3	40374.8 STIFF 1.503
	LONGITUDINAL MOMENT (6)	9019.2	11522.1	10910.4	12102.6	11354.1	13304.7	14137.4 STIFF 1.567
	TRANSVERSE MOMENT (11)	27658.9	34083.4	35380.5	30028.7	30152.4	41792.7	40456.0 STIFF 1.500
	LONGITUDINAL MOMENT (12)	9050.0	11610.1	10900.2	12194.9	11440.0	13405.8	14244.8 STIFF 1.567
272	AXIAL FORCE (1)	343.9	333.3	258.0	329.5	314.7	322.2	361.3 STIFF 1.051
	LONGITUDINAL SHEAR (2)	157.3	197.9	183.5	206.6	194.2	235.9	234.5 STIFF 1.490
	TRANSVERSE SHEAR (3)	183.6	229.4	193.4	263.2	225.8	274.7	239.0 STIFF 1.197
	TORSIONAL MOMENT (4)	3741.0	4567.0	4055.9	4761.3	4340.2	5157.1	5767.6 STIFF 1.464
	TRANSVERSE MOMENT (5)	9575.4	15692.2	16663.2	17897.3	15784.4	17971.7	15939.2 STIFF 1.877
	LONGITUDINAL MOMENT (6)	9711.9	12193.3	11525.2	12750.6	12212.2	14653.9	14226.0 STIFF 1.509
272	TRANSVERSE MOMENT (11)	9588.4	15804.3	16742.7	18019.1	15875.0	18091.3	15931.3 STIFF 1.887
	LONGITUDINAL MOMENT (12)	9792.1	12290.7	11615.5	12052.2	12307.0	14769.3	14611.2 STIFF 1.568
	AXIAL FORCE (1)	350.0	271.6	261.7	329.3	275.6	351.6	282.0 STIFF 1.004
	LONGITUDINAL SHEAR (2)	140.5	177.1	167.0	187.8	176.1	206.0	217.9 STIFF 1.551
	TRANSVERSE SHEAR (3)	179.3	196.1	168.6	223.5	189.3	231.8	197.4 STIFF 1.293
	TORSIONAL MOMENT (4)	4374.4	5112.1	5368.5	5699.3	5663.2	6515.1	6778.8 STIFF 1.550
280	TRANSVERSE MOMENT (5)	22790.9	28656.3	24309.0	31911.2	29471.9	33920.1	31921.4 STIFF 1.408
	LONGITUDINAL MOMENT (6)	10089.7	12893.8	11936.5	13790.4	12761.7	14864.4	15927.9 STIFF 1.569
	TRANSVERSE MOMENT (11)	22691.2	28755.9	24274.8	32025.8	29567.3	34039.4	32021.3 STIFF 1.487
	LONGITUDINAL MOMENT (12)	10150.6	12980.4	12018.6	13832.3	12847.2	14989.5	15934.7 STIFF 1.570
	AXIAL FORCE (1)	305.5	270.4	255.8	304.1	237.2	303.6	246.5 NOM 0.995
	LONGITUDINAL SHEAR (2)	143.4	180.4	173.0	189.4	183.6	218.0	215.8 STIFF 1.525
286	TRANSVERSE SHEAR (3)	152.1	152.8	152.7	174.2	170.3	184.5	175.8 STIFF 1.213
	TORSIONAL MOMENT (4)	4533.3	5599.5	5453.7	5088.6	5770.7	6784.9	6846.6 STIFF 1.510
	TRANSVERSE MOMENT (5)	7268.6	10716.9	11520.3	12267.4	12569.7	12607.3	12460.9 STIFF 1.735
	LONGITUDINAL MOMENT (6)	10240.7	12983.0	12466.4	13660.5	13262.1	15826.2	15545.4 STIFF 1.545
	TRANSVERSE MOMENT (11)	7322.2	10779.9	11596.3	12348.7	12651.3	12688.7	12547.8 STIFF 1.733

TABLE 4-4B CONT.

292	AXIAL FORCE (11)	311.2	349.9	394.4	375.1	434.5	365.9	434.8	434.8	STIFF
	LONGITUDINAL SHEAR (12)	5.0	6.5	6.2	6.9	6.5	7.5	7.5	7.5	STIFF
	TRANSVERSE SHEAR (13)	63.0	97.1	84.8	96.1	95.1	96.0	98.1	98.1	STIFF
	TRANSLATIONAL MOMENT (4)	41.3	42.0	53.4	40.6	56.1	57.7	57.3	57.7	STIFF
	TRANSVERSE MOMENT (5)	5659.1	6060.3	4551.5	5938.6	4681.9	6003.4	5257.3	6060.3	SOFT
	LONGITUDINAL MOMENT (6)	255.1	329.1	510.6	352.0	326.0	303.5	401.4	407.5	STIFF
	TRANSVERSE MOMENT (11)	5851.4	6080.5	6762.1	5932.7	6727.3	6026.1	5105.6	6090.5	SOFT
	LONGITUDINAL MOMENT (12)	258.2	332.4	313.7	395.5	331.7	380.3	411.5	411.5	STIFF
293	AXIAL FORCE (11)	290.3	400.8	358.4	468.5	390.1	392.6	385.7	408.5	NDH
	LONGITUDINAL SHEAR (12)	5.1	6.9	6.1	7.2	6.6	7.9	7.9	7.9	STIFF
	TRANSVERSE SHEAR (13)	116.2	132.2	132.8	148.5	147.6	165.7	164.7	166.7	STIFF
	TRANSLATIONAL MOMENT (4)	43.4	51.7	47.2	53.3	50.1	59.2	62.5	62.5	STIFF
	TRANSVERSE MOMENT (5)	48011.7	5016.9	7244.2	5351.6	7269.0	5739.2	6354.2	7269.0	NDH
	LONGITUDINAL MOMENT (6)	261.8	344.4	312.1	361.6	335.9	405.6	403.8	403.6	STIFF
	TRANSVERSE MOMENT (11)	4822.9	5301.2	7295.8	5165.3	7321.3	5801.0	6101.1	7321.3	NDH
	LONGITUDINAL MOMENT (12)	263.6	347.6	315.2	365.2	339.2	409.6	407.9	409.6	STIFF

UNITS: FORCES - KIPS  
MOMENTS - KIP-IN

TABLE 4.4C: COMPARISON BETWEEN CLASS1 COUPLED SSI RESULTS AND LLNL RESPAN RESULTS  
SUMMARY OF MAGNET HANGER AND STRUT FORCES

PAGE 2

ELMT NO.	LLNL RESPAN ANALYSIS	COUPLED SSI ANALYSIS						MAX CPLD LLNL
		SOFT SOIL		NOMINAL SOIL		STIFF SOIL		
313	243.6	199.3	209.5	241.4	231.5	296.4	267.9	226.4 STIFF 1.176
314	227.7	209.3	192.8	245.2	239.8	268.7	271.7	271.7 STIFF 1.193
315	334.1	289.0	291.5	342.7	299.1	359.0	320.7	359.0 STIFF 1.075
316	538.9	483.4	449.4	562.7	505.5	582.8	529.6	582.8 STIFF 1.082
317	526.8	557.4	527.7	610.7	590.3	599.8	623.7	623.7 STIFF 1.184
318	555.7	530.7	504.5	590.2	560.9	637.9	551.7	637.9 STIFF 1.146
319	67.9	93.4	94.4	94.5	103.0	77.0	80.6	103.0 NOM 1.517
320	26.3	34.5	35.6	39.7	40.4	40.0	40.5	40.5 STIFF 1.539
321	74.4	80.8	78.9	85.8	78.3	83.5	85.3	93.5 STIFF 1.257
322	21.5	23.0	22.7	23.3	27.8	22.1	23.2	27.8 NOM 1.292
323	9.6	7.4	8.4	8.3	9.5	8.7	10.3	10.3 STIFF 1.074
324	38.1	43.4	43.5	40.9	43.6	45.0	45.1	45.1 STIFF 1.162
325	139.2	141.4	115.8	160.0	133.2	164.4	141.0	164.4 STIFF 1.181
326	79.2	68.8	59.9	71.4	71.9	75.5	86.5	86.5 STIFF 1.092
327	81.0	73.1	70.6	80.7	80.9	87.6	80.9	97.6 STIFF 1.092
328	122.2	111.6	108.7	127.5	123.0	137.6	123.0	137.6 STIFF 1.126
329	25.9	30.4	30.1	33.6	35.0	32.6	38.8	38.8 STIFF 1.443
330	32.1	35.6	34.3	35.8	37.8	41.5	37.8	41.5 STIFF 1.292
331	56.3	64.1	58.2	64.9	64.6	70.6	69.6	70.6 STIFF 1.253
332	51.4	53.2	60.9	62.8	64.8	66.9	57.5	66.9 STIFF 1.302
333	13.4	17.6	16.1	18.2	17.5	17.0	18.7	18.7 STIFF 1.353
334	16.9	18.5	19.3	20.9	21.4	22.1	22.5	22.5 STIFF 1.330
335	36.1	44.7	42.6	46.1	41.6	48.2	44.5	48.2 STIFF 1.333
336	11.7	12.2	12.3	13.4	12.7	13.7	12.3	13.7 STIFF 1.177
337	14.2	15.6	14.4	16.6	14.4	14.8	14.2	16.6 NOM 1.170
338	34.9	37.4	36.0	37.8	38.8	41.3	43.2	43.2 STIFF 1.238
339	15.1	22.2	18.2	22.0	19.5	14.1	12.5	22.0 NOM 1.455
340	15.0	18.8	17.3	19.3	16.6	17.1	14.0	19.3 NOM 1.290
341	59.4	57.7	53.0	62.6	57.8	67.6	66.5	67.6 STIFF 1.138
342	50.0	52.9	43.9	54.4	50.5	54.3	52.7	54.4 NOM 1.088
343	49.9	44.0	52.1	47.1	57.4	54.9	57.4	57.4 STIFF 1.152
344	44.2	46.1	43.6	46.4	45.9	50.6	52.5	52.5 STIFF 1.187
345	53.2	53.1	49.7	53.5	59.5	59.1	65.1	66.1 STIFF 1.243
346	8.8	5.4	5.2	7.0	7.0	7.9	8.1	8.1 STIFF .922
347	8.2	7.0	6.1	7.1	5.9	7.0	6.7	7.1 NOM .862
348	16.9	15.9	16.7	16.5	18.5	21.2	20.5	21.2 STIFF 1.256
349	16.0	12.6	12.9	15.3	16.3	18.0	18.8	18.8 STIFF 1.117
350	14.5	15.1	15.3	15.8	16.1	16.6	16.7	16.7 STIFF 1.150
351	36.6	34.3	34.2	38.6	37.5	40.8	41.0	41.0 STIFF 1.121
352	14.2	14.4	14.7	14.7	14.7	15.4	15.6	15.6 STIFF 1.099
353	14.1	16.0	15.7	15.4	14.5	15.7	14.2	16.0 SOFT 1.132
354	46.0	44.0	44.5	46.2	46.4	50.1	50.6	50.6 STIFF 1.102
355	25.6	26.5	21.9	30.0	26.9	31.8	30.3	31.8 STIFF 1.243
356	25.3	22.2	26.6	26.3	29.1	30.1	32.7	32.7 STIFF 1.290
357	24.7	22.7	25.0	28.8	28.4	29.9	29.7	29.9 STIFF 1.210
358	26.9	27.9	24.4	28.1	27.9	29.5	30.1	30.1 STIFF 1.119
359	8.5	7.5	8.7	8.0	9.5	9.5	9.9	9.9 STIFF 1.162
360	9.9	10.0	10.1	10.6	10.0	10.9	11.7	11.7 STIFF 1.183
361	9.1	9.6	8.4	9.4	10.4	10.1	11.3	11.3 STIFF 1.234
362	10.5	10.7	9.4	11.1	10.4	11.6	11.4	11.6 STIFF 1.099
363	39.1	34.5	40.7	36.8	44.9	43.0	45.0	45.0 STIFF 1.150
364	34.9	35.1	35.7	36.9	36.6	39.0	41.5	41.5 STIFF 1.188

1  
TABLE 4.4C CONT.

365	43.1	43.6	40.9	42.0	47.9	45.4	51.6	51.6 STIFF	1.195
366	39.5	40.8	34.9	42.0	39.9	43.2	42.1	43.2 STIFF	1.091
367	10.9	11.9	10.0	12.0	11.4	12.3	12.6	12.6 STIFF	1.156
368	13.0	11.2	14.2	12.8	12.4	12.7	12.9	14.2 SOFT	1.099
369	9.4	9.2	9.9	10.2	10.8	10.2	11.2	11.2 STIFF	1.187
370	12.2	14.7	10.9	14.6	12.5	12.8	13.4	14.7 SOFT	1.207
371	4.7	5.2	4.1	5.8	4.9	6.1	5.3	6.1 STIFF	1.209
372	4.6	3.9	4.6	4.5	5.1	5.7	5.9	5.9 STIFF	1.279
373	4.5	4.6	4.4	5.1	4.9	5.8	5.7	5.8 STIFF	1.276
374	4.7	3.9	4.5	4.8	5.1	5.4	5.4	6.4 STIFF	1.155
375	15.2	15.1	13.0	18.4	15.5	19.6	17.2	19.6 STIFF	1.266
376	14.9	13.0	15.3	14.6	16.9	18.1	18.5	18.5 STIFF	1.247
377	14.5	13.2	14.8	16.9	16.2	17.7	18.1	18.1 STIFF	1.252
378	16.3	16.0	15.5	15.9	17.0	17.8	17.7	17.8 STIFF	1.089

COMPONENT: AXIAL  
UNITS: FORCES - KIPS

with an average increase of 20%. This increase was about the same regardless of orientation of the member. Generally, variations from the average were less than 10% for horizontal members and about 20% for vertical members.

#### 4.2.3 Effects of Increased Damping in the Vessel

We investigated the effect that increasing the damping assumed for the vessel has on response by reanalyzing the coupled vessel/vault SSI case using 10% damping for all vessel modes. Only best-estimate soil properties were used for this reanalysis. The results were compared with those from our coupled SSI analysis with composite modal damping and best-estimate soil properties. This comparison is summarized in Tables 4.5A through 4.5C.

Our comparison showed that, overall, forces decreased by about 15%. Foundation forces (Table 4.5A) were reduced on the average by about 10% for both center and end cell forces. Transverse foundation forces decreased more (15 - 20%) than did longitudinal forces (about 5%). Support leg forces (Table 4.5B) showed the same trends. Magnet hanger forces (Table 4.5C) were reduced about 20%. Vertical and transverse struts experienced higher reductions (about 30%) while longitudinal and drag struts were reduced less (about 15%).

TABLE 4.5A: COMPARISON BETWEEN CLASSI: COUPLED SSI ANALYSES  
FOR 10% DAMPING AND COMPOSITE MODAL DAMPING  
SUMMARY OF FOUNDATION FORCES

ELEM	COMPONENT	COUPLED SSI ANALYSES NOMINAL SOIL PROPERTIES				RATIO (1) (2)
		10% DAMPING (1)		COMPOSITE MODAL DAMPING (2)		
COLUMN BASES SUPPORTING CENTER CELL BOX BEAM						
388	AXIAL FORCE (1)	323.2	325.5	358.1	363.6	.895
	LONGITUDINAL SHEAR (2)	217.6	197.8	228.4	210.2	.953
	TRANSVERSE SHEAR (3)	10.3	10.9	11.6	13.5	.808
	TORSIONAL MOMENT (4)	378.3	338.3	438.8	368.9	.862
	TRANSVERSE MOMENT (5)	4412.5	4070.5	5234.9	4653.3	.843
	LONGITUDINAL MOMENT (6)	1368.7	1432.5	1422.5	1494.2	.959
	TRANSVERSE MOMENT (11)	4122.8	3838.7	4691.7	4400.7	.843
	LONGITUDINAL MOMENT (12)	7676.1	7167.4	8059.2	7495.5	.956
389	AXIAL FORCE (1)	288.2	305.8	341.8	334.4	.895
	LONGITUDINAL SHEAR (2)	202.5	215.7	212.5	225.0	.958
	TRANSVERSE SHEAR (3)	3.7	3.9	4.3	4.0	.924
	TORSIONAL MOMENT (4)	364.3	402.9	417.1	465.4	.864
	TRANSVERSE MOMENT (5)	4019.2	4247.3	4651.2	4968.7	.855
	LONGITUDINAL MOMENT (6)	1455.6	1364.2	1536.7	1405.6	.947
	TRANSVERSE MOMENT (11)	4041.6	4226.4	4743.0	4978.2	.849
	LONGITUDINAL MOMENT (12)	7327.6	7618.6	7700.0	7930.0	.861
390	AXIAL FORCE (1)	214.6	191.4	244.3	216.9	.879
	LONGITUDINAL SHEAR (2)	166.0	212.4	201.4	222.4	.956
	TRANSVERSE SHEAR (3)	10.5	11.4	14.0	12.8	.815
	TORSIONAL MOMENT (4)	327.4	311.9	387.4	357.3	.845
	TRANSVERSE MOMENT (5)	4302.2	4178.4	5094.3	4744.1	.845
	LONGITUDINAL MOMENT (6)	1997.3	2035.5	2077.4	2122.1	.959
	TRANSVERSE MOMENT (11)	4501.7	4220.4	5263.2	4602.5	.855
	LONGITUDINAL MOMENT (12)	7391.0	8194.2	7820.9	8572.7	.956
391	AXIAL FORCE (1)	187.3	190.4	211.7	217.7	.875
	LONGITUDINAL SHEAR (2)	213.0	187.7	224.7	203.3	.948
	TRANSVERSE SHEAR (3)	18.2	17.6	19.2	20.0	.908
	TORSIONAL MOMENT (4)	354.4	358.0	408.3	425.4	.842
	TRANSVERSE MOMENT (5)	4457.7	4471.0	5071.0	5281.7	.847
	LONGITUDINAL MOMENT (6)	2059.6	1992.0	2165.9	2050.0	.951
	TRANSVERSE MOMENT (11)	4043.8	4956.5	5525.4	5863.0	.845
	LONGITUDINAL MOMENT (12)	8236.2	7433.6	8892.5	7900.1	.949
400	AXIAL FORCE (1)	395.5	355.2	417.1	417.3	.950
	LONGITUDINAL SHEAR (2)	826.9	821.6	864.7	852.8	.956
	TRANSVERSE SHEAR (3)	435.7	436.3	521.1	509.9	.837
	TORSIONAL MOMENT (4)	9843.0	7892.9	12060.1	9129.6	.816
	TRANSVERSE MOMENT (5)	150103.8	150211.4	176265.0	173293.2	.852
	LONGITUDINAL MOMENT (6)	69327.1	68710.3	72525.9	71402.9	.956
	TRANSVERSE MOMENT (11)	150980.9	151089.3	177304.2	174310.9	.852
	LONGITUDINAL MOMENT (12)	71009.8	70392.2	74285.5	73138.5	.956

1  
TABLE 4.5A CONT.

PIER BASES IN END CELL						
245	AXIAL FORCE (1)	191.0	213.0	203.4	233.5	.912
	LONGITUDINAL SHEAR (2)	252.7	237.3	267.9	246.5	.944
	TRANSVERSE SHEAR (3)	275.5	263.0	339.0	311.1	.813
	TORSIONAL MOMENT (4)	10775.4	8978.4	11473.6	9627.5	.939
	TRANSVERSE MOMENT (5)	84266.4	77672.7	104359.6	92598.5	.807
	LONGITUDINAL MOMENT (6)	29123.0	26379.0	30913.4	27901.5	.942
	TRANSVERSE MOMENT (11)	69713.5	82288.7	111058.5	98739.8	.808
	LONGITUDINAL MOMENT (12)	34082.0	30986.9	36115.0	32359.4	.944
246	AXIAL FORCE (1)	288.3	288.5	305.7	339.2	.850
	LONGITUDINAL SHEAR (2)	264.7	255.9	278.3	269.0	.951
	TRANSVERSE SHEAR (3)	357.0	353.5	441.2	416.0	.809
	TORSIONAL MOMENT (4)	9917.4	12066.8	10909.1	13295.8	.908
	TRANSVERSE MOMENT (5)	72859.4	68725.1	69372.8	82159.0	.815
	LONGITUDINAL MOMENT (6)	25369.2	29150.0	27252.0	30824.3	.946
	TRANSVERSE MOMENT (11)	79561.9	75769.3	98154.7	90466.5	.815
	LONGITUDINAL MOMENT (12)	30555.7	34184.8	32093.4	36078.6	.948
247	AXIAL FORCE (1)	464.6	507.9	541.3	601.2	.845
	LONGITUDINAL SHEAR (2)	250.6	239.7	265.6	280.1	.943
	TRANSVERSE SHEAR (3)	309.3	284.2	371.2	338.8	.831
	TORSIONAL MOMENT (4)	10233.6	10776.3	11918.2	12565.6	.858
	TRANSVERSE MOMENT (5)	71093.1	67326.9	66126.2	79950.9	.825
	LONGITUDINAL MOMENT (6)	27755.4	25125.6	29358.4	27049.6	.945
	TRANSVERSE MOMENT (11)	77222.1	78918.5	93457.0	86733.2	.825
	LONGITUDINAL MOMENT (12)	32487.5	29783.3	34413.3	31595.7	.944
248	AXIAL FORCE (1)	420.0	476.5	469.8	541.4	.880
	LONGITUDINAL SHEAR (2)	246.5	250.0	257.3	263.9	.947
	TRANSVERSE SHEAR (3)	314.9	320.1	383.7	376.3	.834
	TORSIONAL MOMENT (4)	5955.1	5801.2	6379.1	6882.8	.864
	TRANSVERSE MOMENT (5)	60402.5	57928.9	73063.4	66839.5	.827
	LONGITUDINAL MOMENT (6)	24381.5	28907.3	27402.4	31179.8	.927
	TRANSVERSE MOMENT (11)	65620.3	64256.9	80562.0	76240.2	.827
	LONGITUDINAL MOMENT (12)	29266.2	33776.9	31937.8	36457.1	.926
305	AXIAL FORCE (1)	840.6	922.7	957.5	1034.9	.892
	LONGITUDINAL SHEAR (2)	1012.4	982.6	1063.8	1029.3	.952
	TRANSVERSE SHEAR (3)	1255.6	1220.7	1535.0	1440.8	.818
	TORSIONAL MOMENT (4)	43359.0	35606.3	65246.7	50724.0	.665
	TRANSVERSE MOMENT (5)	490449.0	482471.3	557941.2	573379.7	.820
	LONGITUDINAL MOMENT (6)	160518.7	141051.4	165953.9	154904.4	.968
	TRANSVERSE MOMENT (11)	485702.5	477616.8	591848.5	567846.2	.821
	LONGITUDINAL MOMENT (12)	156652.3	137193.9	161654.9	151216.2	.968

UNITS: FORCES - KIPS  
MOMENTS - KIP-IN

TABLE 4.53: COMPARISON BETWEEN CLASSI COUPLED SSI ANALYSES  
FOR 10% DAMPING AND COMPOSITE MODAL DAMPING  
SUMMARY OF VESSEL END CELL SUPPORT LEG FORCES

ELEM NO.	COMPONENT	COUPLED SSI ANALYSES NOMINAL SOIL PROPERTIES			RATIO (1) (2)
		10% DAMPING (1)	COMPOSITE MODAL DAMPING (2)		
253	AXIAL FORCE (1)	100.0	94.8	108.2	103.6 .924
	LONGITUDINAL SHEAR (2)	8.1	7.9	8.5	8.2 .950
	TRANSVERSE SHEAR (3)	99.7	94.6	116.2	112.0 .844
	TORSIONAL MOMENT (4)	147.0	133.7	154.7	140.4 .950
	TRANSVERSE MOMENT (5)	13323.3	13316.5	16179.6	15925.0 .823
	LONGITUDINAL MOMENT (6)	506.4	496.1	532.1	516.0 .952
	TRANSVERSE MOMENT (11)	13372.3	13363.4	16228.4	15980.0 .823
259	AXIAL FORCE (1)	94.9	75.9	106.5	91.8 .891
	LONGITUDINAL SHEAR (2)	6.4	6.3	6.7	6.5 .956
	TRANSVERSE SHEAR (3)	131.5	129.1	155.6	148.8 .845
	TORSIONAL MOMENT (4)	70.3	59.0	74.8	65.0 .940
	TRANSVERSE MOMENT (5)	9098.4	9201.7	10559.2	10566.1 .839
	LONGITUDINAL MOMENT (6)	424.4	419.3	446.0	435.8 .951
	TRANSVERSE MOMENT (11)	9165.6	9264.8	11048.6	10762.1 .839
265	AXIAL FORCE (1)	203.9	213.0	209.3	231.8 .919
	LONGITUDINAL SHEAR (2)	177.4	167.8	166.5	173.7 .951
	TRANSVERSE SHEAR (3)	145.4	158.1	171.2	163.1 .863
	TORSIONAL MOMENT (4)	3072.8	3027.6	3205.6	3175.4 .958
	TRANSVERSE MOMENT (5)	31979.4	32708.1	37956.7	38361.5 .853
	LONGITUDINAL MOMENT (6)	11508.9	10958.4	12102.6	11354.1 .951
	TRANSVERSE MOMENT (11)	32051.3	32797.1	38029.7	38452.4 .853
272	AXIAL FORCE (1)	312.8	261.4	329.5	314.7 .849
	LONGITUDINAL SHEAR (2)	196.0	187.3	205.6	194.2 .949
	TRANSVERSE SHEAR (3)	216.0	189.9	263.2	225.8 .821
	TORSIONAL MOMENT (4)	4542.0	4092.7	4761.3	4340.2 .954
	TRANSVERSE MOMENT (5)	15707.2	13440.8	17897.3	15784.4 .878
	LONGITUDINAL MOMENT (6)	12096.3	11767.1	12750.6	12212.2 .949
	TRANSVERSE MOMENT (11)	15811.9	13518.4	18019.4	15875.0 .877
	LONGITUDINAL MOMENT (12)	12192.7	11859.3	12852.2	12307.8 .949

I  
TABLE 4.59 CONT.

280	AXIAL FORCE (1)	283.1	242.2	329.3	275.6	.860
	LONGITUDINAL SHEAR (2)	177.6	169.6	187.8	176.1	.946
	TRANSVERSE SHEAR (3)	183.1	157.6	223.5	189.3	.819
	TORSIONAL MOMENT (4)	5451.9	5420.4	5659.3	5653.2	.957
	TRANSVERSE MOMENT (5)	29969.4	24217.5	31911.2	29471.9	.814
	LONGITUDINAL MOMENT (6)	12955.3	12165.3	13740.4	12761.7	.943
	TRANSVERSE MOMENT (11)	26063.4	24297.4	32025.8	29567.3	.814
	LONGITUDINAL MOMENT (12)	13043.2	12248.7	13832.3	12847.2	.943
286	AXIAL FORCE (1)	270.5	214.9	304.1	237.2	.890
	LONGITUDINAL SHEAR (2)	180.0	176.7	189.4	183.6	.951
	TRANSVERSE SHEAR (3)	141.3	143.5	174.2	170.3	.824
	TORSIONAL MOMENT (4)	5610.7	5529.6	5888.6	5770.7	.954
	TRANSVERSE MOMENT (5)	10083.9	10647.8	12257.4	12569.7	.847
	LONGITUDINAL MOMENT (6)	12974.6	12757.7	13660.5	13252.1	.950
	TRANSVERSE MOMENT (11)	10151.9	10715.9	12348.7	12654.3	.847
	LONGITUDINAL MOMENT (12)	13065.8	12857.2	13756.4	13355.1	.950
292	AXIAL FORCE (1)	332.8	389.5	375.1	434.5	.896
	LONGITUDINAL SHEAR (2)	6.5	6.3	6.9	6.5	.942
	TRANSVERSE SHEAR (3)	82.6	81.3	96.1	95.1	.859
	TORSIONAL MOMENT (4)	42.5	52.5	48.6	56.1	.936
	TRANSVERSE MOMENT (5)	5295.8	4473.4	5939.8	4684.9	.892
	LONGITUDINAL MOMENT (6)	331.5	315.7	352.0	328.4	.942
	TRANSVERSE MOMENT (11)	5310.0	4506.7	5962.7	4727.3	.892
	LONGITUDINAL MOMENT (12)	334.7	318.9	355.5	331.7	.942
299	AXIAL FORCE (1)	369.1	353.0	408.5	390.1	.904
	LONGITUDINAL SHEAR (2)	6.8	6.3	7.2	6.6	.950
	TRANSVERSE SHEAR (3)	121.2	125.5	148.5	147.6	.845
	TORSIONAL MOMENT (4)	51.4	47.6	53.3	50.1	.953
	TRANSVERSE MOMENT (5)	5005.8	6381.4	5391.6	7269.0	.875
	LONGITUDINAL MOMENT (6)	343.2	321.4	361.6	335.9	.949
	TRANSVERSE MOMENT (11)	5065.3	6406.2	5465.3	7321.3	.875
	LONGITUDINAL MOMENT (12)	346.6	324.5	365.2	339.2	.949

UNITS: FORCES - KIPS  
MOMENTS - KIP-IN

TABLE 4.5C: COMPARISON BETWEEN CLASSI COUPLED SSI ANALYSES  
FOR 10% DAMPING AND COMPOSITE MODAL DAMPING  
SUMMARY OF MAGNET HANGER AND STRUT FORCES

ELEM NO.	COUPLED SSI ANALYSES NOMINAL SOIL PROPERTIES				RATIO (1) (2)
	10% DAMPING (1)	COMPOSITE MODAL DAMPING (2)	10% DAMPING (1)	COMPOSITE MODAL DAMPING (2)	
313	176.9	187.6	241.4	231.5	.777
314	201.6	198.8	245.2	239.8	.822
315	251.2	254.8	342.7	299.1	.762
316	452.9	421.3	562.7	505.5	.805
317	522.0	516.6	610.7	590.3	.855
318	522.9	489.2	590.2	560.9	.886
319	59.6	56.2	94.5	103.0	.579
320	29.9	19.0	39.7	40.4	.517
321	68.1	66.0	85.6	78.3	.795
322	18.3	19.0	23.3	27.8	.684
323	5.7	6.3	8.3	9.5	.662
324	33.7	34.6	40.9	43.6	.794
325	134.6	116.3	160.0	133.2	.841
326	67.3	62.2	71.4	71.9	.935
327	72.7	70.3	80.1	80.9	.899
328	111.2	106.3	127.5	123.0	.873
329	23.5	21.5	33.6	36.0	.692
330	33.9	33.1	36.8	37.8	.896
331	54.3	53.2	64.9	64.6	.837
332	42.9	41.0	62.8	64.8	.662
333	14.7	14.4	18.2	17.5	.804
334	13.5	13.5	20.9	21.4	.633
335	33.8	34.0	46.1	41.6	.736
336	10.1	10.7	13.4	12.7	.799
337	11.4	10.0	16.8	14.4	.690
338	29.7	30.4	37.8	38.8	.781
339	12.4	11.7	22.0	19.5	.564
340	12.0	11.1	19.3	16.6	.623
341	44.2	41.1	62.8	57.8	.706
342	48.6	38.4	54.4	50.5	.893
343	39.7	50.6	47.1	57.4	.881
344	43.6	35.2	48.4	45.9	.901
345	44.0	44.8	53.5	59.5	.753
346	4.6	4.4	7.0	7.0	.662
347	5.2	4.9	7.1	5.9	.730
348	14.3	14.7	16.5	18.5	.805
349	10.0	9.9	15.3	16.3	.616
350	8.6	8.7	15.8	16.1	.540
351	30.1	30.2	38.6	37.5	.782
352	11.5	11.6	14.7	14.7	.786
353	10.7	10.6	15.4	14.5	.695
354	35.9	36.4	46.2	46.4	.785
355	26.2	21.1	30.0	26.9	.874
356	21.3	26.6	26.3	29.1	.914
357	20.9	25.2	28.8	28.4	.877
358	25.9	21.4	28.1	27.9	.922
359	6.8	8.5	8.0	9.5	.894

TABLE 4.5C CON'T.

360	9.4	8.8	10.6	10.0	.886
361	8.2	7.9	2.4	10.4	.791
362	10.0	8.9	11.1	10.4	.904
363	29.9	39.4	35.8	44.9	.876
364	33.3	28.3	36.9	36.6	.903
365	35.5	36.4	42.0	47.9	.769
366	37.7	30.1	42.0	39.9	.898
367	10.9	8.6	12.0	11.4	.911
368	10.5	11.6	12.8	12.4	.901
369	8.6	8.8	10.2	10.8	.822
370	12.0	9.8	14.6	12.5	.819
371	5.1	3.9	5.8	4.9	.870
372	4.0	4.6	4.6	5.1	.908
373	4.3	4.3	5.1	4.9	.850
374	3.8	4.6	4.8	5.1	.906
375	15.2	11.7	18.4	15.5	.830
376	11.2	15.2	14.8	16.9	.897
377	12.0	13.9	16.9	16.2	.825
378	14.1	12.6	15.9	17.0	.827

UNITS: FORCES - KIPS

Vessel shell, support legs and magnets (welded stainless steel)	3%
Magnet hangers and struts (stainless steel, pinned connections)	5%
Foundation slabs, end cell piers and local soil springs (reinforced concrete)	10%
Center cell columns knees and cross-bracing (welded steel)	7%

To implement these values in the CLASSI SSI analyses we used the composite modal damping approach to determine an equivalent modal damping matrix for the structure. This method uses the assembled stiffness matrix of the individual element groups as weighting factors as shown in the formulation below:

$$\bar{\beta}_j = \frac{\{ \phi_j \}^T [\bar{K}] \{ \phi_j \}}{\{ \phi_j \}^T [K] \{ \phi_j \}}$$

where  $\bar{\beta}_j$  = equivalent modal damping ratio of the  $j$ th mode

$[K]$  = assembled structure stiffness matrix

$$[\bar{K}] = \sum_g \beta_g k_g \quad (\text{summed over element group})$$

The calculation of composite damping involved computer program SAPPAC, described in Ref. 7. The damping ratios we calculated are shown in Table 3.2.

## 5. CONCLUSIONS AND RECOMMENDATIONS

This report documents the seismic analyses performed by SMA for the MFTF-B Axicell vacuum vessel. In the course of this study we performed response spectrum analyses, CLASSI fixed-base analyses, and SSI analyses that included interaction effects between the vessel and vault. The response spectrum analysis served to benchmark certain modeling differences between the LLNL and SMA versions of the vessel model. The fixed-base analysis benchmarked the differences between analysis techniques. The SSI analyses provided our best estimate of vessel response to the postulated seismic excitation for the MFTF-B facility, and included consideration of uncertainties in soil properties by calculating response for a range of soil shear moduli. Our results are presented in this report as tables of comparisons of specific member forces from our analyses and the analyses performed by LLNL. Also presented are tables of maximum accelerations and relative displacements and plots of response spectra at various selected locations. Based on these results we made the following observations.

- The basic difference between the original LLNL vessel model and the revised model we used was in the way local soil flexibility beneath the foundation piers and support columns was represented. The effect of these modeling differences was most pronounced near the foundation; at the bases of the end cell piers, transverse bending moments increased by 15% and longitudinal bending moments increased by a factor of two; at the bases of the center cell support columns forces generally decreased by 20%. Forces in magnet hangers and struts were minimally affected (less than 5%).
- The effect of differences in analysis methods was an increase of 5% to 10% in CLASSI results over our response spectrum results. This difference was fairly uniform throughout the model and is within the range of differences one would expect between these two methods. At least part of the difference can be attributed to the difference between the frequency content of the time histories we used and the design spectra used for the response

spectrum analysis.

- The general effects of SSI and interaction with the vault were to reduce forces by 10 - 30%. Reductions in forces in foundation members and support legs were slightly higher than in magnet hangers and struts. Transverse forces generally experienced less reduction than did longitudinal forces. The overall reduction was about 20%, not as much as the 25% initially anticipated for the MFTF-B project, and used for its seismic design.
- The comparison of our best estimate results, enveloped for uncertainty in soil properties, with the LLNL analysis, using for input design spectra factored by 0.75, reflect the cumulative effects of the differences described above. Magnet hanger and strut forces calculated by CLASSI generally were 10% to 30% higher than the LLNL forces. Forces at the bases of the center cell support columns were generally 10% higher. Forces in the vessel end cell support legs were 40% to 50% higher. At the bases of the end cell piers, transverse bending moments were about 50% higher while longitudinal moments were higher by factors of 2.5 or more. In the transverse direction, the effect of model differences was responsible for over one-third of the increase (15%), the remainder coming from analysis methods (10%), enveloping effects (10%) and a less than average reduction due to SSI (15%). In the longitudinal direction the increase was predominantly due to modeling differences, namely the differences in rotational foundation stiffness and coupling effects between pier bases.
- An additional coupled SSI analysis showed that increasing modal damping in the vessel to 10% for all modes resulted in a reduction of 10% to 20% in calculated forces, compared to our best estimate results which used composite modal damping for the vessel.
- For structural members for which stresses are calculated using a

combination of force components, such as transverse and longitudinal bending moments at the bases of columns and piers, an inspection of the times at which the maxima occur showed that they do not generally coincide. In addition, in our previous investigation of the A-cell vessel (Ref. 1), a limited study showed that combination by direct superposition of stress time histories agreed reasonably well with maximum stresses combined using the SRSS (square-root-sum-of-squares) method. Thus it would appear that combination by the SRSS method is reasonable for the Axicell results.

- The differences between our results and the LLNL results are reported herein as ratios of maximum values without regard for the importance of the forces relative to other members or to design capacities. For example, the ratios between longitudinal bending moments at the bases of the piers from our best estimate analyses and from the LLNL response spectrum analysis were in excess of 2.5. The ratios for the transverse bending moments were about 1.5. However, transverse moments were generally three times as large as longitudinal moments. Thus the combined stress due to both would be expected to result in ratios closer to 1.5. As another example, ratios may be high for one of a number of identical members. However, unless the forces in that member control the design of all members, the results are not important.

In summary, the overall trend of a reduction in calculated vessel forces due to the combined effects of SSI and interaction with the vault was observed (although it was not quite as large as initially anticipated) when comparisons were made between comparable analysis methods using the same modeling assumptions. The use of different modeling assumptions was responsible for significant differences in calculated forces in some structural members, in particular the end cell piers. Considerable effort was spent by SMA in studying the different modelling assumptions. Based on this, we conclude that the representation we used was more appropriate for seismic analysis, assuming failure does not occur in any structural members. We recommend that the member forces presented in Tables 4.4A to 4.4C be reviewed

and used for comparison with design capacities. If excessive yielding should be observed to occur in any major structural elements, it may be of value to conduct a reanalysis using degraded properties.

## 6. REFERENCES

1. Maslenikov, O. R., Tiong, L. W., Johnson, J. J., Seismic Analyses for the Mirror Fusion Test Facility: Soil Structure Interaction Analyses of the Vessel, Structural Mechanics Associates, San Ramon, CA, SMA 12210.01, Prepared for Lawrence Livermore National Laboratory, (1984).
2. Maslenikov, O. R., Tiong, L. W., Johnson, J. J., Seismic Analysis of the MFTF-B Facility: Soil Structure Interaction of the Vault, Structural Mechanics Associates, San Ramon, CA, SMA 12210.02, Prepared for Lawrence Livermore National Laboratory, (1984).
3. Johnson, J. J., Maslenikov, O. R., Mraz, M. J., Seismic Analysis of the Mirror Fusion Test Facility: Building 431, Structural Mechanics Associates, San Ramon, CA, SMA 12210.03, Prepared for Lawrence Livermore National Laboratory, (1984).
4. Wong, H. L., and Luco, J. E., Soil Structure Interaction: A Linear Continuum Mechanics Approach (CLASSI), Department of Civil Engineering, University of Southern California, Los Angeles, CA, CE 79-03 (1980).
5. Chen, J. C., Bernreuter, D. L., Development of Soil Models and Basemat Input Motion for SSI Analysis of MFTF-B Vessel/Foundation/Vault System, Nuclear Systems, Nuclear Systems Safety Program, Lawrence Livermore National Laboratory, Interdepartmental Letter EG-82-25/0304t to J. W. Gerich, June 14, 1982.
6. Richart, F. E., Jr., Hall, J. R., Jr., Woods, R. D., Vibration of Soils and Foundations, Prentice-Hall, (1970).
7. G. L. Goudreau, SAPPAC - A Multisupport Modal Time and Transfer Function Plotter for SAP4 Models, Lawrence Livermore National Laboratory, UCID-19054, July, 1983.

APPENDIX A

IN-STRUCTURE MAXIMUM ACCELERATIONS,  
DISPLACEMENTS AND RESPONSE SPECTRA  
FROM COUPLED SSI ANALYSES

TABLE A.1A: CLASSI COUPLED SSI ANALYSIS RESULTS  
SUMMARY OF MAXIMUM ACCELERATIONS  
DIAGNOSTICS AND HANGER ATTACHMENTS

NODE NO.	COMPONENT	COUPLED SSI ANALYSIS					
		SOFT SOIL		NOMINAL SOIL		STIFF SOIL	
604	TRANSVERSE	260.12	269.67	203.28	267.06	301.70	293.42
	VERTICAL	97.80	95.47	108.10	108.21	122.20	129.12
	LONGITUDINAL	205.22	214.99	211.55	221.45	237.59	263.63
601	TRANSVERSE	216.52	199.60	248.18	227.08	251.62	234.62
	VERTICAL	95.06	99.57	91.24	96.84	92.78	92.43
	LONGITUDINAL	196.89	189.88	210.45	199.32	228.50	255.62
613	TRANSVERSE	191.09	189.41	198.47	201.94	198.54	209.73
	VERTICAL	103.56	104.65	100.87	103.85	90.32	101.07
	LONGITUDINAL	215.25	203.79	219.96	203.28	256.62	230.19
563	TRANSVERSE	253.58	251.01	262.46	260.10	273.21	256.44
	VERTICAL	114.53	108.85	99.21	107.20	105.02	100.29
	LONGITUDINAL	211.29	220.94	215.68	244.63	258.12	252.75
577	TRANSVERSE	235.66	210.25	270.69	239.79	284.92	251.12
	VERTICAL	97.27	104.03	97.50	95.51	93.32	93.02
	LONGITUDINAL	197.01	189.91	210.69	193.49	228.86	256.44
569	TRANSVERSE	200.65	219.69	203.06	233.00	202.65	199.57
	VERTICAL	101.29	105.60	98.23	98.57	98.70	96.80
	LONGITUDINAL	215.42	204.01	220.20	203.46	255.90	230.46
750	TRANSVERSE	255.92	261.70	262.08	274.77	253.73	259.35
	VERTICAL	79.23	85.30	76.07	87.62	78.75	89.61
	LONGITUDINAL	155.34	153.56	203.14	207.80	231.98	229.89
745	TRANSVERSE	252.70	251.10	245.61	253.91	256.96	259.42
	VERTICAL	95.08	90.67	98.17	87.03	84.62	78.24
	LONGITUDINAL	156.13	192.59	207.73	203.87	222.66	240.19
755	TRANSVERSE	148.53	146.40	156.28	157.58	152.37	161.79
	VERTICAL	89.80	95.17	90.76	92.76	86.27	92.36
	LONGITUDINAL	192.19	184.42	199.13	197.38	222.95	227.10
879	TRANSVERSE	260.97	263.60	263.39	269.38	255.50	260.77
	VERTICAL	94.47	95.79	86.66	85.48	81.85	76.66
	LONGITUDINAL	198.26	192.17	207.06	204.55	222.97	234.50
885	TRANSVERSE	262.10	260.64	265.44	266.67	256.68	263.74
	VERTICAL	88.46	91.45	85.91	87.94	86.82	87.45
	LONGITUDINAL	194.31	191.58	206.14	204.02	232.87	228.71
891	TRANSVERSE	149.34	149.27	157.66	159.54	158.62	163.96
	VERTICAL	88.72	91.70	88.56	92.53	88.31	87.12
	LONGITUDINAL	185.96	182.32	196.65	194.39	216.20	220.26
129	TRANSVERSE	123.01	123.78	120.90	119.81	129.93	129.14
	VERTICAL	88.19	88.70	84.41	87.20	81.58	83.77
	LONGITUDINAL	156.76	155.35	167.05	162.28	173.60	168.93

TABLE 4.14: CONT.

347	TRANSVERSE	277.64	269.61	279.05	264.16	267.43	267.02
	VERTICAL	157.88	142.72	119.29	129.30	122.91	116.74
	LONGITUDINAL	215.60	208.37	219.91	232.08	255.76	251.26
355	TRANSVERSE	317.74	292.63	358.14	319.11	367.38	333.28
	VERTICAL	137.01	143.11	129.80	139.10	137.92	141.63
	LONGITUDINAL	215.99	242.02	220.07	267.02	291.39	283.21
556	TRANSVERSE	263.71	229.77	302.83	255.97	267.80	274.41
	VERTICAL	84.27	95.70	84.74	66.93	84.81	82.16
	LONGITUDINAL	194.67	200.90	206.66	210.44	225.35	265.79
349	TRANSVERSE	312.93	278.02	323.80	253.61	326.51	295.60
	VERTICAL	172.91	165.33	133.34	142.65	143.85	146.07
	LONGITUDINAL	216.33	240.87	229.34	243.78	261.30	302.69
341	TRANSVERSE	251.67	260.37	246.82	253.53	269.25	254.36
	VERTICAL	82.74	95.87	65.98	69.12	91.76	95.81
	LONGITUDINAL	210.56	208.66	214.31	229.96	254.33	260.54
343	TRANSVERSE	323.48	294.34	363.87	352.97	410.99	402.88
	VERTICAL	119.59	134.68	105.00	124.02	126.77	150.89
	LONGITUDINAL	207.59	227.11	236.09	238.06	264.76	304.07
362	TRANSVERSE	245.16	243.76	266.18	273.54	251.67	289.93
	VERTICAL	160.64	169.73	204.05	194.20	195.18	178.30
	LONGITUDINAL	254.94	234.39	255.73	266.14	278.35	287.96
445	TRANSVERSE	215.50	208.65	253.95	253.06	250.91	269.25
	VERTICAL	140.87	160.14	138.57	142.20	136.13	147.85
	LONGITUDINAL	206.46	195.67	229.03	222.05	242.45	242.01

UNITS: ACCELERATION - INCHES/SEC/SEC

TABLE A.1B: CLASSI COUPLED SSI ANALYSIS RESULTS  
SUMMARY OF MAXIMUM ACCELERATIONS  
VESSEL SHELL AND SUPPORTS

NODE NO.	COMPONENT	COUPLED SSI ANALYSIS					
		SOFT SOIL		NOMINAL SOIL		STIFF SOIL	
531	TRANSVERSE	284.33	243.95	326.04	285.04	320.08	301.60
	VERTICAL	90.95	100.71	94.17	89.59	93.22	88.48
	LONGITUDINAL	195.21	200.94	206.81	210.22	225.20	265.34
537	TRANSVERSE	280.98	270.54	279.58	276.25	312.08	300.53
	VERTICAL	197.26	171.20	167.42	168.34	157.09	190.55
	LONGITUDINAL	216.22	210.71	221.05	234.15	257.27	231.53
549	TRANSVERSE	159.64	153.80	178.10	168.68	178.01	168.10
	VERTICAL	153.37	165.92	169.95	155.80	147.91	157.78
	LONGITUDINAL	168.05	193.91	197.96	203.48	217.44	248.89
649	TRANSVERSE	200.53	199.28	215.23	213.69	225.73	221.73
	VERTICAL	85.82	89.82	85.56	84.32	80.87	76.71
	LONGITUDINAL	156.25	162.81	205.76	203.03	223.73	252.08
655	TRANSVERSE	248.76	249.45	244.90	254.89	255.67	249.20
	VERTICAL	79.14	92.62	93.30	95.37	83.98	80.68
	LONGITUDINAL	205.38	213.34	210.39	232.98	250.95	255.10
667	TRANSVERSE	140.85	141.55	158.86	152.32	164.23	154.64
	VERTICAL	112.05	119.50	119.36	119.43	109.84	121.31
	LONGITUDINAL	183.67	195.41	194.53	205.70	217.51	245.23
697	TRANSVERSE	209.05	205.37	205.00	211.05	223.65	223.14
	VERTICAL	85.19	87.47	82.31	81.71	79.17	81.73
	LONGITUDINAL	191.87	193.64	204.27	204.79	215.32	241.63
703	TRANSVERSE	248.82	250.68	247.24	258.24	254.26	253.61
	VERTICAL	99.08	114.64	119.84	123.97	114.11	102.17
	LONGITUDINAL	204.79	192.95	213.95	211.27	236.36	232.71
715	TRANSVERSE	144.34	143.22	156.13	150.67	162.24	157.05
	VERTICAL	123.74	129.65	130.09	125.52	119.29	129.13
	LONGITUDINAL	168.98	183.19	197.43	196.86	219.73	225.29
812	TRANSVERSE	259.41	259.53	255.80	263.58	249.23	258.84
	VERTICAL	109.20	115.57	113.13	118.09	105.73	110.66
	LONGITUDINAL	200.06	191.14	208.66	206.20	231.29	230.96
824	TRANSVERSE	143.96	142.21	154.03	155.16	153.28	160.09
	VERTICAL	132.01	133.15	143.72	140.76	138.88	148.04
	LONGITUDINAL	189.10	163.32	197.22	197.18	221.19	222.90
401	TRANSVERSE	194.43	193.34	211.84	214.40	239.42	241.18
	VERTICAL	82.67	85.28	81.56	82.75	77.55	77.64
	LONGITUDINAL	193.77	191.28	203.56	201.88	216.31	236.99
923	TRANSVERSE	199.51	199.85	221.78	221.89	222.64	225.54
	VERTICAL	85.13	85.91	82.14	82.15	78.21	75.46
	LONGITUDINAL	194.19	187.92	202.48	200.10	217.47	227.77

TABLE A-15: CON<sup>T</sup>

459	TRANSVERSE	269.03	269.29	262.81	263.33	251.38	250.99
	VERTICAL	103.53	102.01	111.53	105.81	99.34	103.45
	LONGITUDINAL	197.89	193.06	209.04	204.60	230.30	231.55
940	TRANSVERSE	145.54	145.00	163.25	163.59	166.55	168.05
	VERTICAL	117.07	118.24	124.95	123.80	125.62	125.17
	LONGITUDINAL	166.43	162.31	197.17	194.49	219.11	219.20
1238	TRANSVERSE	130.76	133.73	137.81	132.51	136.39	129.90
	VERTICAL	81.52	83.01	83.91	82.95	76.11	76.82
	LONGITUDINAL	148.00	143.51	160.85	148.85	145.11	140.35
1250	TRANSVERSE	96.28	97.28	89.48	90.46	91.99	91.41
	VERTICAL	80.29	66.95	84.02	78.24	77.74	76.33
	LONGITUDINAL	136.16	131.85	134.14	133.69	122.98	124.79
1276	TRANSVERSE	108.61	108.75	109.35	103.62	113.56	110.93
	VERTICAL	91.10	94.15	83.07	91.29	84.31	91.32
	LONGITUDINAL	154.60	155.17	164.67	160.91	171.03	166.49
1303	TRANSVERSE	94.54	95.08	89.79	90.35	91.19	91.25
	VERTICAL	93.53	94.92	81.47	91.82	86.02	90.31
	LONGITUDINAL	131.92	135.62	133.72	133.67	124.84	123.16

UNITS: ACCELERATION = INCHES/SEC<sup>2</sup>

TABLE A.10. CLASSI COUPLED SSI ANALYSIS RESULTS  
SUMMARY OF MAXIMUM ACCELERATIONS  
FOR THE VAULT

NODE NO.	COMPONENT	COUPLED SSI ANALYSIS		
		SOFT SOIL	NOMINAL SOIL	STIFF SOIL
30	LONGITUDINAL	126.2	119.3	108.5
	TRANSVERSE	135.8	155.0	163.5
	VERTICAL	96.3	94.7	91.5
140	LONGITUDINAL	130.8	127.4	114.4
	TRANSVERSE	138.4	152.7	168.6
	VERTICAL	142.6	124.8	111.0
153	LONGITUDINAL	126.9	125.1	113.5
	TRANSVERSE	114.9	123.7	114.0
	VERTICAL	142.1	124.1	110.6
154	LONGITUDINAL	126.9	124.9	113.5
	TRANSVERSE	117.3	141.6	155.8
	VERTICAL	134.9	118.1	105.1
155	LONGITUDINAL	126.9	124.7	113.0
	TRANSVERSE	125.9	151.3	160.9
	VERTICAL	127.8	112.5	100.9
157	LONGITUDINAL	127.3	124.5	112.9
	TRANSVERSE	116.2	129.9	140.7
	VERTICAL	114.1	101.6	93.4
160	LONGITUDINAL	127.8	124.4	113.0
	TRANSVERSE	127.3	179.5	176.3
	VERTICAL	102.7	92.3	87.6
162	LONGITUDINAL	127.8	124.4	113.0
	TRANSVERSE	182.1	195.3	179.5
	VERTICAL	92.9	84.1	77.1
166	LONGITUDINAL	122.6	122.2	112.7
	TRANSVERSE	116.6	106.0	116.6
	VERTICAL	141.5	123.2	108.6
167	LONGITUDINAL	122.6	122.0	112.5
	TRANSVERSE	113.3	108.2	125.3
	VERTICAL	134.4	117.4	104.2
168	LONGITUDINAL	122.6	121.8	112.2
	TRANSVERSE	111.2	110.5	129.9
	VERTICAL	127.4	111.8	100.1
170	LONGITUDINAL	122.3	121.3	112.0
	TRANSVERSE	105.8	105.2	119.1
	VERTICAL	113.6	100.8	92.6
173	LONGITUDINAL	120.5	120.5	112.3
	TRANSVERSE	103.7	100.9	107.0
	VERTICAL	102.5	92.0	86.9

TABLE A-1C CONT.

175	LONGITUDINAL	119.4	120.2	112.0
	TRANSVERSE	117.9	113.4	113.5
	VERTICAL	92.2	83.5	76.6
235	LONGITUDINAL	141.4	144.5	156.7
	TRANSVERSE	127.2	132.7	147.7
	VERTICAL	130.9	110.4	86.7
353	LONGITUDINAL	120.7	117.9	106.9
	TRANSVERSE	103.3	98.2	106.3
	VERTICAL	85.8	78.8	73.1

UNITS ACCELERATION = INCHES/SEC/SEC

TABLE A-2A: CLASSI COUPLED SSI ANALYSIS RESULTS  
SUMMARY OF MAXIMUM RELATIVE DISPLACEMENTS  
IN THE VESSEL EAST HALF

NODE	COMPONENT	COUPLED SSI ANALYSIS			MAXIMUM
		SOFT SOIL	NOMINAL SOIL	STIFF SOIL	
<b>VESSEL EAST HALF</b>					
539	TRANS	.497	.259	.239	.297
539	VERT	.179	.151	.137	.179
539	LONG	.066	.062	.060	.066
586	TRANS	.222	.204	.176	.222
586	VERT	.138	.119	.095	.138
586	LONG	.071	.067	.062	.071
745	TRANS	.052	.054	.050	.054
745	VERT	.026	.027	.025	.036
745	LONG	.007	.008	.008	.008
755	TRANS	.372	.332	.312	.372
755	VERT	.097	.065	.051	.097
755	LONG	.043	.037	.028	.043
885	TRANS	.023	.025	.029	.020
885	VERT	.105	.055	.043	.105
885	LONG	.046	.041	.038	.046
972	TRANS	.035	.035	.035	.035
972	VERT	.016	.019	.007	.016
972	LONG	.004	.005	.006	.006
<b>VESSEL WEST HALF</b>					
539	TRANS	.260	.224	.220	.260
539	VERT	.227	.160	.153	.227
539	LONG	.044	.039	.043	.044
586	TRANS	.210	.171	.166	.210
586	VERT	.179	.107	.091	.179
586	LONG	.047	.041	.042	.047
745	TRANS	.054	.051	.055	.056
745	VERT	.060	.038	.025	.060
745	LONG	.050	.039	.034	.050
755	TRANS	.365	.327	.313	.365
755	VERT	.118	.072	.049	.118
755	LONG	.041	.032	.020	.041

1  
TABLE A.2a CONT.

685	TRANS	.029	.026	.040	.040
685	VERT	.111	.061	.040	.111
685	LONG	.020	.018	.015	.020
972	TRANS	.036	.031	.032	.035
972	VERT	.016	.010	.008	.016
972	LONG	.043	.036	.025	.043

UNITS: INCHES

NOTES: ALL DISPLACEMENTS ARE RELATIVE TO NOSE 879 OF THE VESSELS  
EAST HALF

TABLE A-29: CLASSI COUPLED SSI ANALYSIS RESULTS  
SUMMARY OF MAXIMUM RELATIVE DISPLACEMENTS  
IN THE VAULT

NODE	COMPONENT	COUPLED SSI ANALYSIS			
		SOFT SOIL	NOMINAL SOIL	STIFF SOIL	MAXIMUM
30	LONG	.013	.014	.016	.016
30	TRANS	.171	.193	.199	.199
30	VERT	.014	.014	.017	.017
140	LONG	.011	.011	.012	.012
140	TRANS	.178	.202	.200	.202
140	VERT	.009	.008	.009	.009
153	LONG	.005	.007	.006	.007
153	TRANS	.065	.077	.080	.080
153	VERT	.005	.006	.007	.007
154	LONG	.006	.007	.006	.007
154	TRANS	.121	.143	.139	.143
154	VERT	.004	.005	.005	.005
155	LONG	.005	.007	.006	.007
155	TRANS	.151	.177	.167	.177
155	VERT	.003	.004	.004	.004
157	LONG	.008	.008	.008	.008
157	TRANS	.131	.134	.128	.134
157	VERT	.002	.002	.002	.002
160	LONG	.009	.010	.009	.010
160	TRANS	.250	.265	.253	.260
160	VERT	.003	.003	.003	.003
162	LONG	.009	.010	.009	.010
162	TRANS	.666	.617	.616	.666
162	VERT	.005	.005	.005	.005
165	LONG	.001	.001	.002	.002
165	TRANS	.024	.025	.023	.025
165	VERT	.004	.005	.005	.005
167	LONG	.001	.001	.001	.001
167	TRANS	.017	.023	.025	.025
167	VERT	.003	.004	.005	.005
168	LONG	.001	.001	.001	.001
168	TRANS	.020	.028	.031	.031
168	VERT	.003	.004	.004	.004

TABLE A.2B CONT.

173	LONG	.005	.005	.004	.005
173	TRANS	.032	.043	.049	.049
173	VERT	.002	.002	.002	.002
175	LONG	.008	.008	.006	.008
175	TRANS	.062	.078	.075	.078
175	VERT	.008	.005	.005	.005
236	LONG	.082	.109	.122	.122
236	TRANS	.072	.094	.089	.089
236	VERT	.062	.066	.065	.066
363	LONG	.023	.026	.028	.028
363	TRANS	.025	.032	.034	.034
363	VERT	.045	.043	.043	.045

UNITS: INCHES

NOTES: ALL DISPLACEMENTS ARE RELATIVE TO NODE 170 OF THE VAULT

TABLE A-2C: CLASS: COUPLED SSI ANALYSIS RESULTS  
SUMMARY OF MAXIMUM RELATIVE DISPLACEMENTS  
BETWEEN THE VESSEL AND THE VAULT

COMPONENT	COUPLED SSI ANALYSIS			
	SOFT SOIL	NOMINAL SOIL	STIFF SOIL	MAXIMUM
LONG.	.295	.320	.388	.388
TRANS.	.561	.492	.498	.591
VERT.	.340	.218	.121	.340

UNITS: INCHES

NOTES: DISPLACEMENTS ARE FOR NODE 170 OF THE VAULT  
RELATIVE TO NODE 879 OF THE VESSEL'S EAST HALF

LIST OF APPENDIX FIGURES

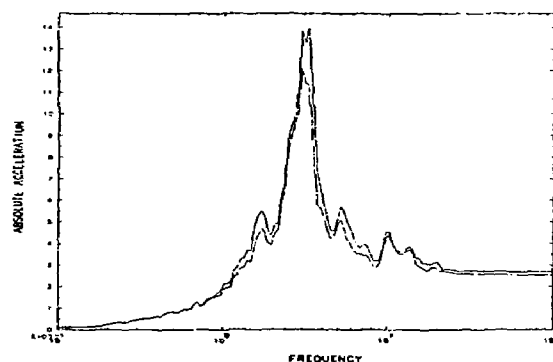
In-Structure Response Spectra from Coupled SSI Analyses, Vessel Model

<u>Fig.</u>	<u>Description</u>	<u>Fig.</u>	<u>Description</u>
A.1	Node 341	A.21	Node 655
A.2	Node 343	A.22	Node 667
A.3	Node 347	A.23	Node 697
A.4	Node 349	A.24	Node 703
A.5	Node 355	A.25	Node 715
A.6	Node 382	A.26	Node 745
A.7	Node 401	A.27	Node 750
A.8	Node 445	A.28	Node 755
A.9	Node 458	A.29	Node 812
A.10	Node 531	A.30	Node 824
A.11	Node 537	A.31	Node 879
A.12	Node 549	A.32	Node 885
A.13	Node 555	A.33	Node 891
A.14	Node 577	A.34	Node 923
A.15	Node 583	A.35	Node 940
A.16	Node 589	A.36	Node 1238
A.17	Node 601	A.37	Node 1250
A.18	Node 604	A.38	Node 1276
A.19	Node 613	A.39	Node 1296
A.20	Node 649	A.40	Node 1303

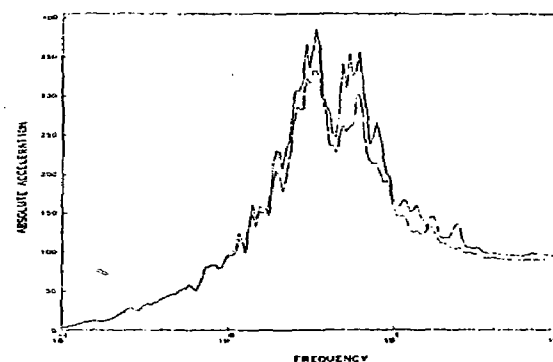
In-Structure Response Spectra from Coupled SSI Analyses, Vault Model

<u>Fig.</u>	<u>Description</u>
A.41	Node 30
A.42	Node 140
A.43	Node 153
A.44	Node 154
A.45	Node 155
A.46	Node 157
A.47	Node 160
A.48	Node 162
A.49	Node 166
A.50	Node 167
A.51	Node 168
A.52	Node 170
A.53	Node 173
A.54	Node 175
A.55	Node 236
A.56	Node 353

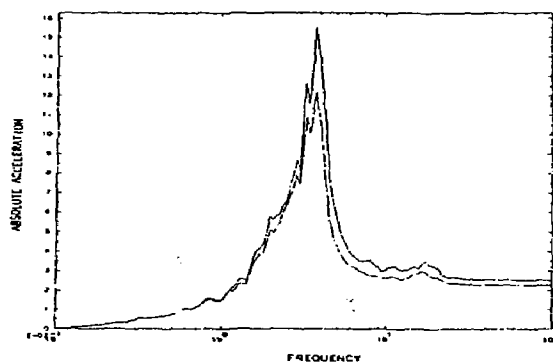
a) Transverse



b) Vertical



c) Longitudinal



Legend

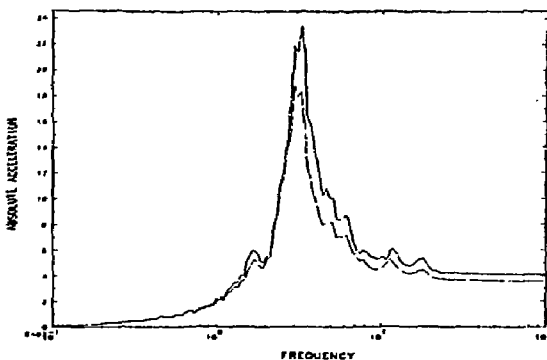
Maximum \_\_\_\_\_  
Mean \_\_\_\_\_

Notes

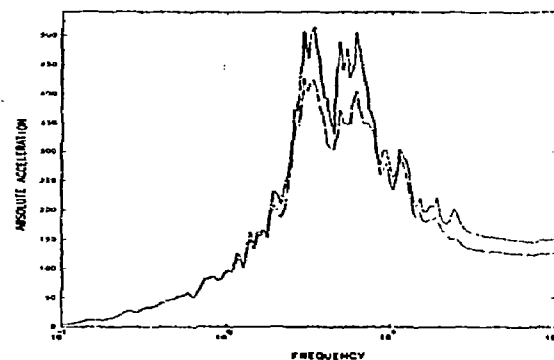
All spectra at 5% damping  
All frequencies in Hz  
All accelerations in in/sec<sup>2</sup>

Figure A.1 In-Structure Response Spectra from Coupled SSI Analyses  
Node 341, Vessel Model

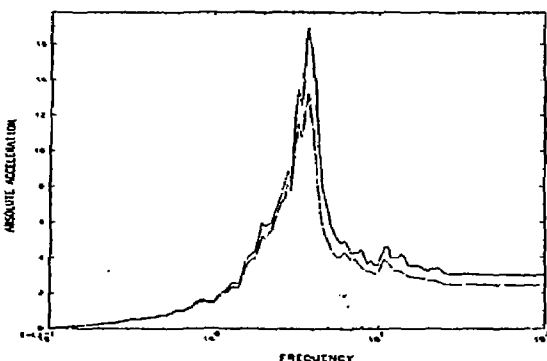
a) Transverse



b) Vertical



c) Longitudinal



Legend

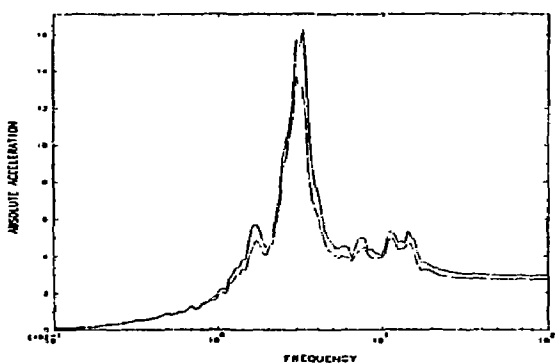
Maximum ——————  
Mean ——————

Notes

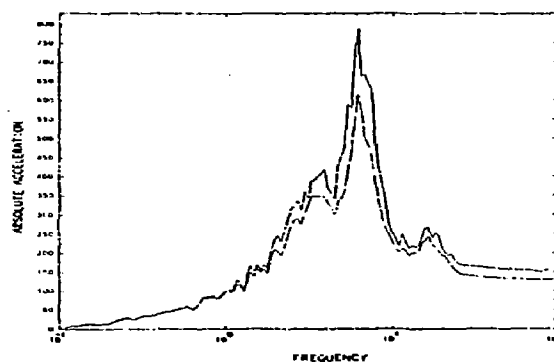
All spectra at 5% damping  
All frequencies in Hz  
All accelerations in in/sec<sup>2</sup>

Figure A.2 In-Structure Response Spectra from Coupled SSI Analyses  
Node 343, Vessel Model

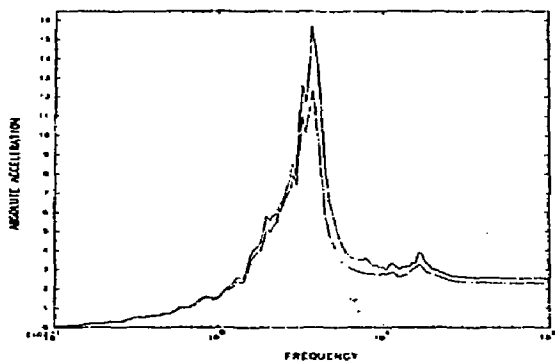
a) Transverse



b) Vertical



c) Longitudinal



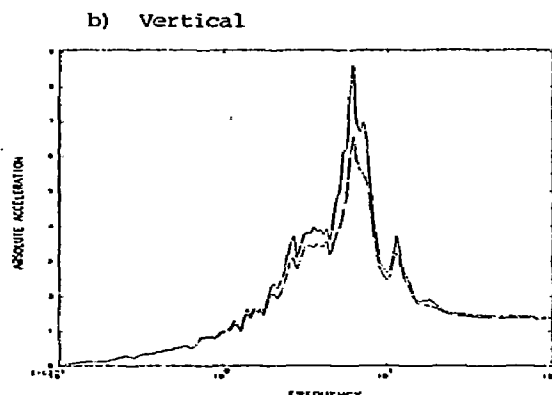
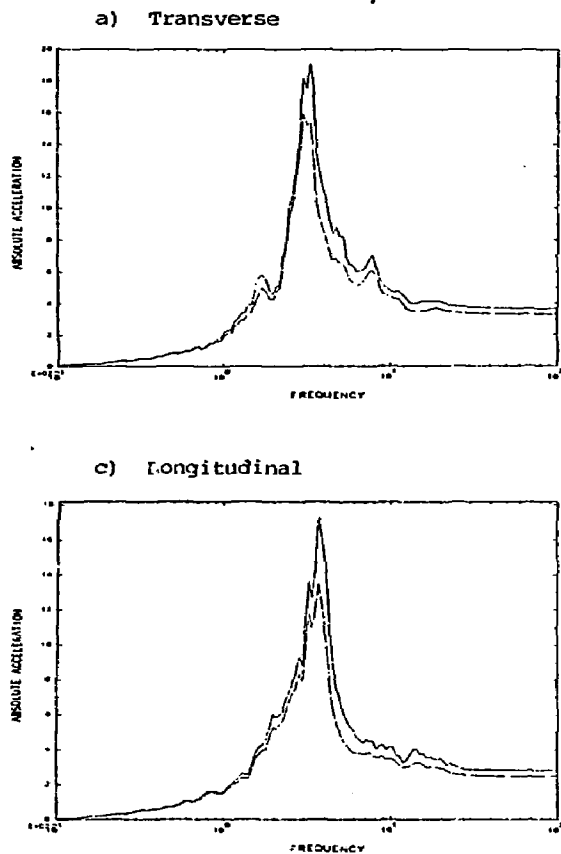
Legend

Maximum \_\_\_\_\_  
Mean \_\_\_\_\_

Notes

All spectra at 5% damping  
All frequencies in Hz  
All accelerations in in/sec<sup>2</sup>

Figure A.3 In-Structure Response Spectra from Coupled SSI Analyses  
Node 347 Vessel Model



Legend

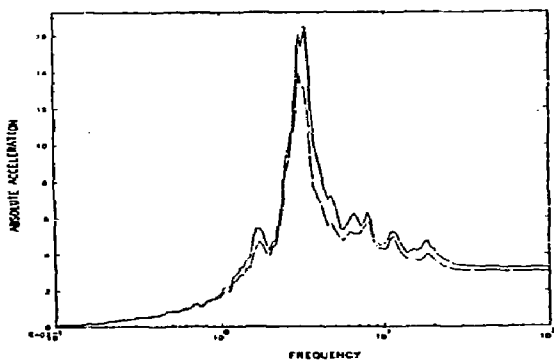
Maximum \_\_\_\_\_  
 Mean \_\_\_\_\_

Notes

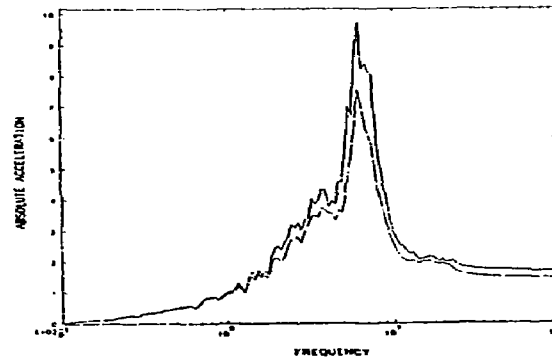
All spectra at 5% damping  
 All frequencies in Hz  
 All accelerations in in/sec<sup>2</sup>

Figure A.4 In-Structure Response Spectra from Coupled SSI Analyses  
 Node 355, Vessel Model

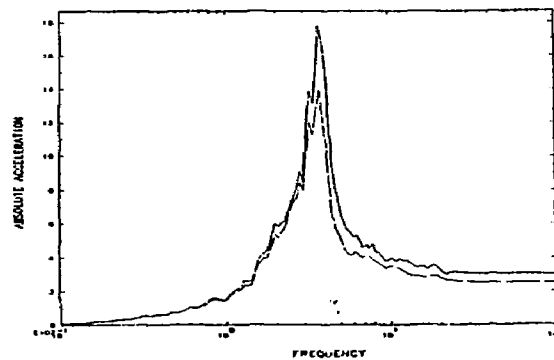
a) Transverse



b) Vertical



c) Longitudinal



Legend

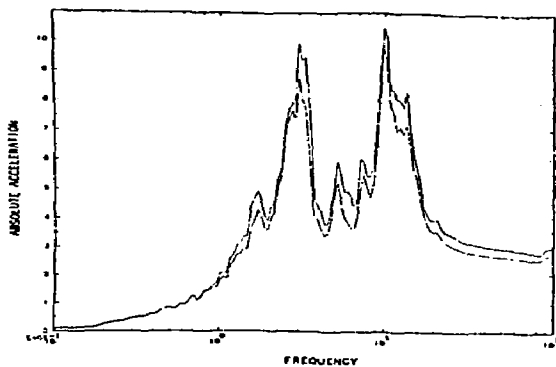
Maximum \_\_\_\_\_  
Mean \_\_\_\_\_

Notes

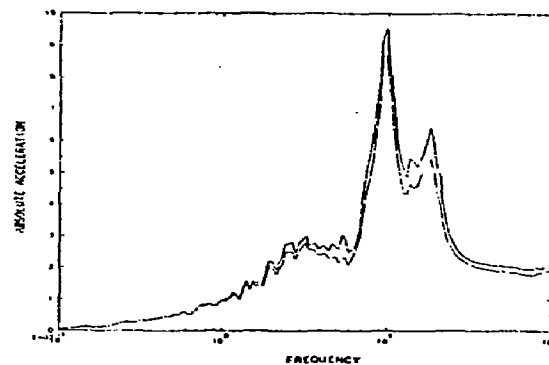
All spectra at 5% damping  
All frequencies in Hz  
All accelerations in in/sec<sup>2</sup>

Figure A.5 In-Structure Response Spectra from Coupled SSI Analyses  
Node 349, Vessel Model

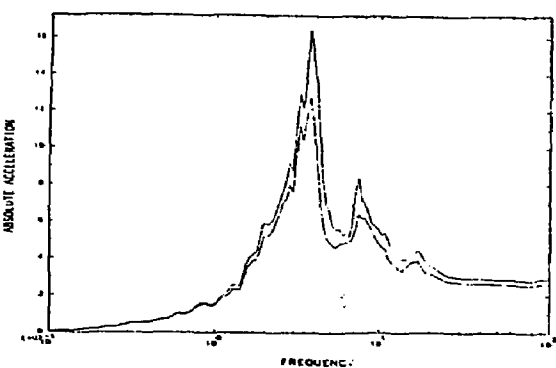
a) Transverse



b) Vertical



c) Longitudinal



Legend

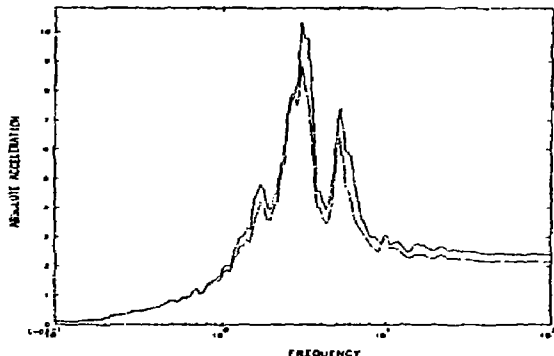
Maximum \_\_\_\_\_  
Mean \_\_\_\_\_

Notes

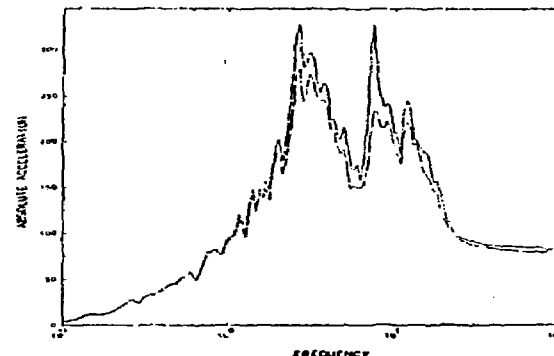
All spectra at 5% damping  
All frequencies in Hz  
All accelerations in in/sec<sup>2</sup>

Figure A.6 In-Structure Response Spectra from Coupled SSI Analyses  
Node 382, Vessel Model

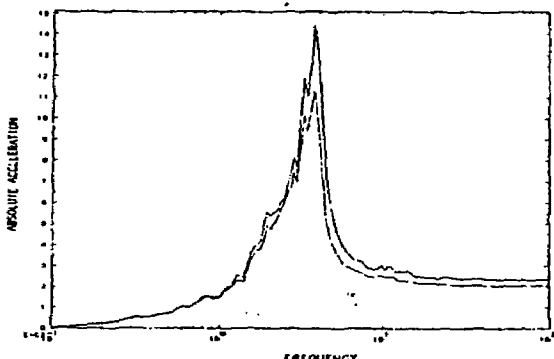
a) Transverse



b) Vertical



c) Longitudinal



Legend

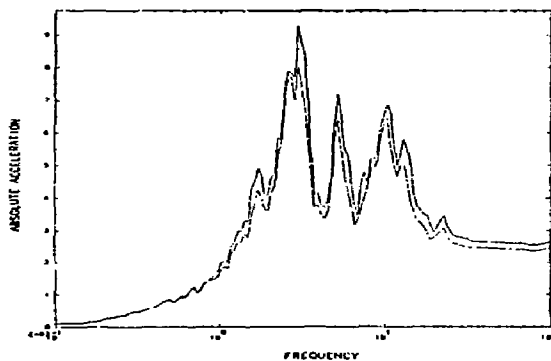
Maximum \_\_\_\_\_  
Mean \_\_\_\_\_

Notes

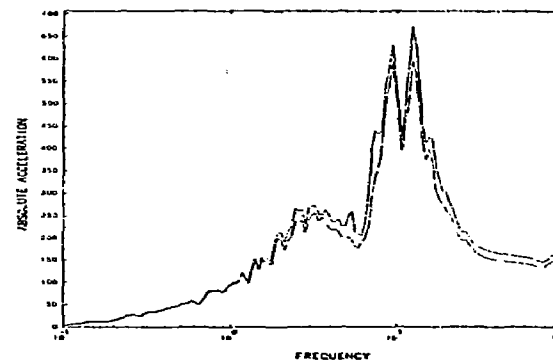
All spectra at 5% damping  
All frequencies in Hz  
All accelerations in in/sec<sup>2</sup>

Figure A.7 In-Structure Response Spectra from Coupled SSI Analyses  
Node 401, Vessel Model

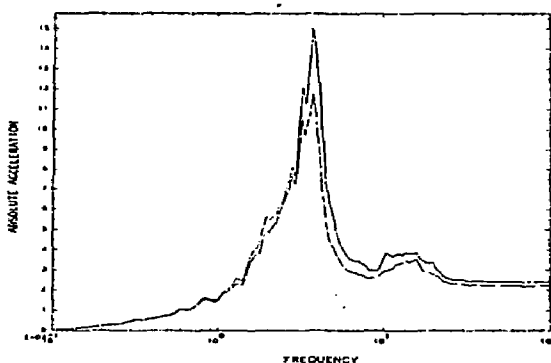
a) Transverse



b) Vertical



c) Longitudinal



Legend

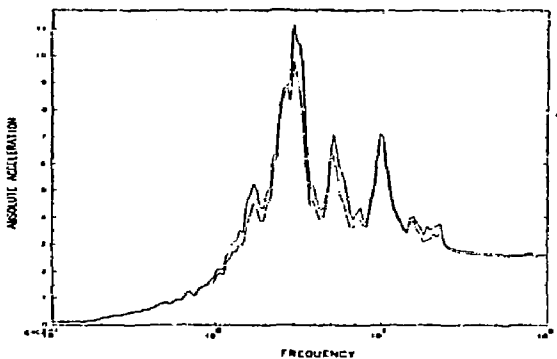
Maximum ——————  
Mean ——————

Notes

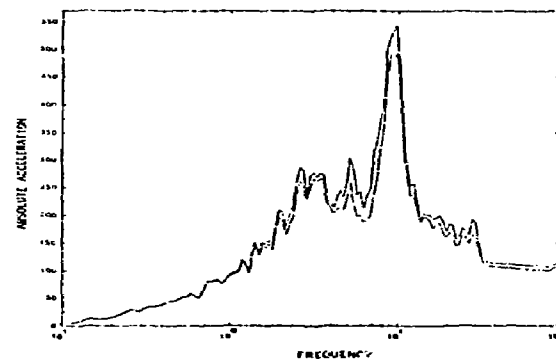
All spectra at 5% damping  
All frequencies in Hz  
All accelerations in in/sec<sup>2</sup>

Figure A.8 In-Structure Response Spectra from Coupled SSI Analyses  
Node 445, Vessel Model

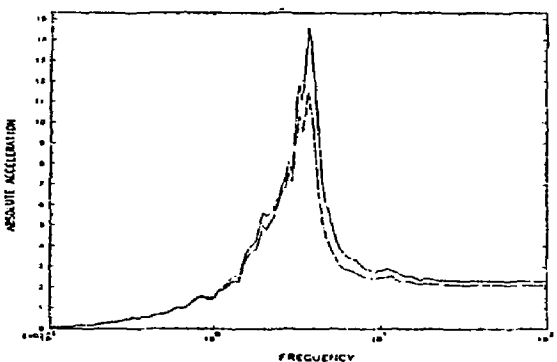
a) Transverse



b) Vertical



c) Longitudinal



Legend

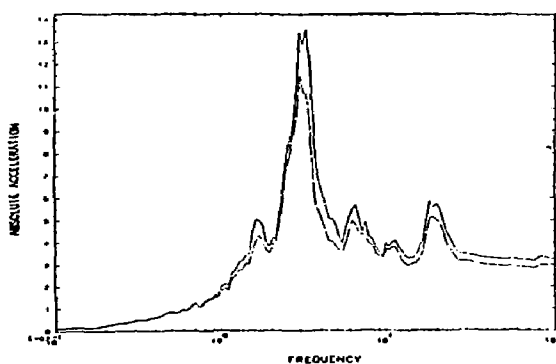
Maximum \_\_\_\_\_  
Mean \_\_\_\_\_

Notes

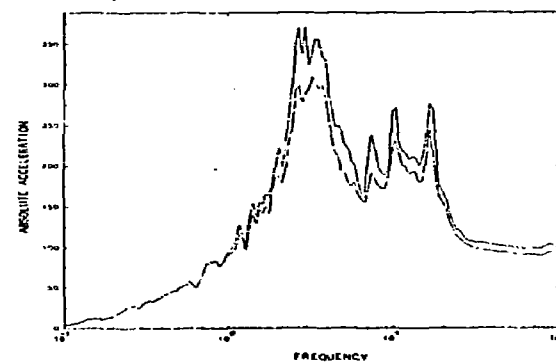
All spectra at 5% damping  
All frequencies in Hz  
All accelerations in in/sec<sup>2</sup>

Figure A.9 In-Structure Response Spectra from Coupled SSI Analyses  
Node 458 Vessel Model

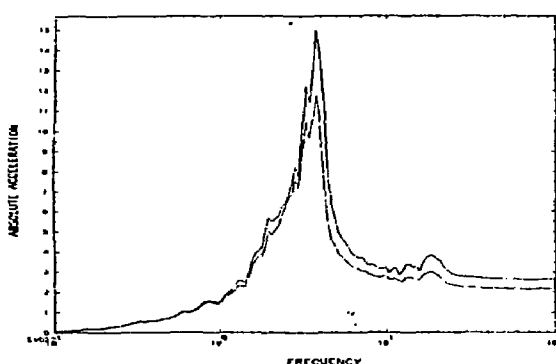
a) Transverse



b) Vertical



c) Longitudinal



Legend

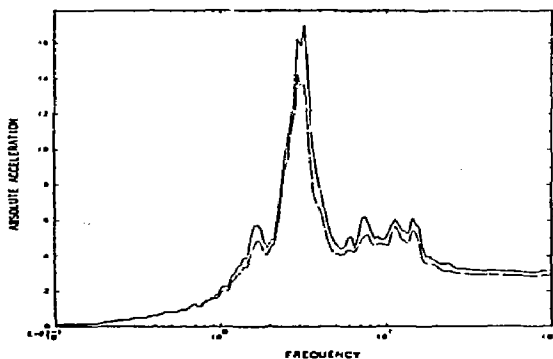
Maximum    —  
Mean    ——

Notes

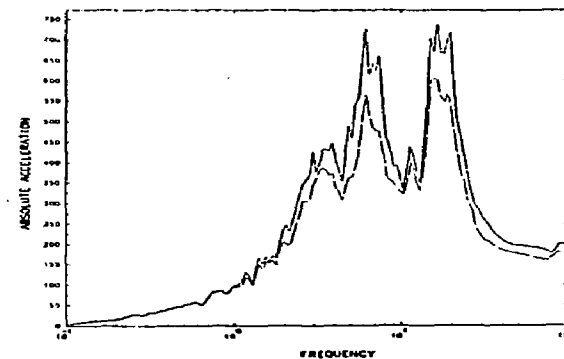
All spectra at 5% damping  
All frequencies in Hz  
All accelerations in in/sec<sup>2</sup>

Figure A.10 In-Structure Response Spectra from Coupled SSI Analyses  
Node 531, Vessel Model

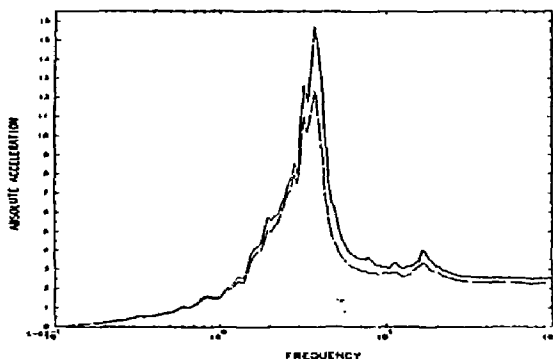
a) Transverse



b) Vertical



c) Longitudinal



Legend

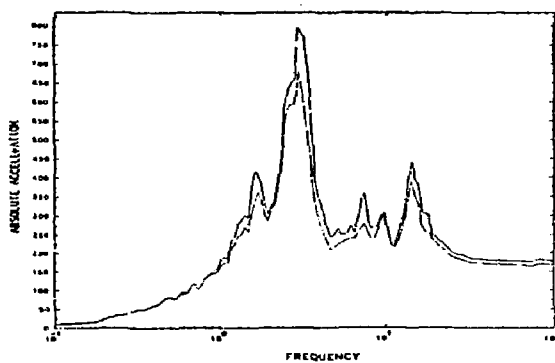
Maximum \_\_\_\_\_  
Mean \_\_\_\_\_

Notes

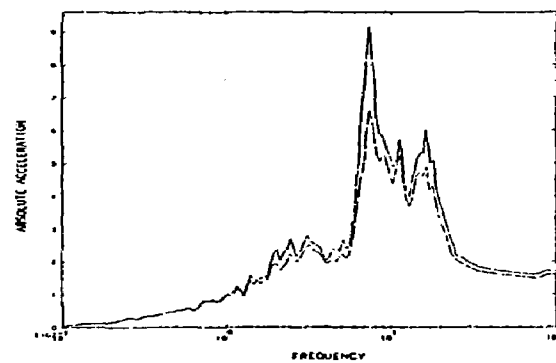
All spectra at 5% damping  
All frequencies in Hz  
All accelerations in in/sec<sup>2</sup>

Figure A.11 In-Structure Response Spectra from Coupled SSI Analyses  
Node 537, Vessel Model

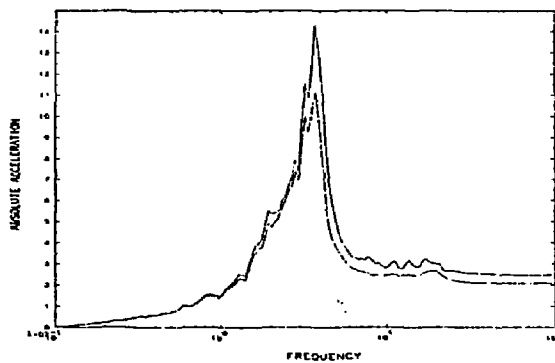
a) Transverse



b) Vertical



c) Longitudinal



Legend

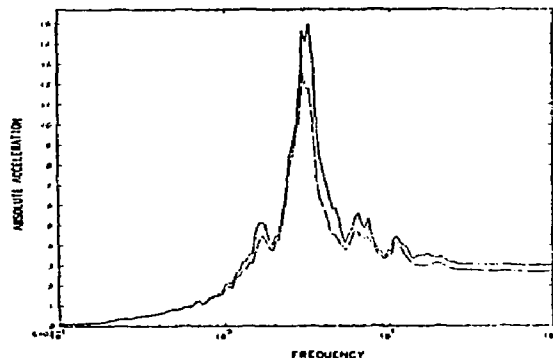
Maximum ——————  
Mean ————

Notes

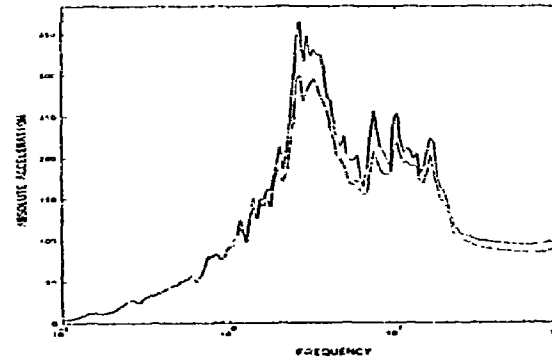
All spectra at 5% damping  
All frequencies in Hz  
All accelerations in in/sec<sup>2</sup>

Figure A.12 In-Structure Response Spectra from Coupled SSI Analyses  
Node 549, Vessel Model

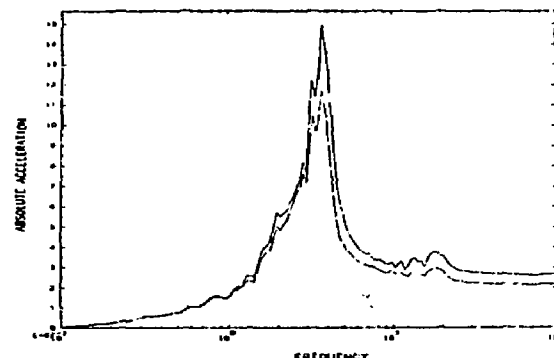
a) Transverse



b) Vertical



c) Longitudinal



Legend

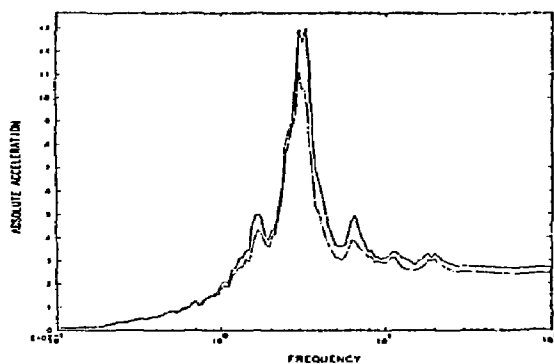
Maximum \_\_\_\_\_  
Mean \_\_\_\_\_

Notes

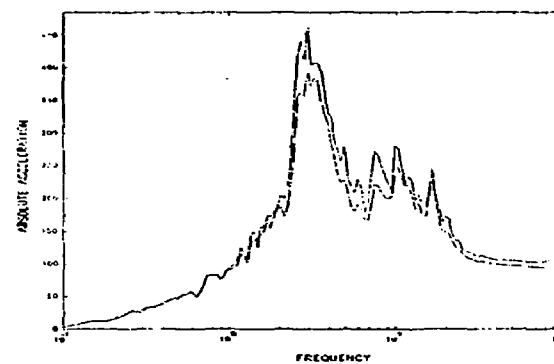
All spectra at 5% damping  
All frequencies in Hz  
All accelerations in in/sec<sup>2</sup>

Figure A.13 In-Structure Response Spectra from Coupled SSI Analyses  
Node 555 Vessel Model

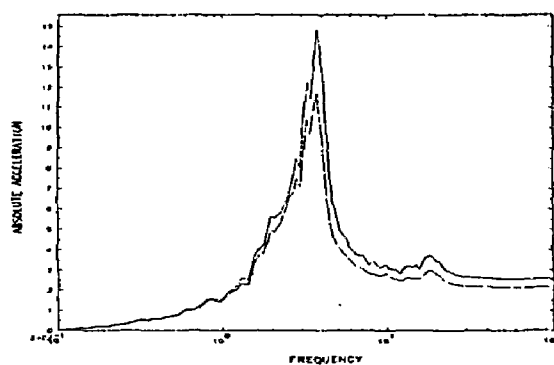
a) Transverse



b) Vertical



c) Longitudinal



Legend

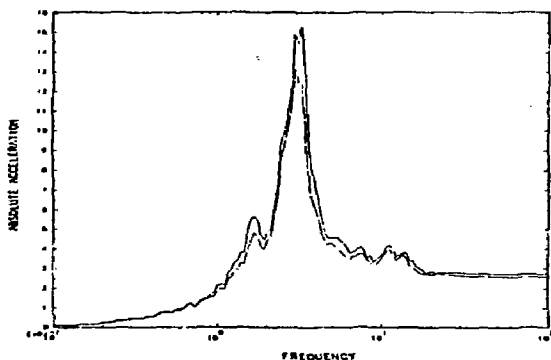
Maximum ——————  
Mean - - - - -

Notes

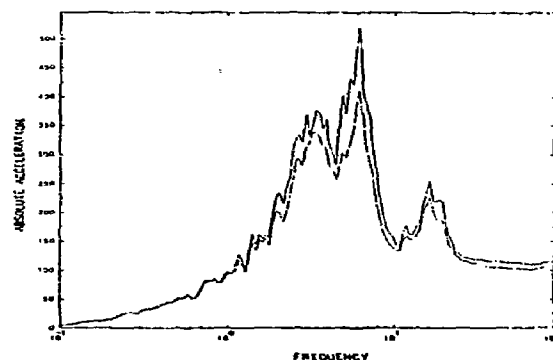
All spectra at 5% damping  
All frequencies in Hz  
All accelerations in in/sec<sup>2</sup>

Figure A.14 In-Structure Response Spectra from Coupled SSI Analyses  
Node 577, Vessel Model

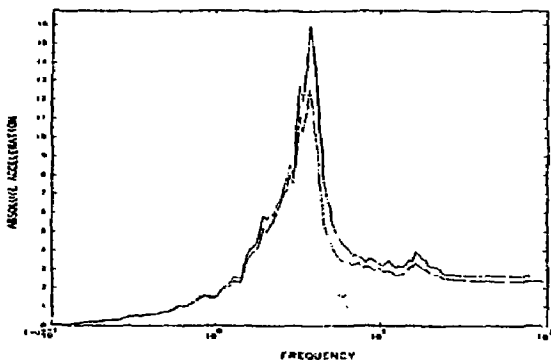
a) Transverse



b) Vertical



c) Longitudinal



Legend

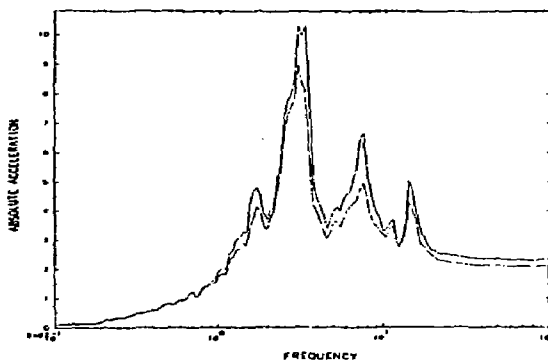
Maximum \_\_\_\_\_  
Mean \_\_\_\_\_

Notes

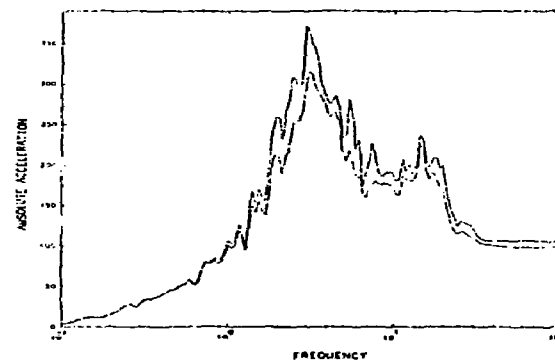
All spectra at 5% damping  
All frequencies in Hz  
All accelerations in in/sec<sup>2</sup>

Figure A.15 In-Structure Response Spectra from Coupled SSI Analyses  
Node 583, Vessel Model

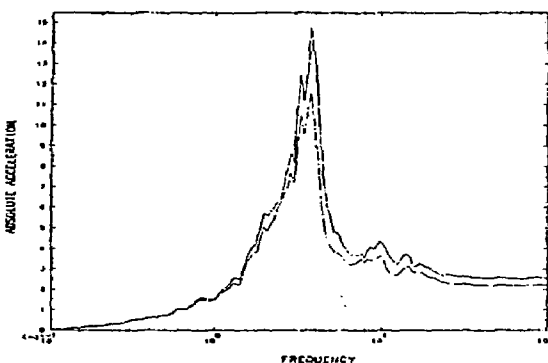
a) Transverse



b) Vertical



c) Longitudinal



Legend

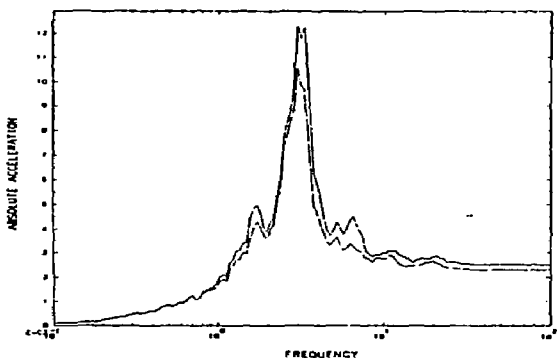
Maximum \_\_\_\_\_  
Mean \_\_\_\_\_

Notes

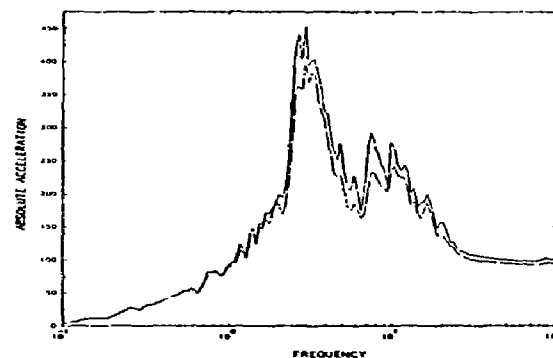
All spectra at 5% damping  
All frequencies in Hz  
All accelerations in in/sec<sup>2</sup>

Figure A.16 In-Structure Response Spectra from Coupled SSI Analyses  
Node 589, Vessel Model

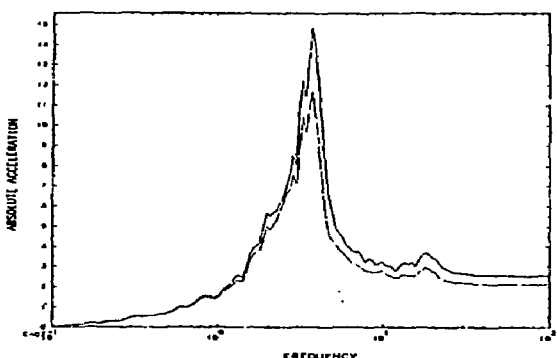
a) Transverse



b) Vertical



c) Longitudinal



Legend

Maximum \_\_\_\_\_

Mean \_\_\_\_\_

Notes

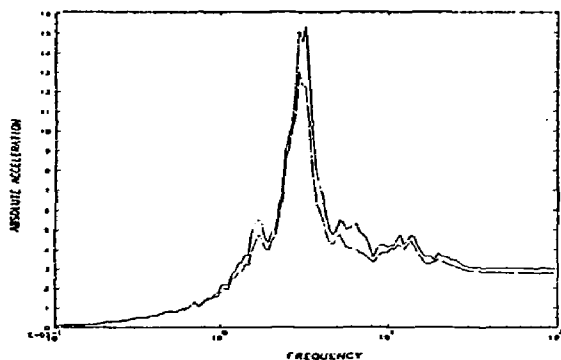
All spectra at 5% damping

All frequencies in Hz

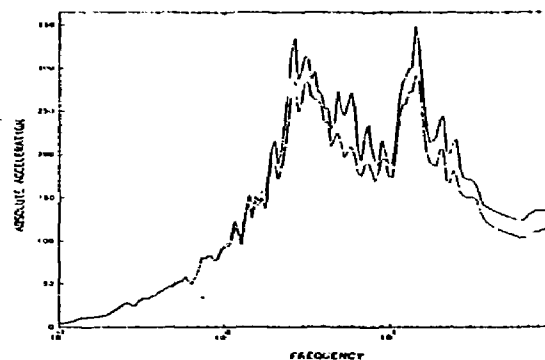
All accelerations in in/sec<sup>2</sup>

Figure A.17 In-Structure Response Spectra from Coupled SSI Analyses  
Node 601, Vessel Model

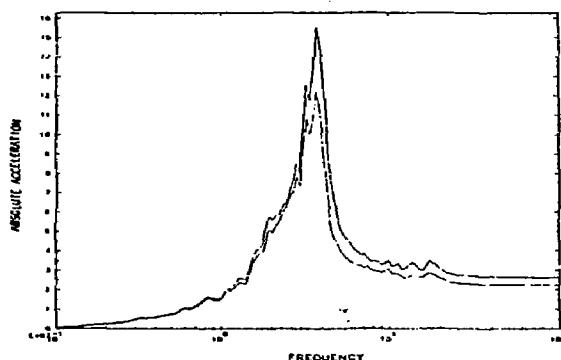
a) Transverse



b) Vertical



c) Longitudinal



Legend

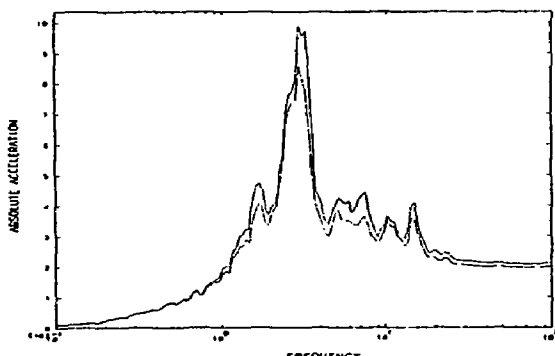
Maximum            —  
Mean            —

Notes

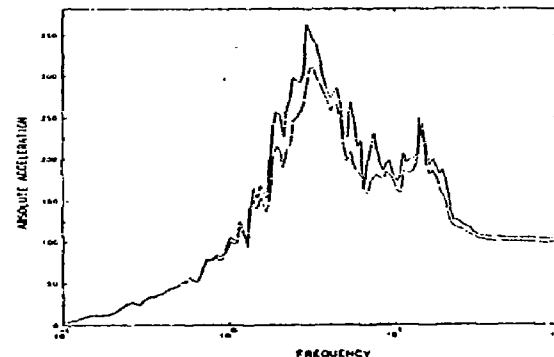
All spectra at 5% damping  
All frequencies in Hz  
All accelerations in in/sec<sup>2</sup>

Figure A.18 In-Structure Response Spectra from Coupled SSI Analyses  
Node 604, Vessel Model

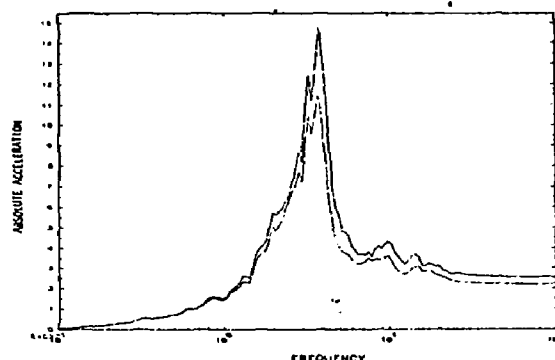
a) Transverse



b) Vertical



c) Longitudinal



Legend

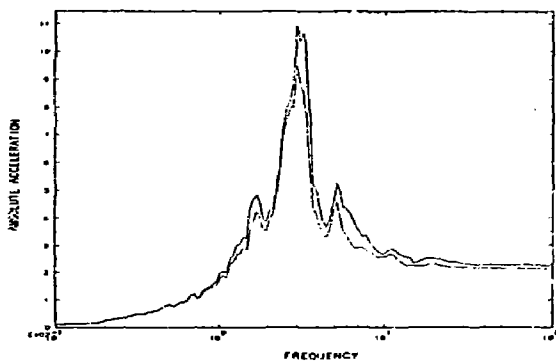
Maximum \_\_\_\_\_  
Mean \_\_\_\_\_

Notes

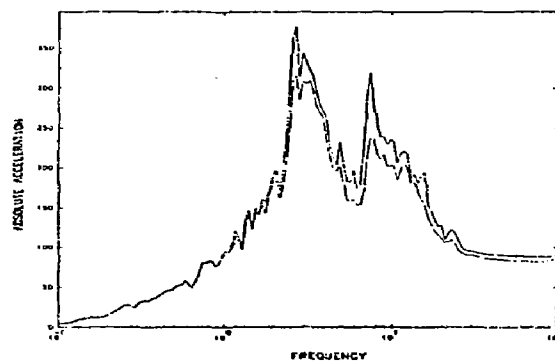
All spectra at 5% damping  
All frequencies in Hz  
All accelerations in in/sec<sup>2</sup>

Figure A.19 In-Structure Response Spectra from Coupled SSI Analyses  
Node 613 Vessel Model

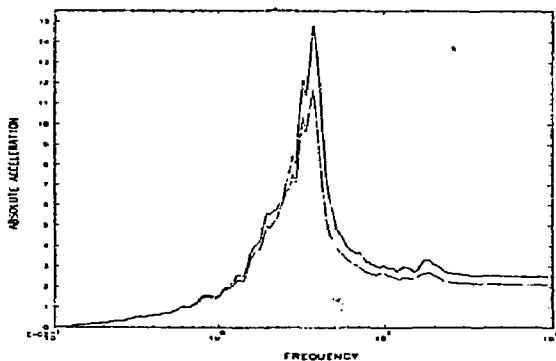
a) Transverse



b) Vertical



c) Longitudinal



Legend

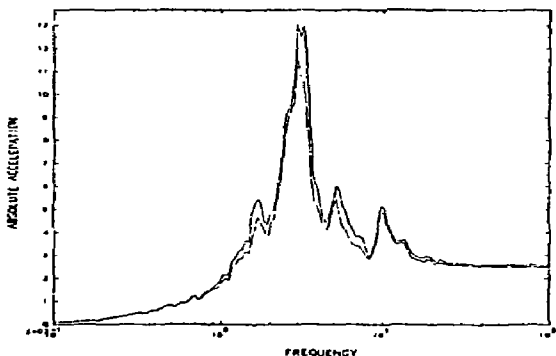
Maximum \_\_\_\_\_  
Mean \_\_\_\_\_

Notes

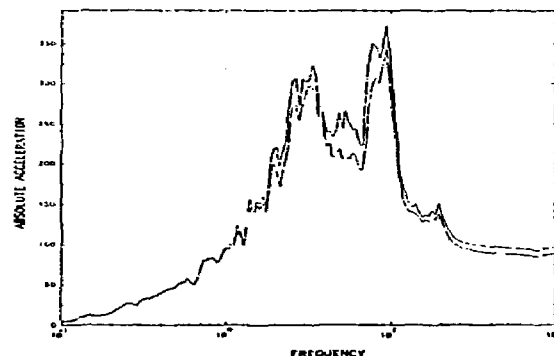
All spectra at 5% damping  
All frequencies in Hz  
All accelerations in in/sec<sup>2</sup>

Figure A.20 In-Structure Response Spectra from Coupled SSI Analyses  
Node 649, Vessel Model

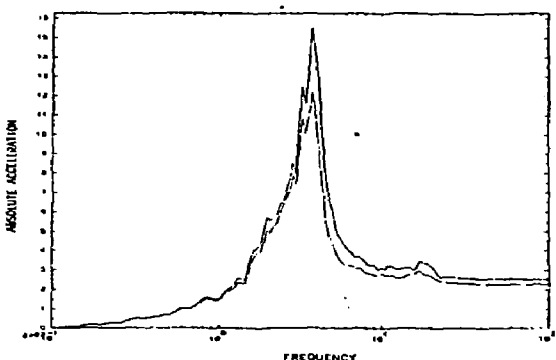
a) Transverse



b) Vertical



c) Longitudinal



Legend

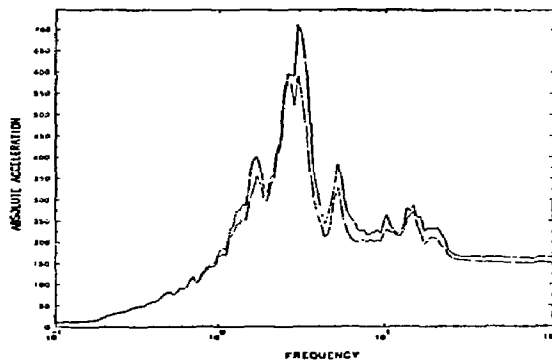
Maximum   
Mean 

Notes

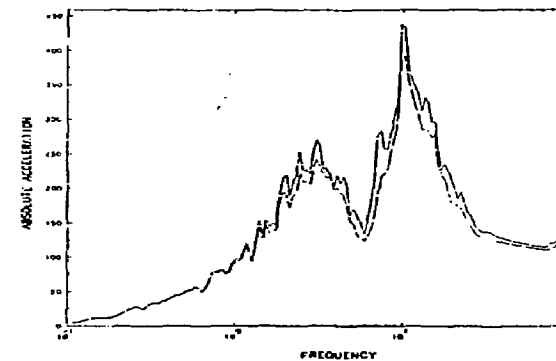
All spectra at 5% damping  
All frequencies in Hz  
All accelerations in in/sec<sup>2</sup>

Figure A.21 In-Structure Response Spectra from Coupled SSI Analyses  
Node 655, Vessel Model

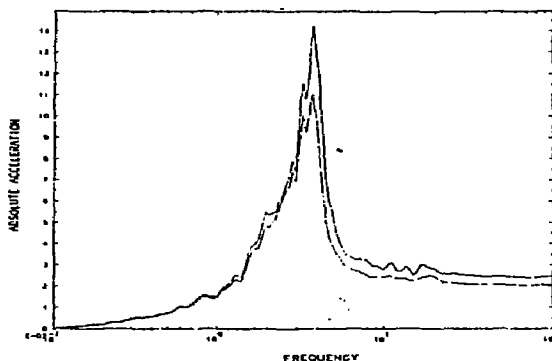
a) Transverse



b) Vertical



c) Longitudinal



Legend

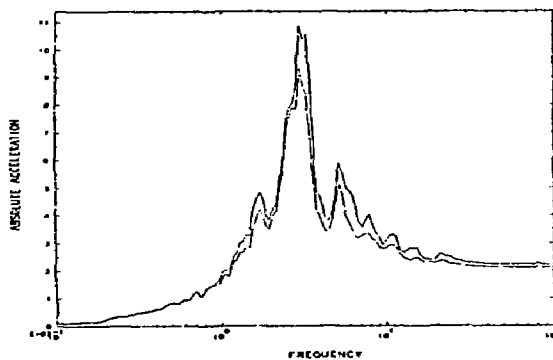
Maximum \_\_\_\_\_  
Mean \_\_\_\_\_

Notes

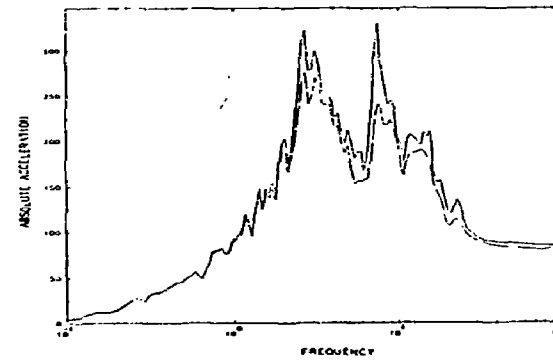
All spectra at 5% damping  
All frequencies in Hz  
All accelerations in in/sec<sup>2</sup>

Figure A.22 In-Structure Response Spectra from Coupled SSI Analyses  
Node 667, Vessel Model

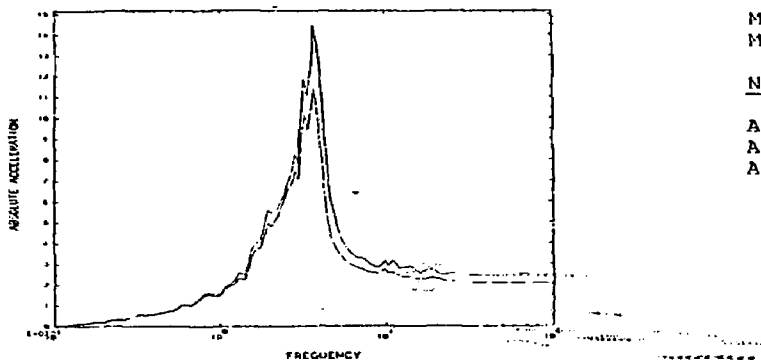
a) Transverse



b) Vertical



c) Longitudinal



Legend

Maximum

Mean

Notes

All spectra at 5% damping

All frequencies in Hz

All accelerations in in/sec<sup>2</sup>

Figure A.23 In-Structure Response Spectra from Coupled SSI Analyses  
Node 697 Vessel Model

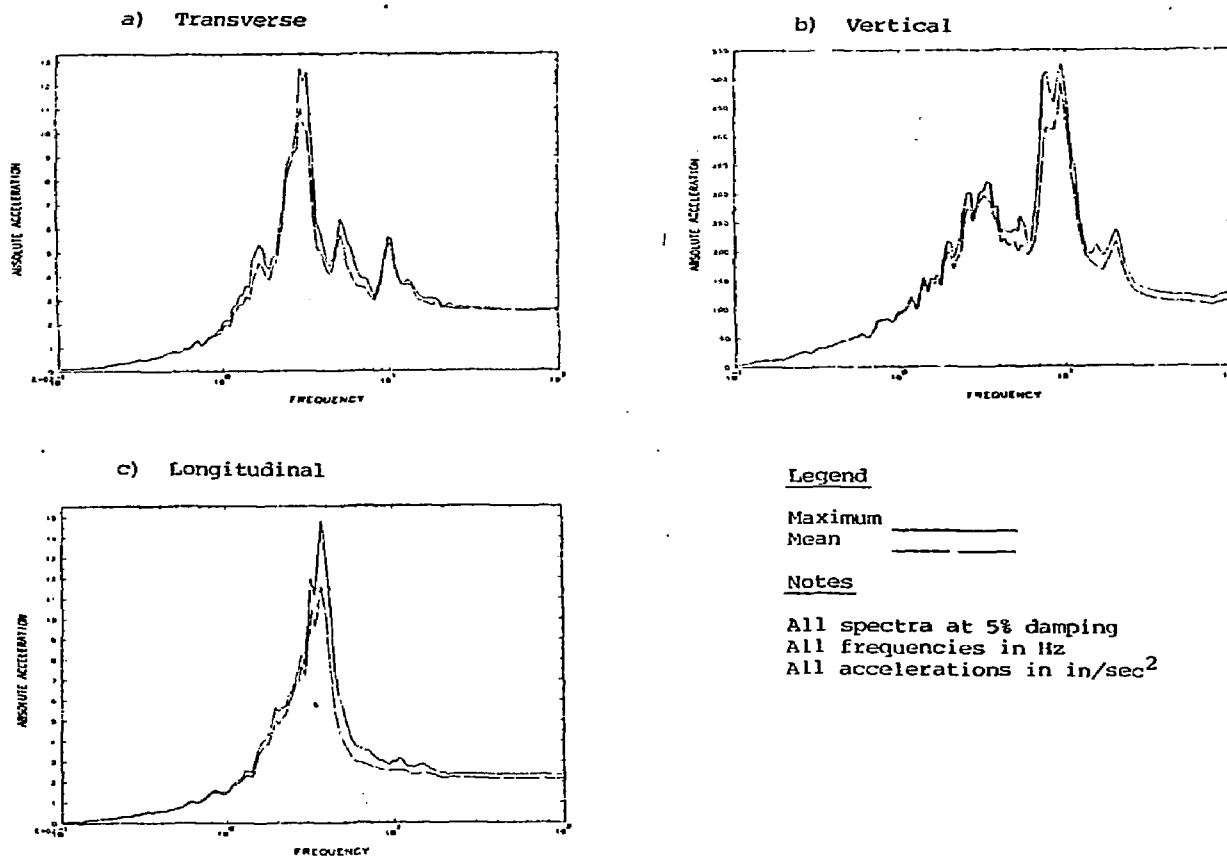


Figure A.24 In-Structure Response Spectra from Coupled SSI Analyses  
Node 703, Vessel Model

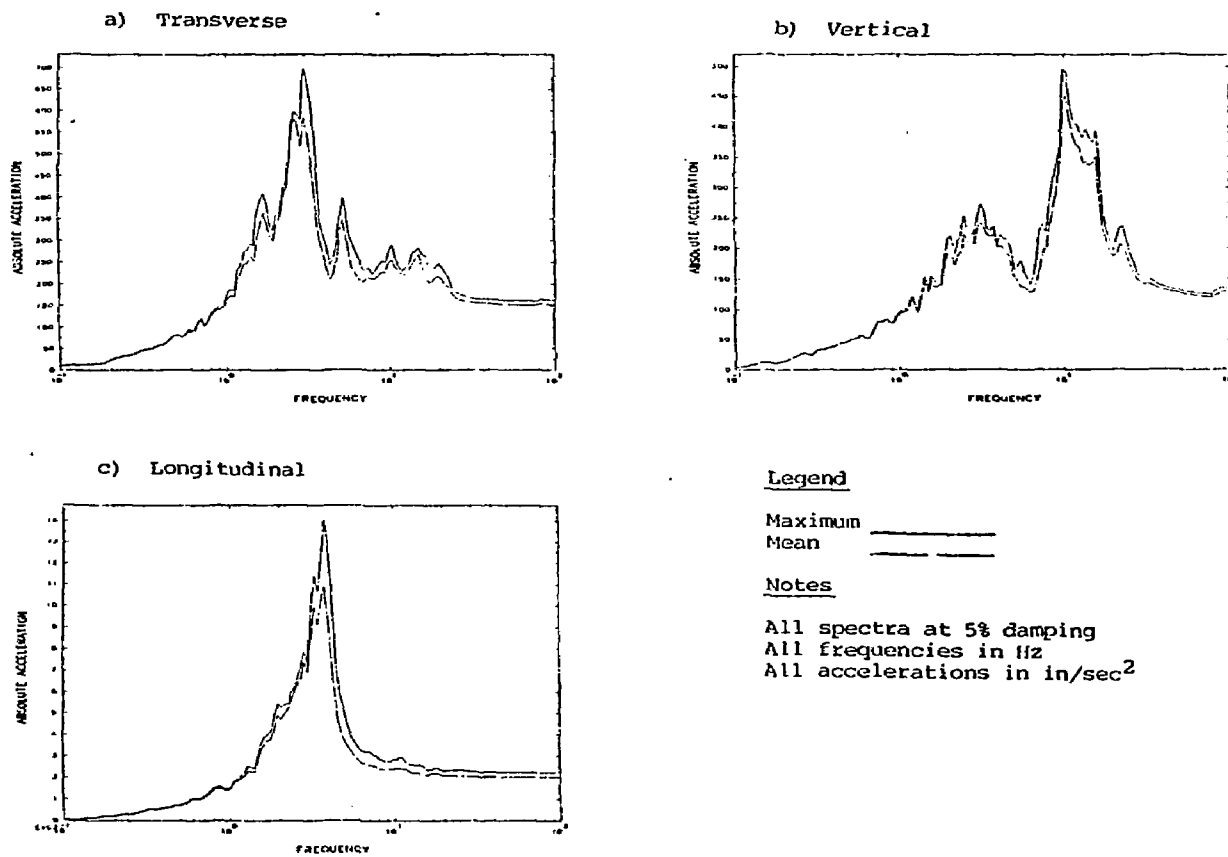
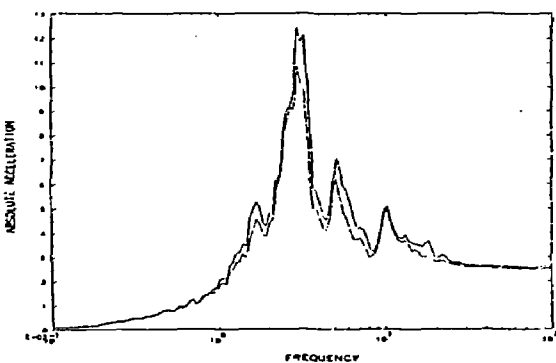
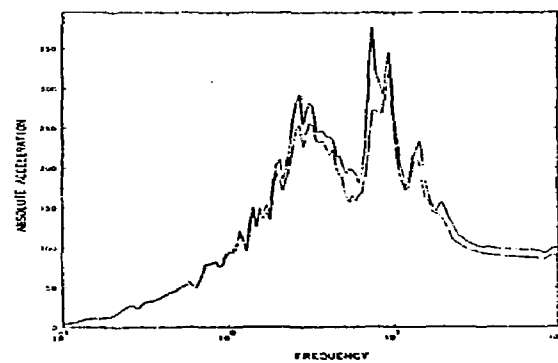


Figure A.25 In-Structure Response Spectra from Coupled SSI Analyses  
 Node 715, Vessel Model

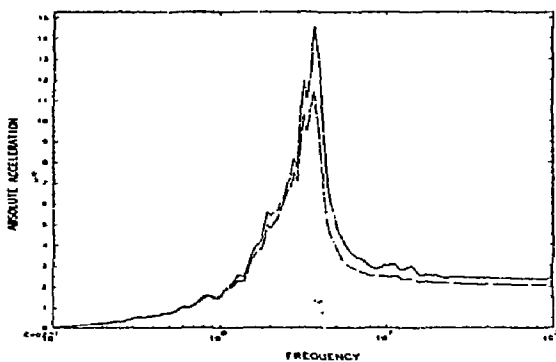
a) Transverse



b) Vertical



c) Longitudinal



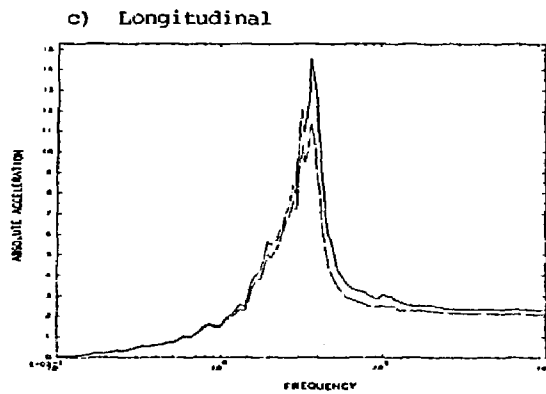
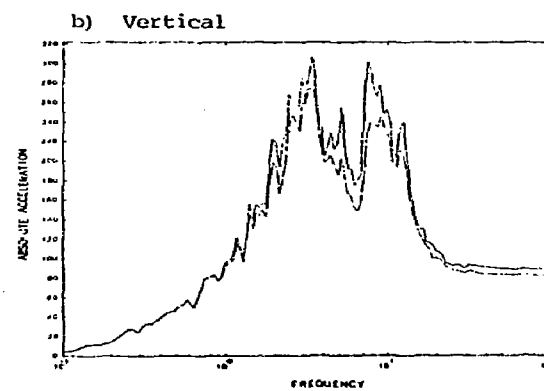
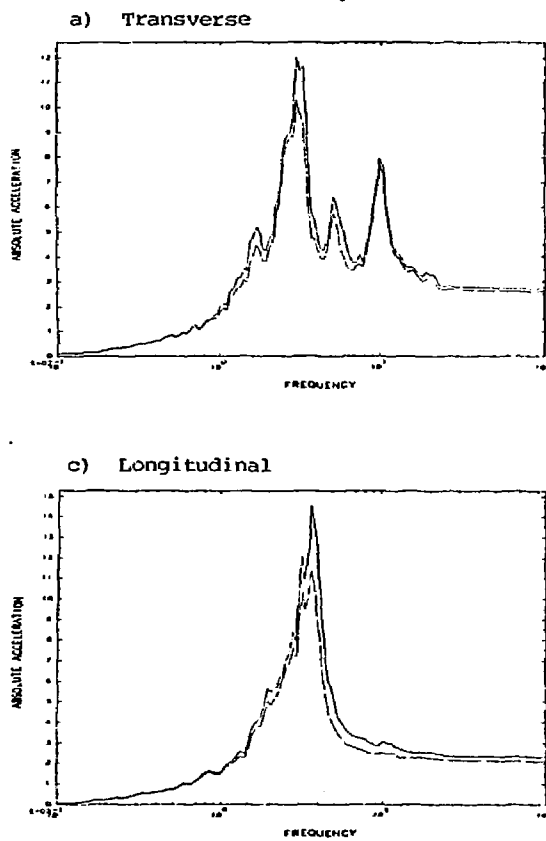
Legend

Maximum \_\_\_\_\_  
Mean \_\_\_\_\_

Notes

All spectra at 5% damping  
All frequencies in Hz  
All accelerations in in/sec<sup>2</sup>

Figure A.26 In-Structure Response Spectra from Coupled SSI Analyses  
Node 745, Vessel Model



Legend

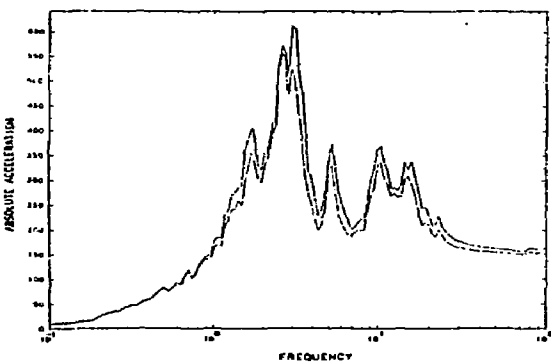
Maximum \_\_\_\_\_  
 Mean \_\_\_\_\_

Notes

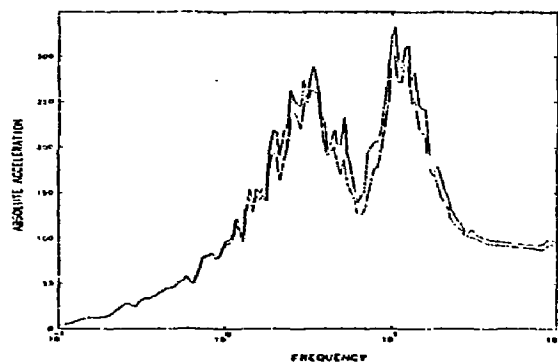
All spectra at 5% damping  
 All frequencies in Hz  
 All accelerations in in/sec<sup>2</sup>

Figure A.27 In-Structure Response Spectra from Coupled SSI Analyses  
 Node 750, Vessel Model

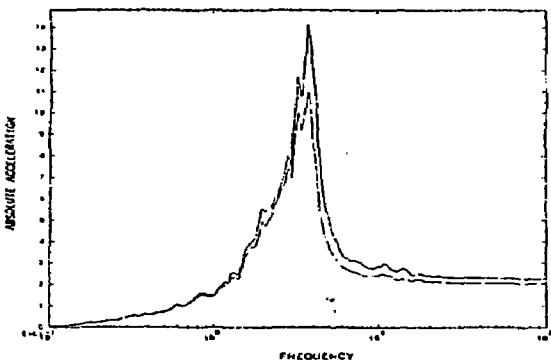
a) Transverse



b) Vertical



c) Longitudinal



Legend

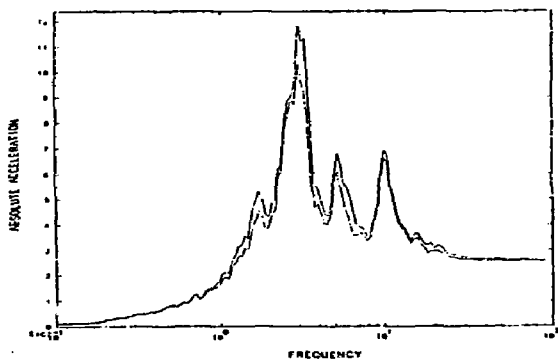
Maximum \_\_\_\_\_  
Mean \_\_\_\_\_

Notes

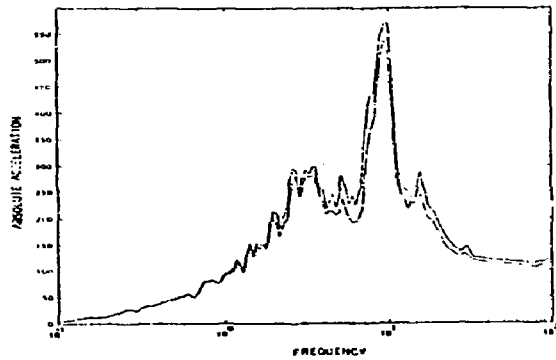
All spectra at 5% damping  
All frequencies in Hz  
All accelerations in in/sec<sup>2</sup>

Figure A.28 In-Structure Response Spectra from Coupled SSI Analyses  
Node 755, Vessel Model

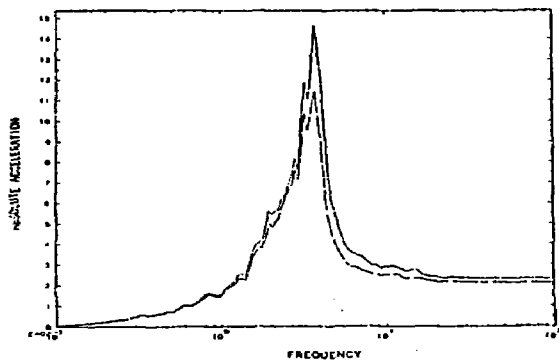
a) Transverse



b) Vertical



c) Longitudinal



Legend

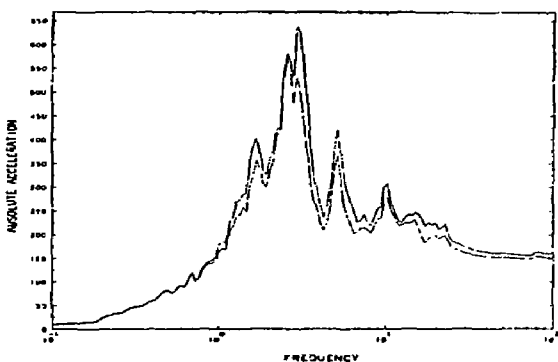
Maximum \_\_\_\_\_  
Mean \_\_\_\_\_

Notes

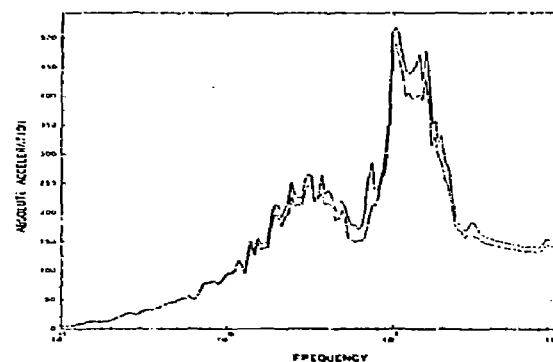
All spectra at 5% damping  
All frequencies in Hz  
All accelerations in in/sec<sup>2</sup>

Figure A.29 In-Structure Response Spectra from Coupled SSI Analyses  
Node 812 Vessel Model

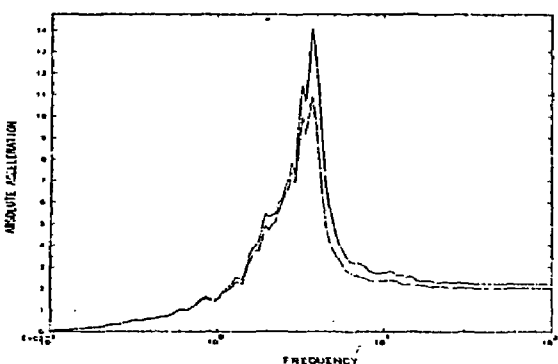
a) Transverse



b) Vertical



c) Longitudinal



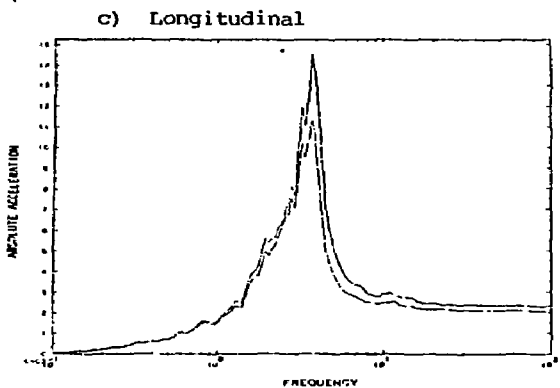
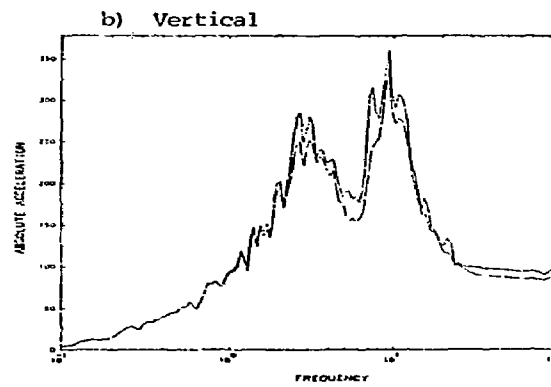
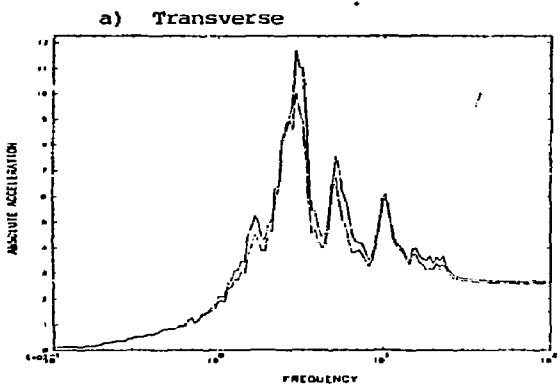
Legend

Maximum \_\_\_\_\_  
Mean \_\_\_\_\_

Notes

All spectra at 5% damping  
All frequencies in Hz  
All accelerations in in/sec<sup>2</sup>

Figure A.30 In-Structure Response Spectra from Coupled SSI Analyses  
Node 824, Vessel Model



Legend

Maximum   
Mean 

Notes

All spectra at 5% damping  
All frequencies in Hz  
All accelerations in in/sec<sup>2</sup>

Figure A.31 In-Structure Response Spectra from Coupled SSI Analyses  
Node 879, Vessel Model

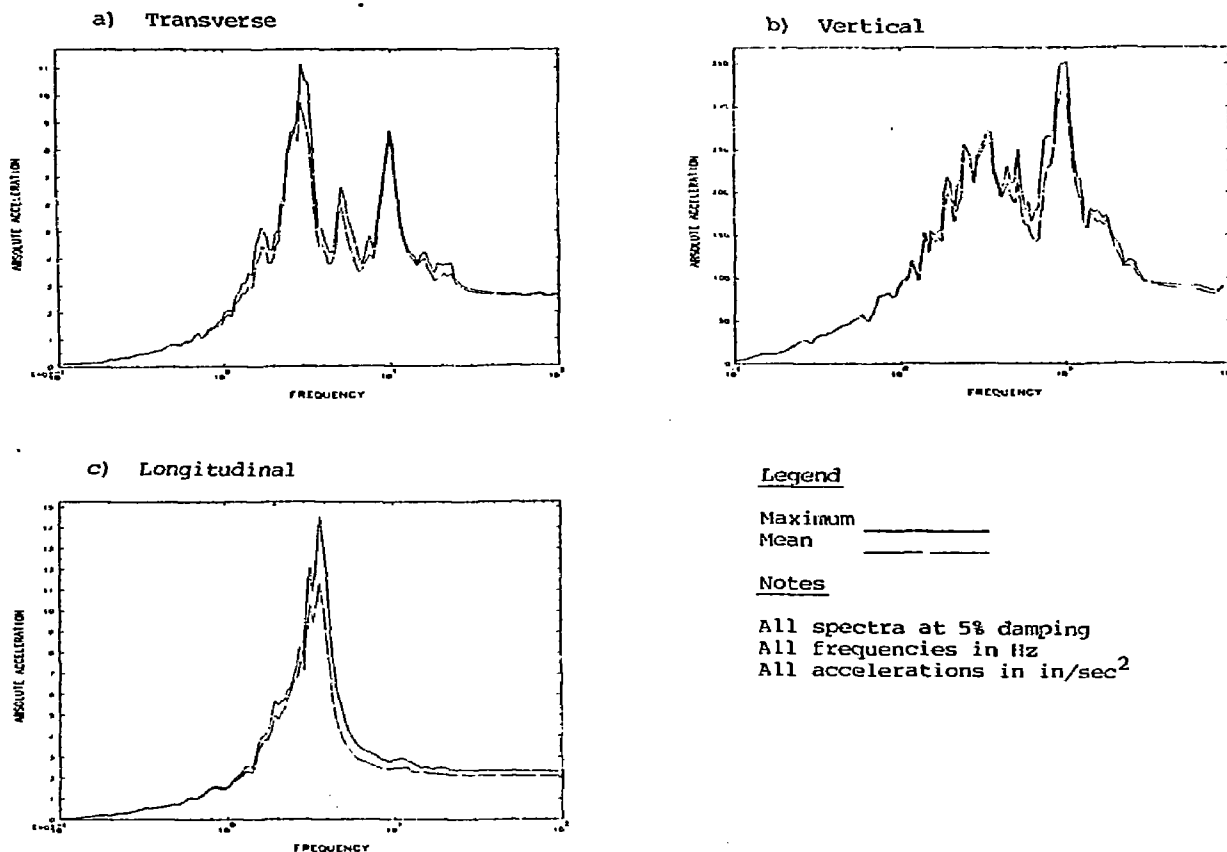
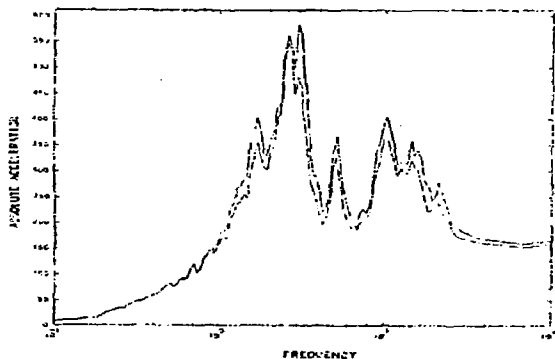
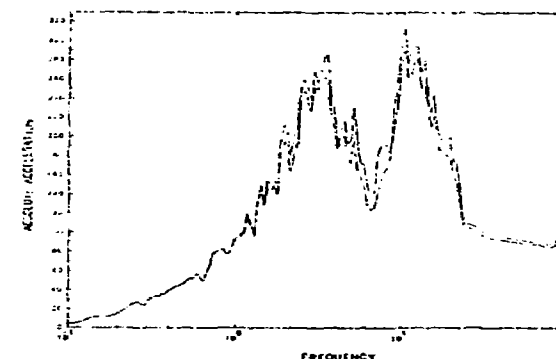


Figure A.32 In-Structure Response Spectra from Coupled SSI Analyses  
Node 885, Vessel Model

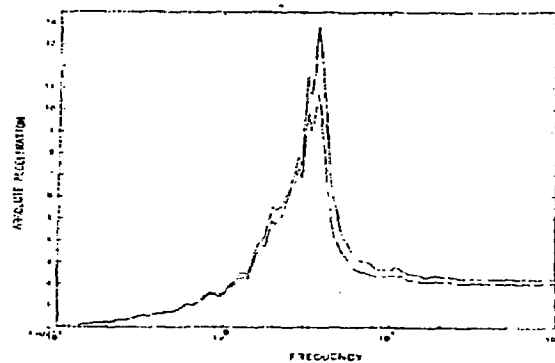
a) Transverse



b) Vertical



c) Longitudinal



Legend

Maximum \_\_\_\_\_  
Mean \_\_\_\_\_

Notes

All spectra at 5% damping  
All frequencies in Hz  
All accelerations in in/sec<sup>2</sup>

Figure A.33 In-Structure Response Spectra from Coupled SSI Analyses  
Node 891 Vessel Model

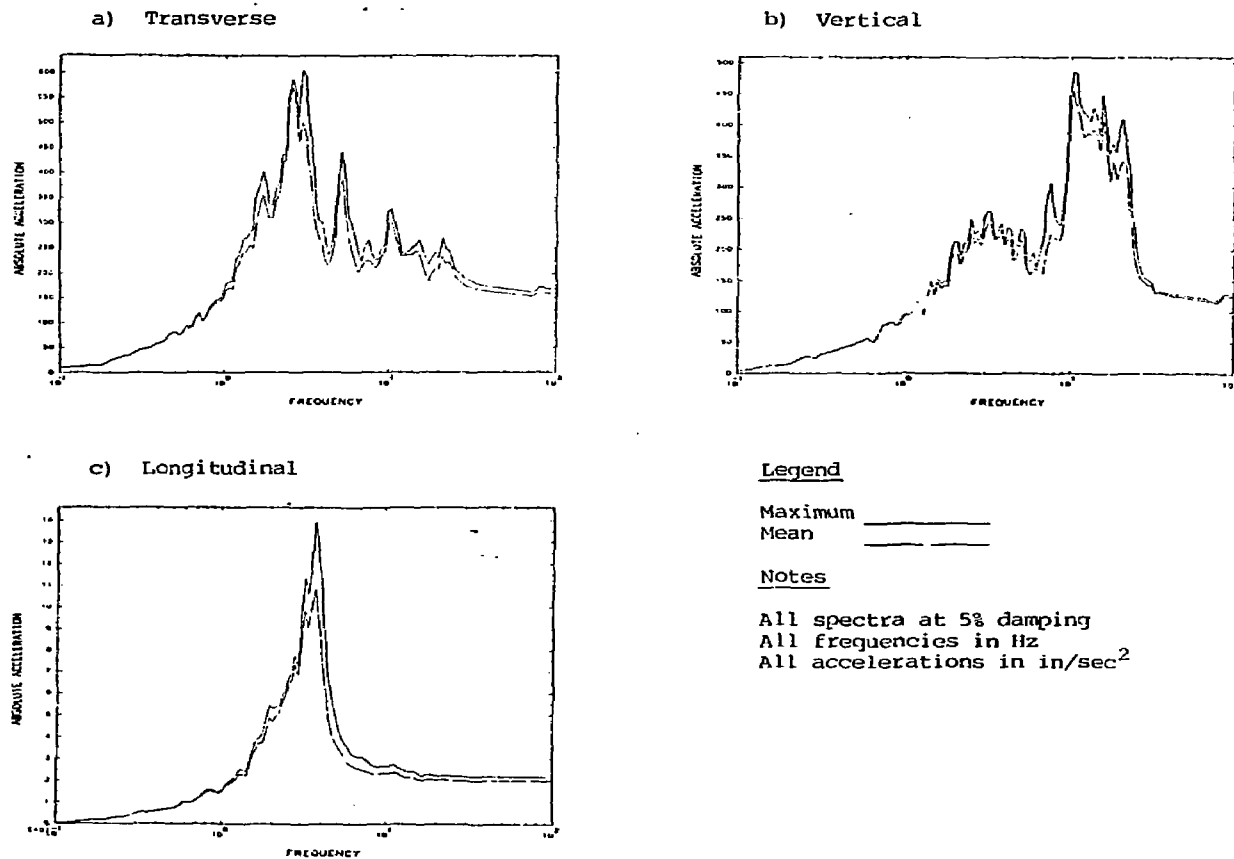
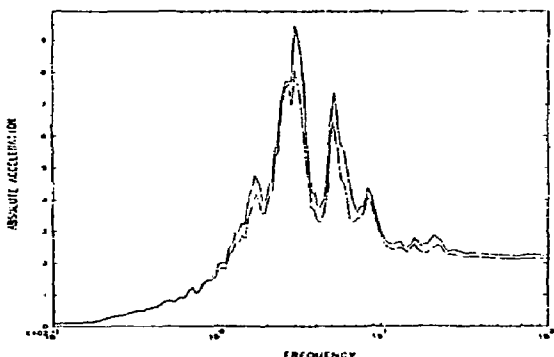
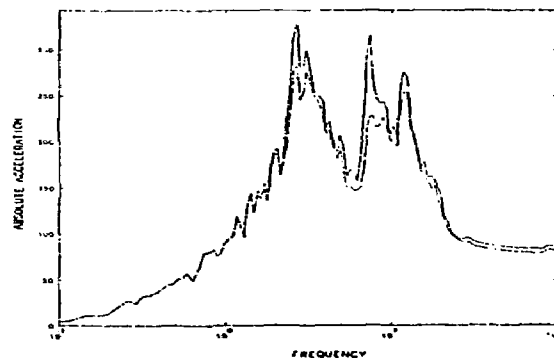


Figure A.34 In-Structure Response Spectra from Coupled SSI Analyses  
 Node 940, Vessel Model

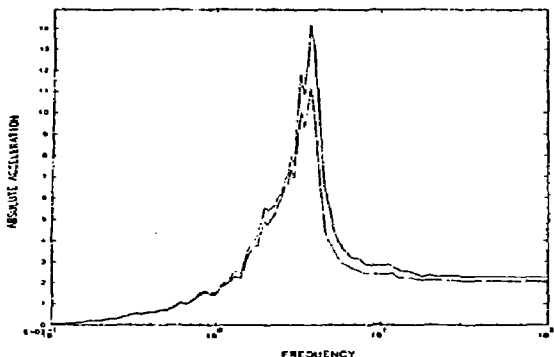
a) Transverse



b) Vertical



c) Longitudinal



Legend

Maximum \_\_\_\_\_  
Mean \_\_\_\_\_

Notes

All spectra at 5% damping  
All frequencies in Hz  
All accelerations in in/sec<sup>2</sup>

Figure A.35 In-Structure Response Spectra from Coupled SSI Analyses  
Node 923, Vessel Model

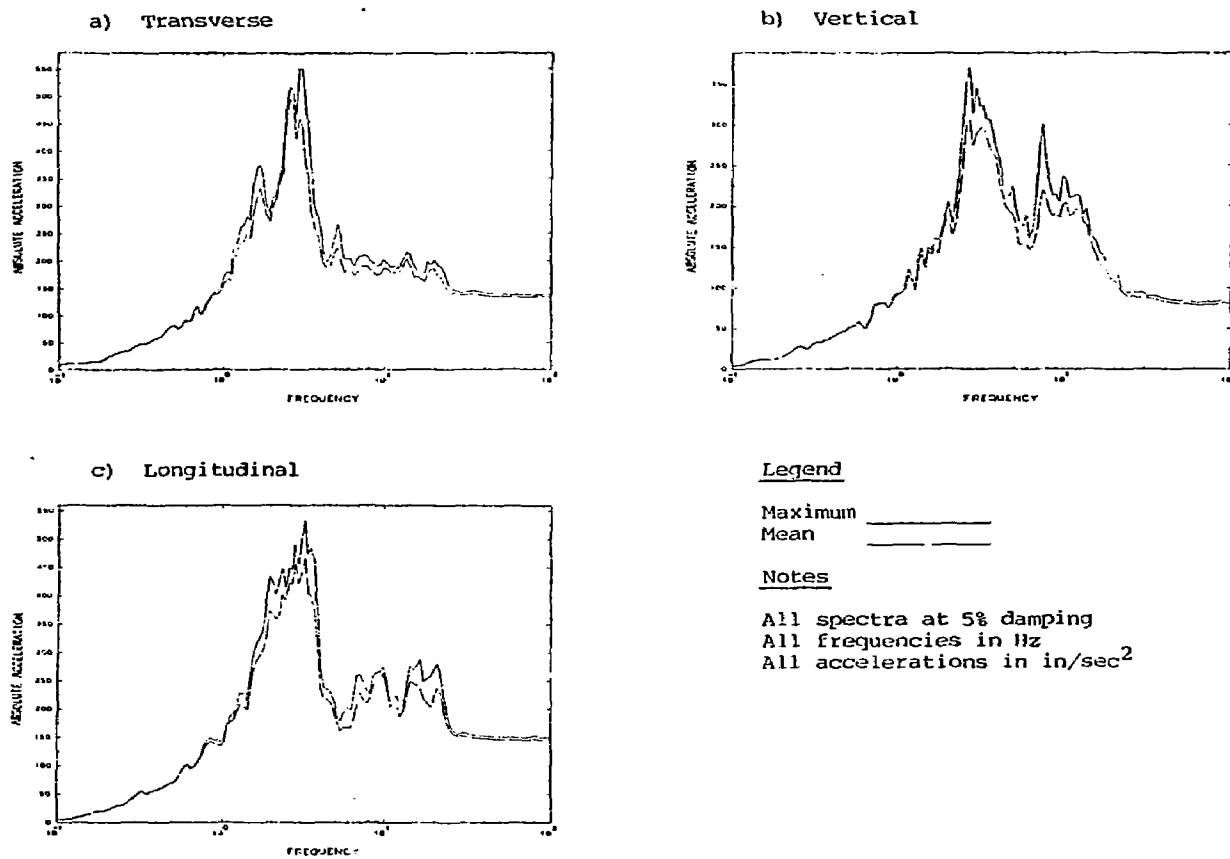
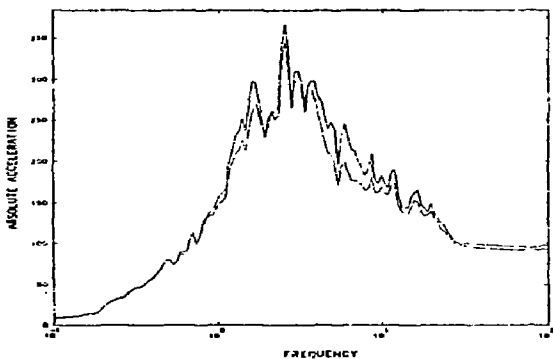
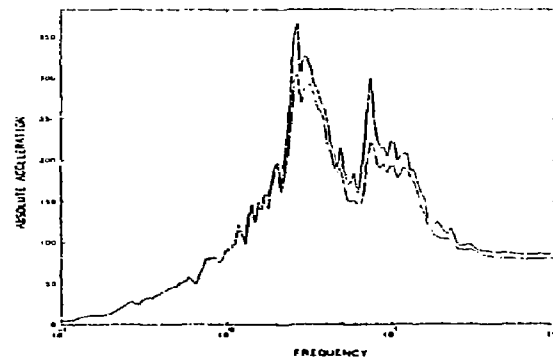


Figure A.36 In-Structure Response Spectra from Coupled SSI Analyses  
 Node 1238, Vessel Model

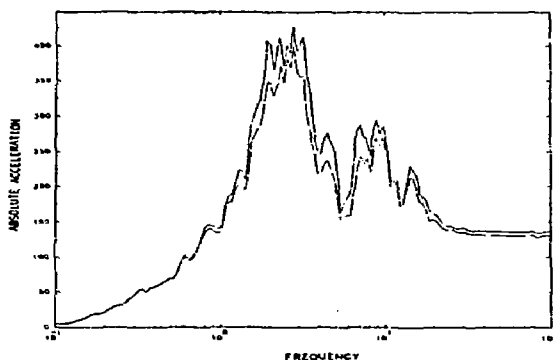
a) Transverse



b) Vertical



c) Longitudinal



Legend

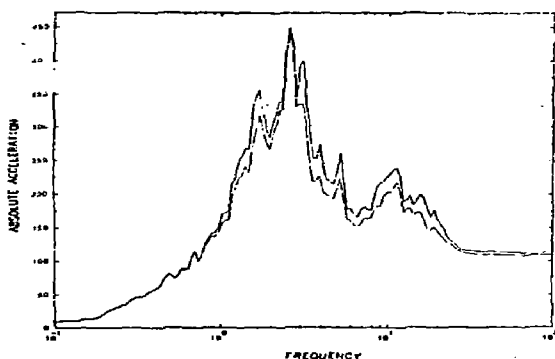
Maximum \_\_\_\_\_  
Mean \_\_\_\_\_

Notes

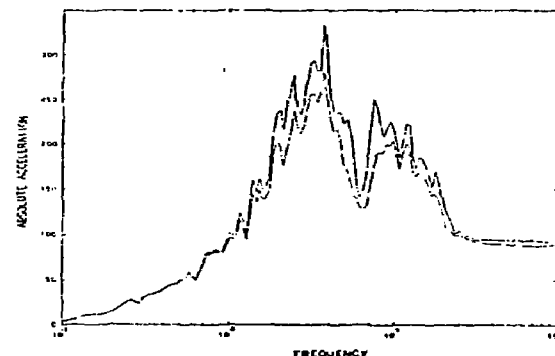
All spectra at 5% damping  
All frequencies in Hz  
All accelerations in in/sec<sup>2</sup>

Figure A.37 In-Structure Response Spectra from Coupled SSI Analyses  
Node 1250, Vessel Model

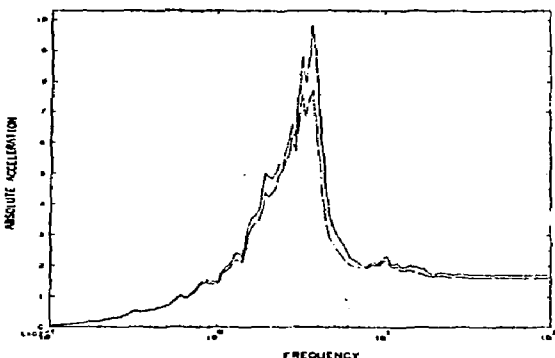
a) Transverse



b) Vertical



c) Longitudinal



Legend

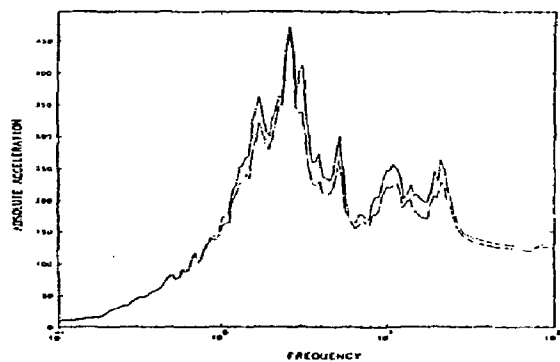
Maximum ———  
Mean - - -

Notes

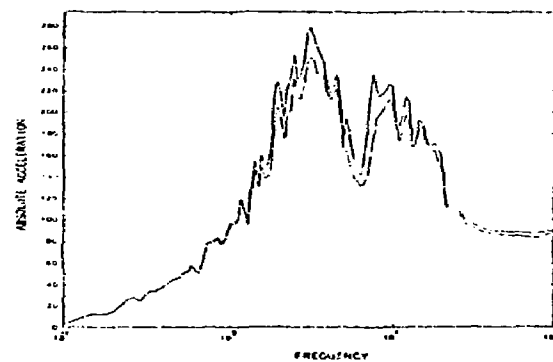
All spectra at 5% damping  
All frequencies in Hz  
All accelerations in in/sec<sup>2</sup>

Figure A.38 In-Structure Response Spectra from Coupled SSI Analyses  
Node 1276, Vessel Model

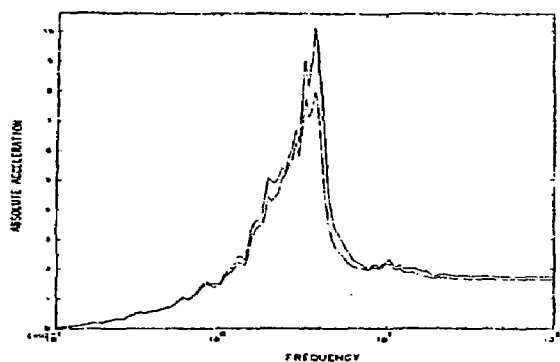
a) Transverse



b) Vertical



c) Longitudinal



Legend

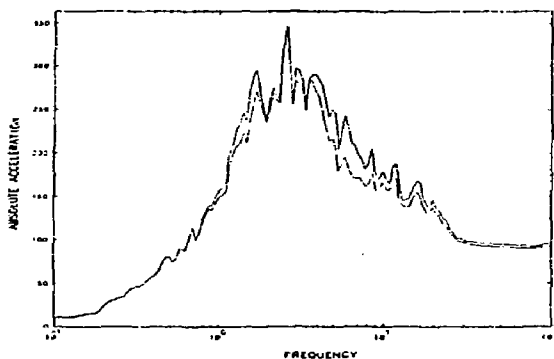
Maximum \_\_\_\_\_  
Mean \_\_\_\_\_

Notes

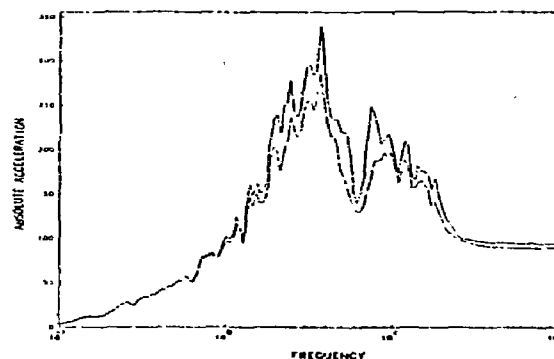
All spectra at 5% damping  
All frequencies in Hz  
All accelerations in in/sec<sup>2</sup>

Figure A.39 In-Structure Response Spectra from Coupled SSI Analyses  
Node 1296 Vessel Model

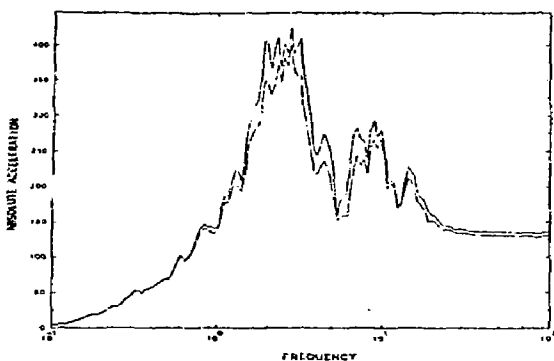
a) Transverse



b) Vertical



c) Longitudinal



Legend

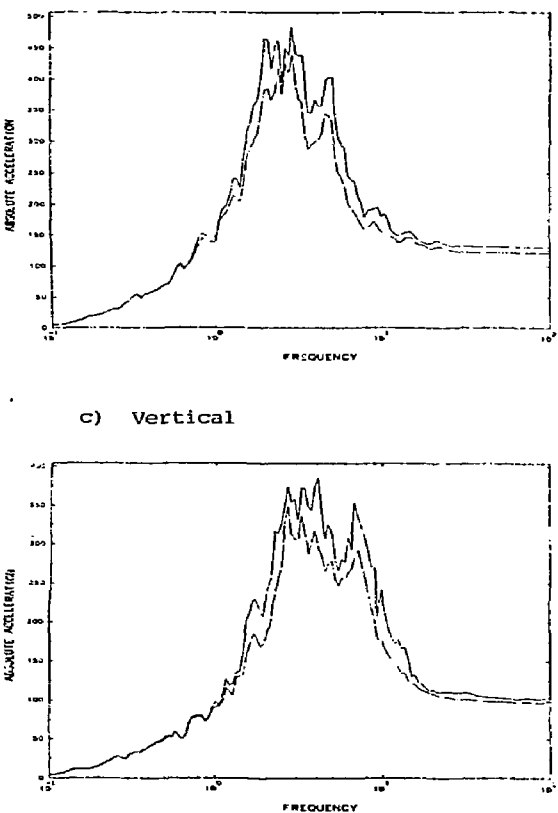
Maximum \_\_\_\_\_  
Mean \_\_\_\_\_

Notes

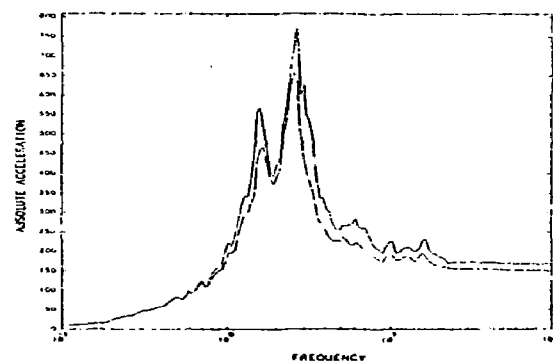
All spectra at 5% damping  
All frequencies in Hz  
All accelerations in in/sec<sup>2</sup>

Figure A.40 In-Structure Response Spectra from Coupled SSI Analyses  
Node 1303, Vessel Model

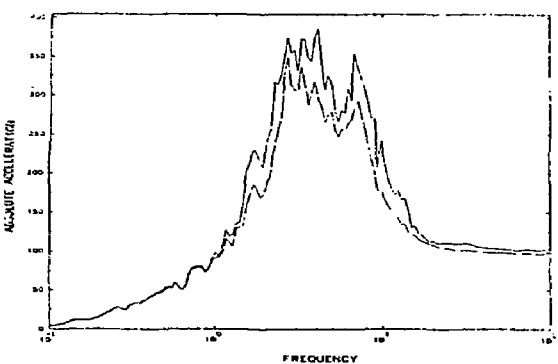
a) Longitudinal



b) Transverse



c) Vertical



Legend

Maximum \_\_\_\_\_  
Mean \_\_\_\_\_

Notes

All spectra at 5% damping  
All frequencies in Hz  
All accelerations in in/sec<sup>2</sup>

Figure A.41 In-Structure Response Spectra from Coupled SSI Analyses  
Node 30, Vault Model

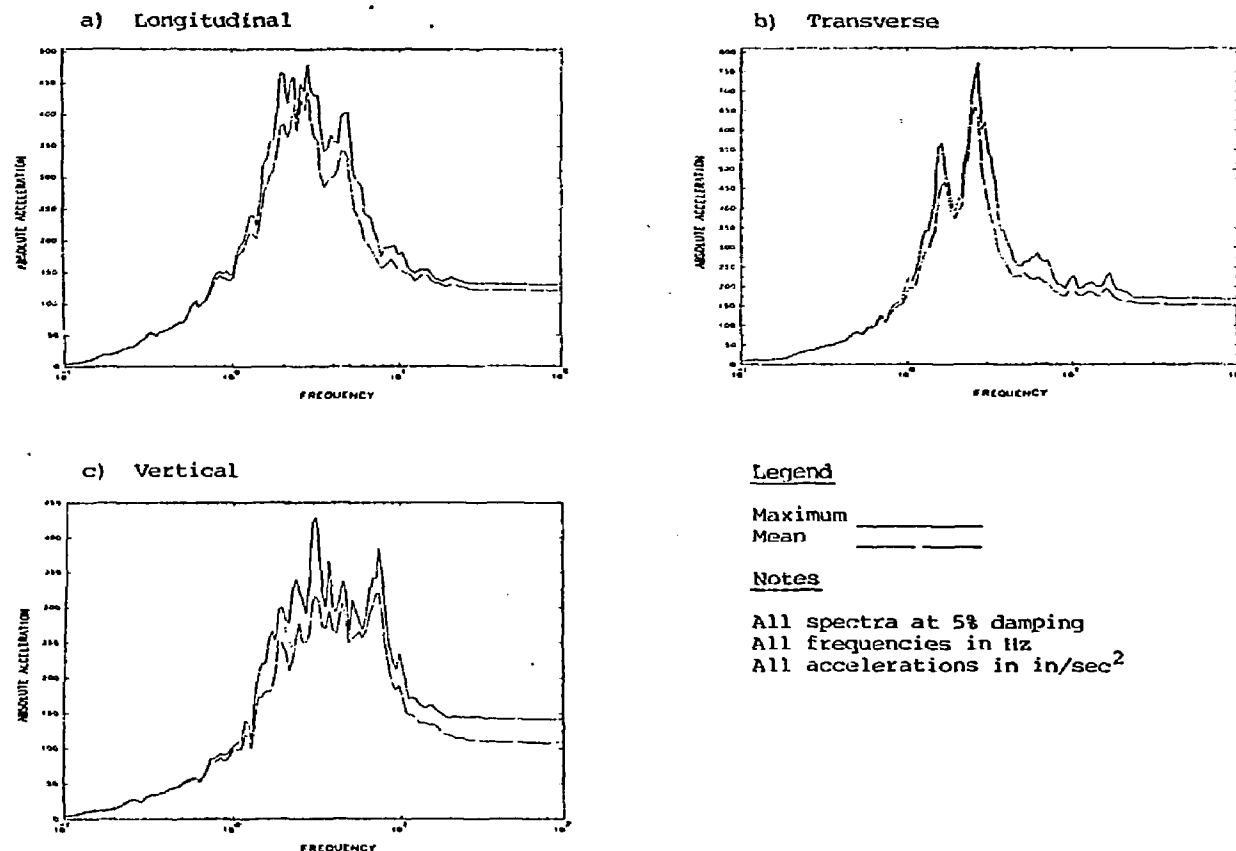
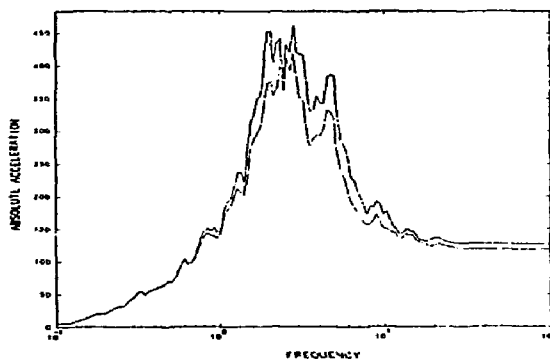
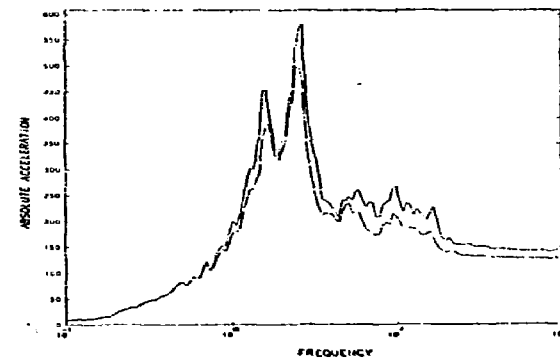


Figure A.42 In-structure Response Spectra from Coupled SSI Analyses  
Node 140, Vault Model

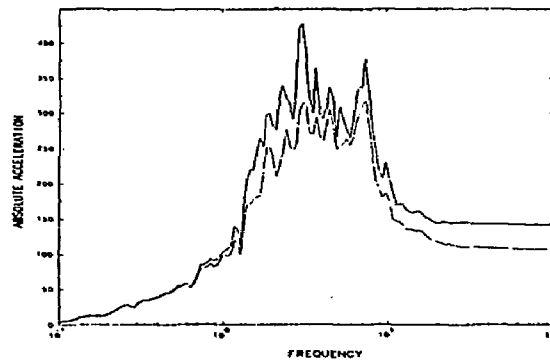
a) Longitudinal



b) Transverse



c) Vertical



Legend

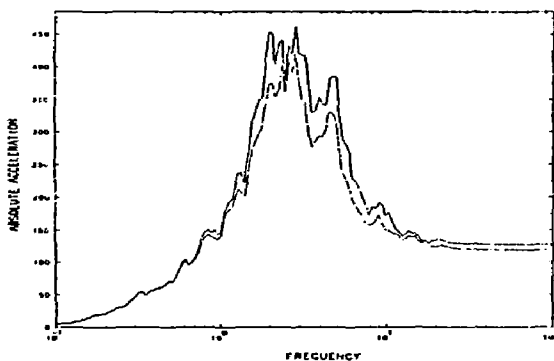
Maximum \_\_\_\_\_  
Mean \_\_\_\_\_

Notes

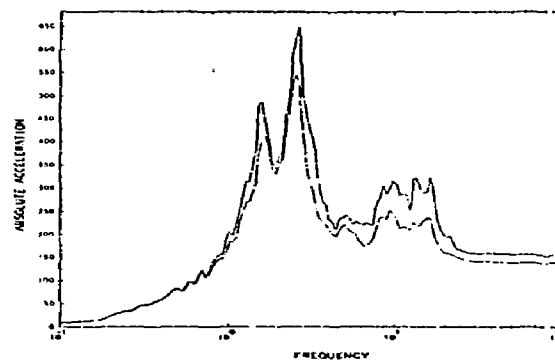
All spectra at 5% damping  
All frequencies in Hz  
All accelerations in in/sec<sup>2</sup>

Figure A.43 In-Structure Response Spectra from Coupled SSI Analyses  
Node 153 Vault Model

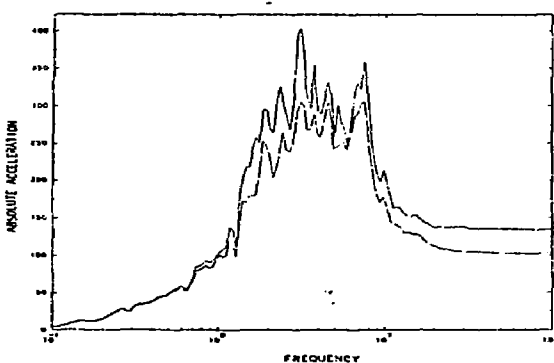
a) Longitudinal



b) Transverse



c) Vertical



Legend

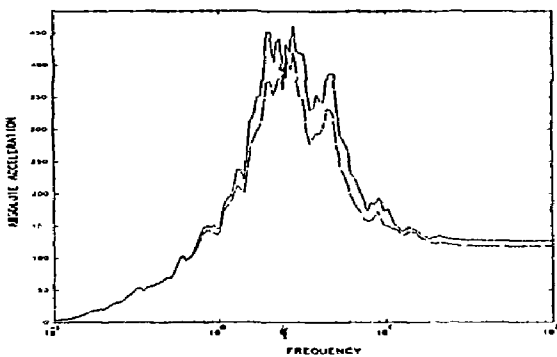
Maximum \_\_\_\_\_  
Mean \_\_\_\_\_

Notes

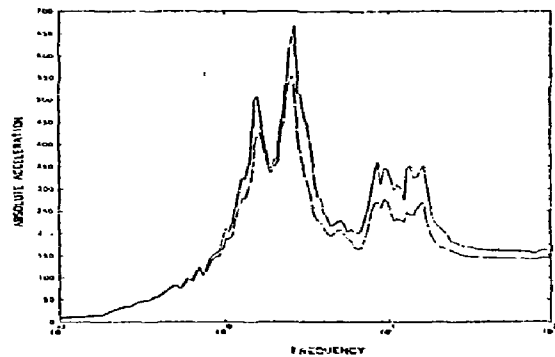
All spectra at 5% damping  
All frequencies in Hz  
All accelerations in in/sec<sup>2</sup>

Figure A.44 In-Structure Response Spectra from Coupled SSI Analyses  
Node 154, Vault Model

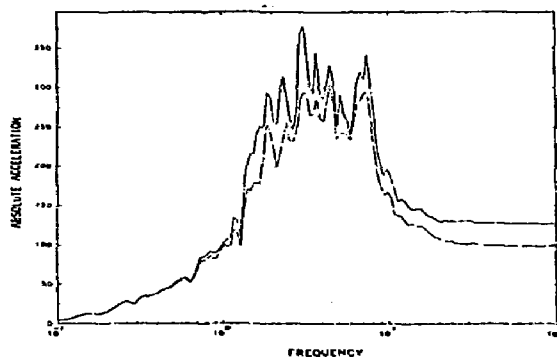
a) Longitudinal



b) Transverse



c) Vertical



Legend

Maximum \_\_\_\_\_  
Mean \_\_\_\_\_

Notes

All spectra at 5% damping  
All frequencies in Hz  
All accelerations in in/sec<sup>2</sup>

Figure A.45 In-Structure Response Spectra from Coupled SSI Analyses  
Node 155, Vault Model

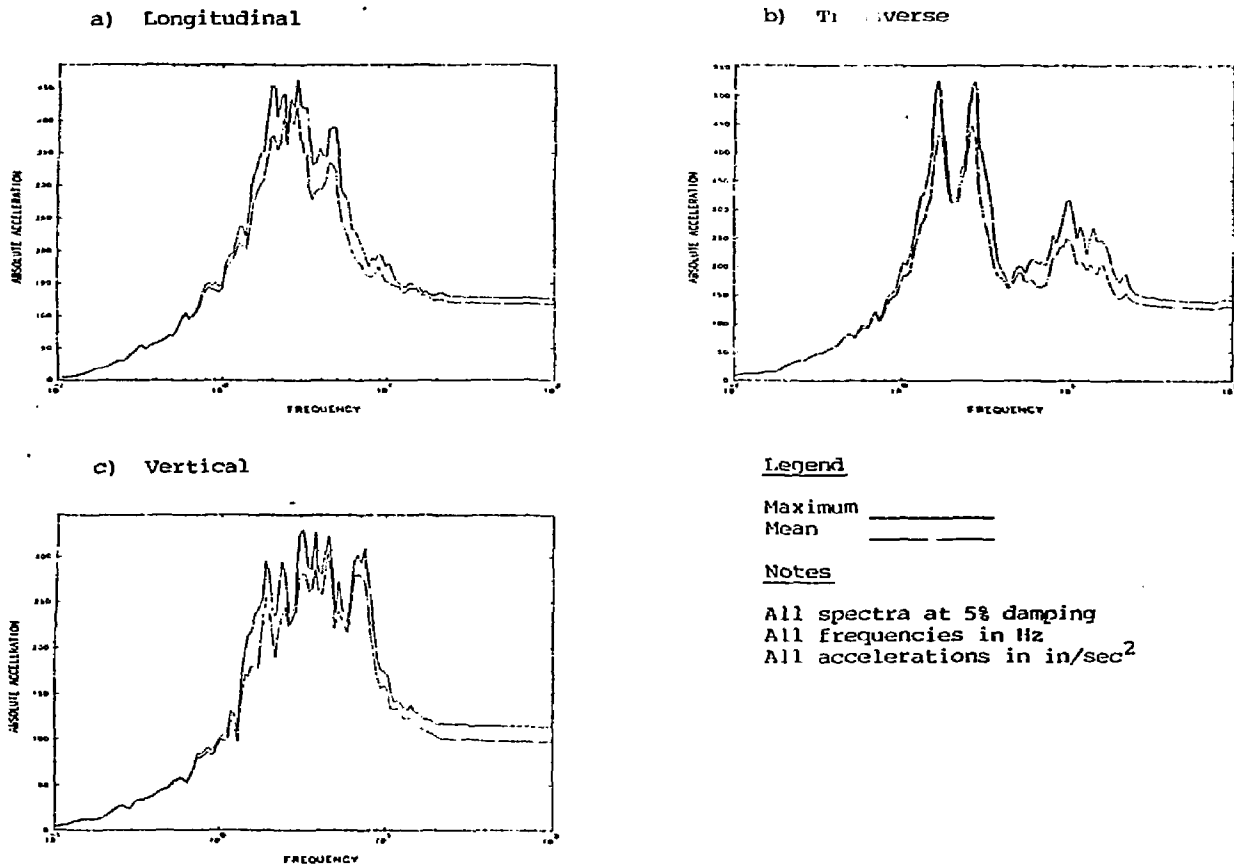
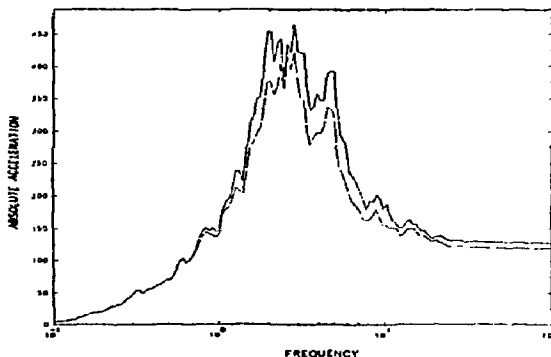
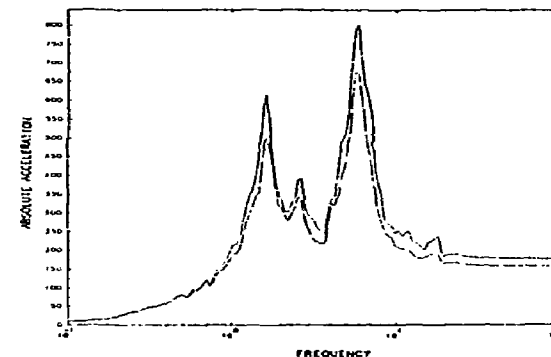


Figure A.46 In-Structure Response Spectra from Coupled SSI Analyses  
Node 157, Vault Model

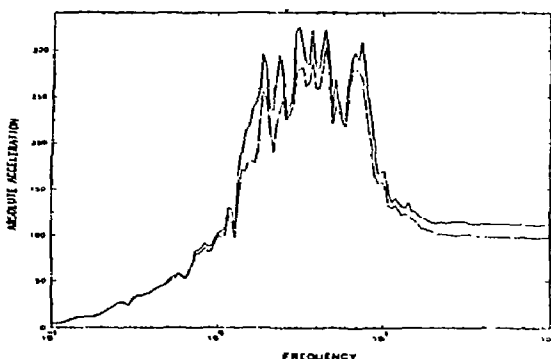
a) Longitudinal



b) Transverse



c) Vertical



Legend

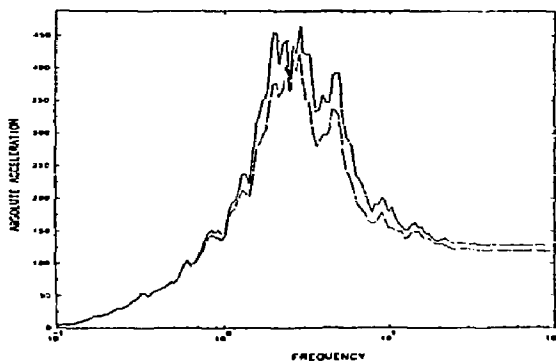
Maximum \_\_\_\_\_  
Mean \_\_\_\_\_

Notes

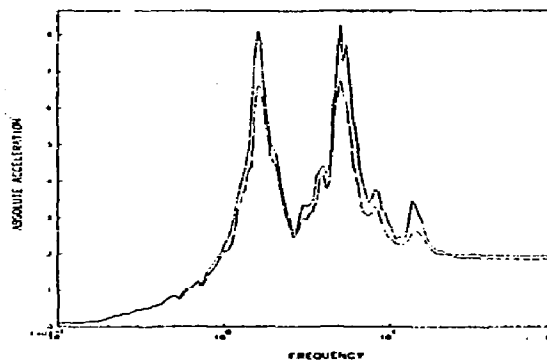
All spectra at 5% damping  
All frequencies in Hz  
All accelerations in in/sec<sup>2</sup>

Figure A.47 In-Structure Response Spectra from Coupled SSI Analyses  
Node 160, Vault Model

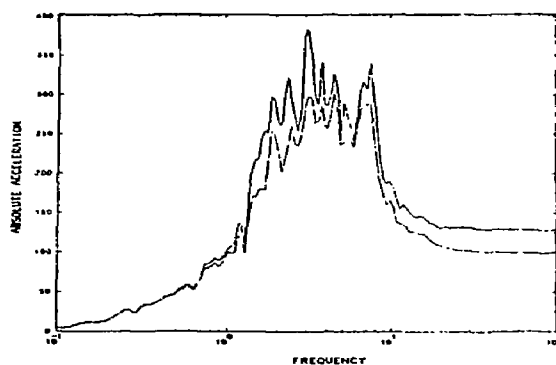
a) Longitudinal



b) Transverse



c) Vertical



Legend

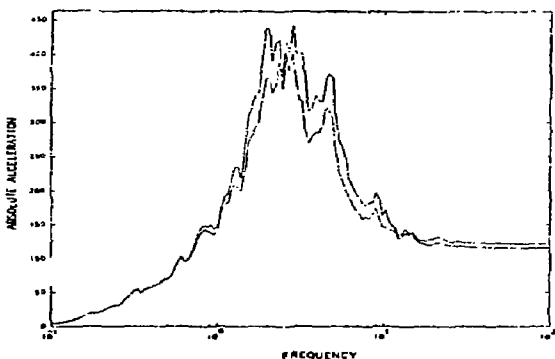
Maximum \_\_\_\_\_  
Mean \_\_\_\_\_

Notes

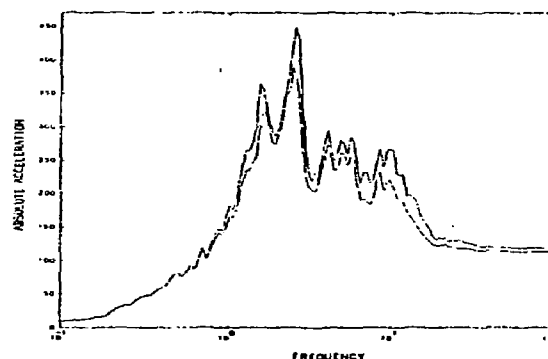
All spectra at 5% damping  
All frequencies in Hz  
All accelerations in in/sec<sup>2</sup>

Figure A.48 In-Structure Response Spectra from Coupled SSI Analyses  
Node 162, Vault Model

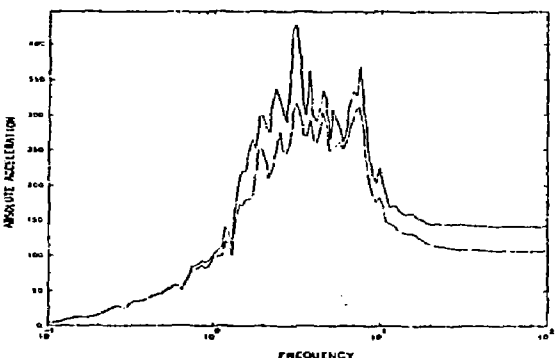
a) Longitudinal



b) Transverse



c) Vertical



Legend

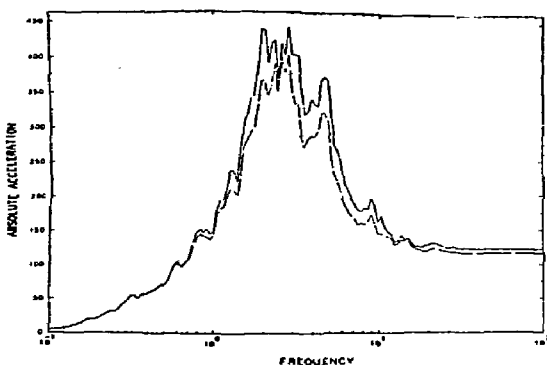
Maximum \_\_\_\_\_  
Mean \_\_\_\_\_

Notes

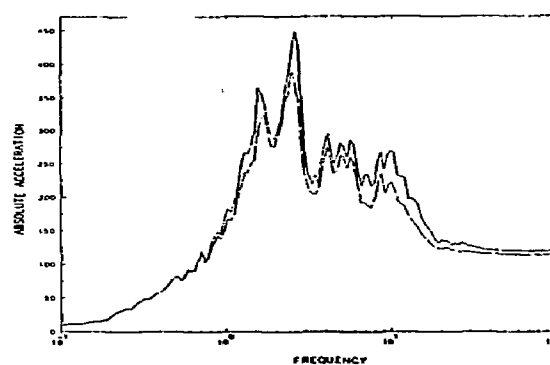
All spectra at 5% damping  
All frequencies in Hz  
All accelerations in in/sec<sup>2</sup>

Figure A.49 In-Structure Response Spectra from Coupled SSI Analyses  
Node 166, Vault Model

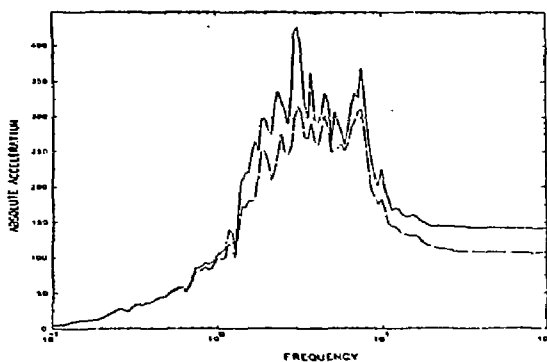
a) Longitudinal



b) Transverse



c) Vertical



Legend

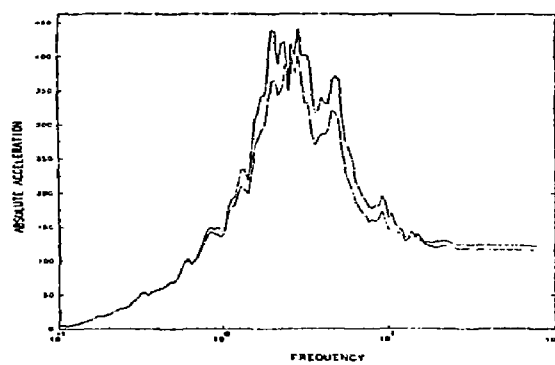
Maximum \_\_\_\_\_  
Mean \_\_\_\_\_

Notes

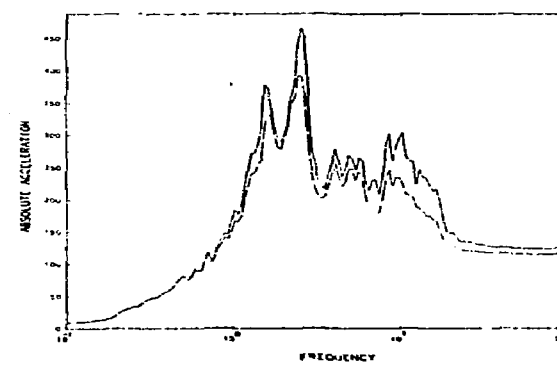
All spectra at 5% damping  
All frequencies in Hz  
All accelerations in in/sec<sup>2</sup>

Figure A.50 In-Structure Response Spectra from Coupled SSI Analyses  
Node 167, Vault Model

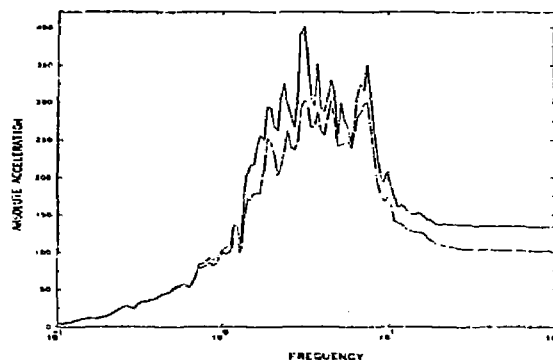
a) Longitudinal



b) Transverse



c) Vertical



Legend

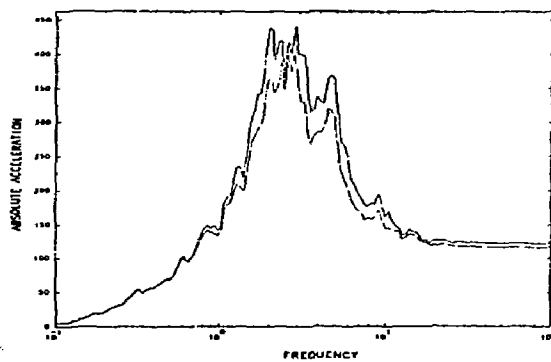
Maximum \_\_\_\_\_  
Mean \_\_\_\_\_

Notes

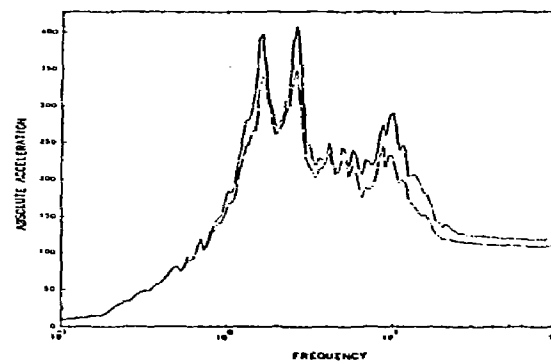
All spectra at 5% damping  
All frequencies in Hz  
All accelerations in in/sec<sup>2</sup>

Figure A.51 In-Structure Response Spectra from Coupled SSI Analyses  
Node 168, Vault Model

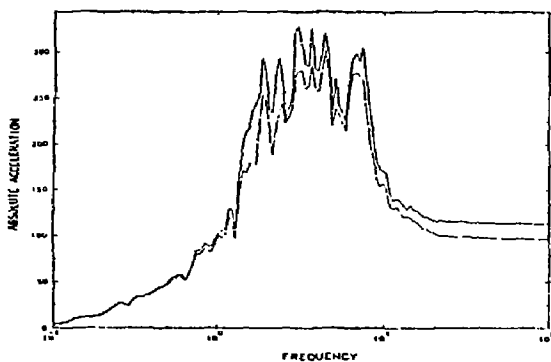
a) Longitudinal



b) Transverse



c) Vertical



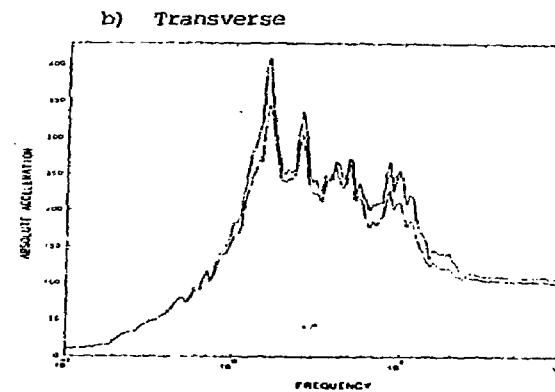
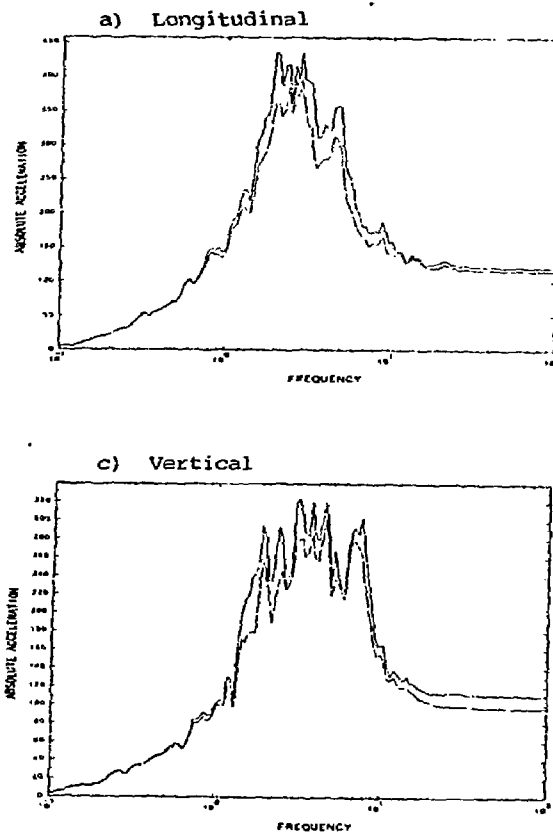
Legend

Maximum \_\_\_\_\_  
Mean \_\_\_\_\_

Notes

All spectra at 5% damping  
All frequencies in Hz  
All accelerations in in/sec<sup>2</sup>

Figure A.52 In-Structure Response Spectra from Coupled SSI Analyses  
Node 170, Vault Model



Legend

Maximum \_\_\_\_\_  
 Mean \_\_\_\_\_

Notes

All spectra at 5% damping  
 All frequencies in Hz  
 All accelerations in in/sec<sup>2</sup>

Figure A.53 In-Structure Response Spectra from Coupled SSI Analyses  
 Node 173, Vault Model

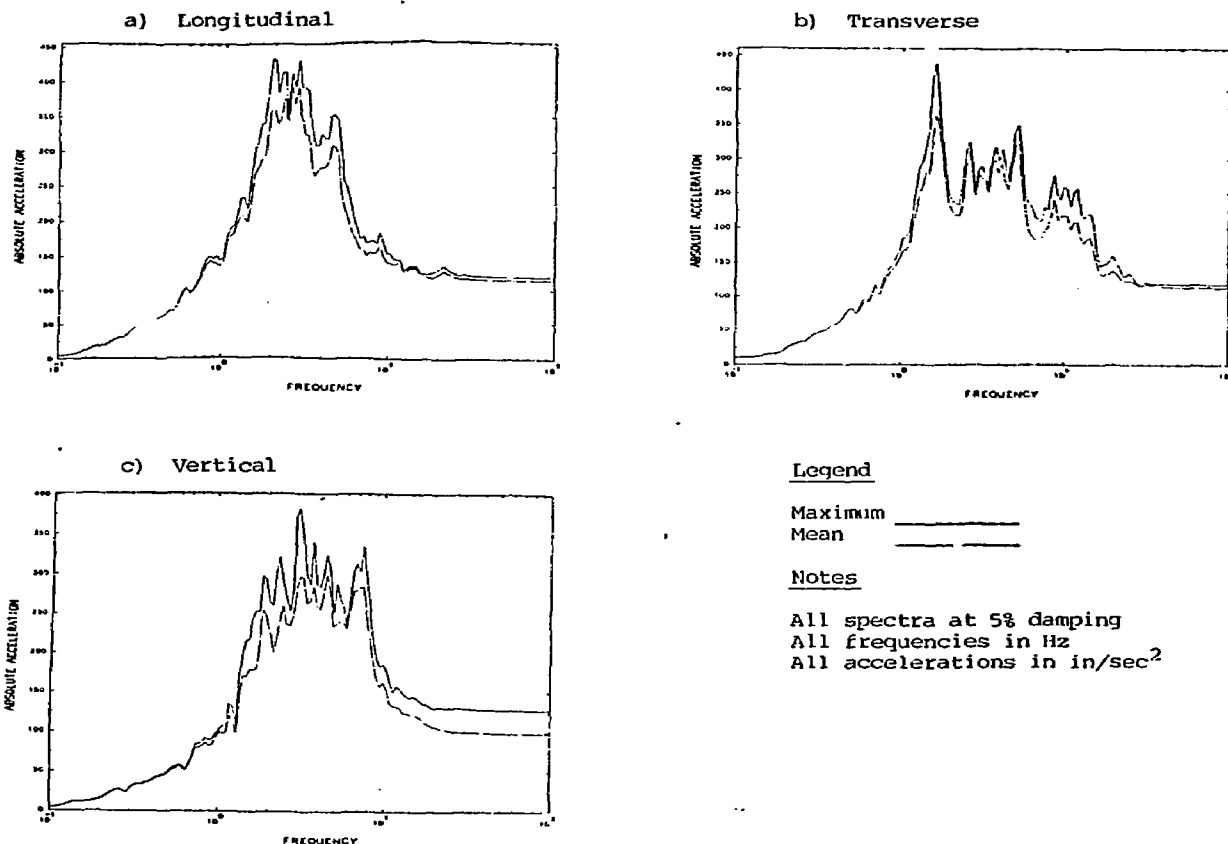
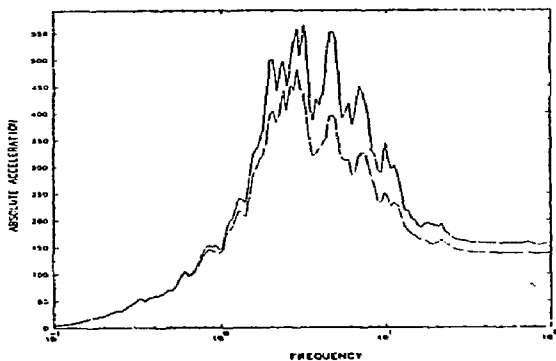
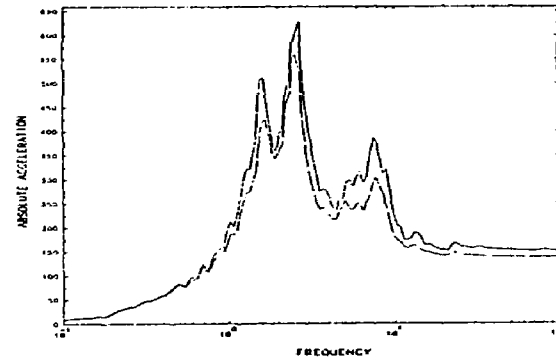


Figure A.54 In-Structure Response Spectra from Coupled SSI Analyses  
 Node 175, Vault Model

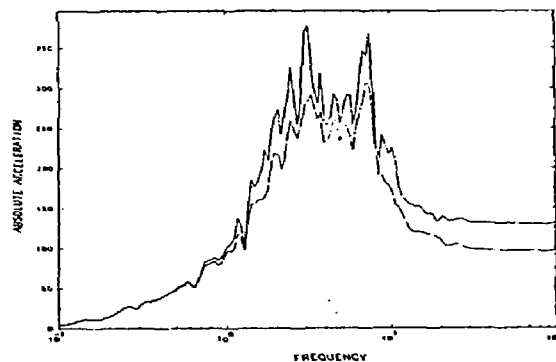
a) Longitudinal



b) Transverse



c) Vertical



Legend

Maximum \_\_\_\_\_  
Mean \_\_\_\_\_

Notes

All spectra at 5% damping  
All frequencies in Hz  
All accelerations in in/sec<sup>2</sup>

Figure A.55 In-Structure Response Spectra from Coupled SSI Analyses  
Node 236, Vault Model

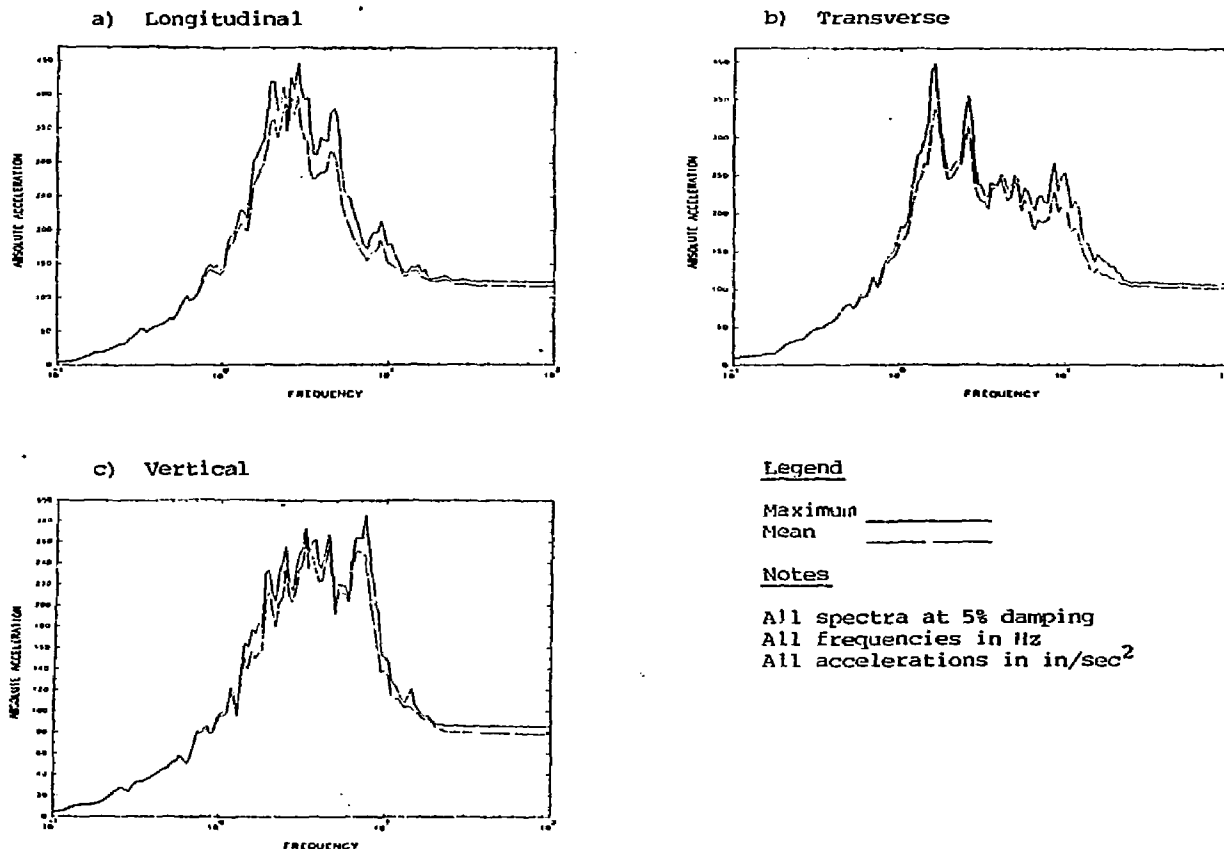


Figure A.56 In-Structure Response Spectra from Coupled SSI Analyses  
Node 353, Vault Model